# THE POTENTIAL OF SONIC WAVE PROPAGATION IN ENGINEERING ROCK CLASSIFICATION

by

Paul P. G. Schilizzi

Thesis submitted to the Faculty of the
Virginia Polytechnic Institute and State University
in partial fulfillment of the requirements for the degree of

MASTER OF SCIENCE

in

Mining Engineering

APPROVED:

M. Kármis, Chairman

J. Costain

G. Faulkner

C. Haycocks

J. R. Lucas

July, 1982

Blacksburg, Virginia

ACKNOWLEDGEMENTS

I would like to express my gratitude to Dr. Michael Karmis and Dr. Gavin Faulkner for their help and guidance during the course of my research. Special thanks to Dr. J. Costain, Dr. C. Haycocks and Dr. J. R. Lucas for their help and suggestions.

The cooperation received by the management of the various quarries is appreciated.

Thanks to Mr. J. Hussey and Mr. B. Grabs for their assistance during the statistical analysis of the experimental data.

Thanks to Mr. Bill Kane and Mr. Jim Overfelt for their help and suggestions during sample collection and testing.

A heartfelt thanks to Mrs. Frances Woodward for her careful editing and typing of the manuscript.

Thanks are extended to the Bodossaki Foundation in Athens, Greece for their financial support during my studies at VPI & SU.

Thanks to all the graduate students in the Mining Engineering Department at VPI & SU for their help and suggestions .

Finally, a great deal of thanks are due my parents for their support throughout my university career.

TABLE OF CONTENTS

TABLE OF CONTENTS

TABLE OF CONTENTS

LIST OF FIGURES

LIST OF FIGURES

LIST OF FIGURES

LIST OF FIGURES

LIST OF FIGURES

LIST OF FIGURES

LIST OF TABLES

# CHAPTER I

## INTRODUCTION

The need for the development of engineering rock classification systems has been widely recognized. The purpose of a classification system is to take into consideration parameters of rock quality, measured in the field and the laboratory and to assess the behavior and response of rocks under stress utilizing these properties.

Over the years, a number of rock classification systems have been developed. The purpose, application and method of assigning an index describing rock quality vary considerably between these systems. Several systems are developed to assess the stability of excavations in rock, whereas other systems have been directed towards estimating a particular feature of a rock mass, i.e., blastability, rippability, etc. In most cases, the rock quality is expressed by meaningful descriptions or by a numerical property index.

Each classification system requires the laboratory or field testing of rock in order to determine the desired parameters. Laboratory work on intact rock usually consists of the measurement of the modulus of elasticity and the unconfined compressive strength. Field investigations may include the determination of the in-situ modulus of deformation and the spacing and characteristics of the discontinuities. The measurement of such parameters requires sample collection and preparation, field preparation, extensive field work and considerable experimental instrumentation.

The estimation or approximation of the above static properties and rock quality characteristics from parameters determined from sonic wave testing, such as the velocity, amplitude and frequency of P- and S-waves, has been the subject of considerable interest among investigators. If such correlation is possible, existing rock classification systems could be modified and new systems could be developed utilizing the much easier to measure sonic parameters.

The objective of this research was to develop relationships between static and dynamic properties describing the competency and behavior of rocks, to identify the most appropriate sonic wave parameters for rock classification purposes and to apply these findings for the establishment of rock quality indexes.

The research demonstrated that the potential of the sonic wave propagation for engineering rock classification is considerable and that sonic wave properties could provide reliable qualitative and quantitative means of rock quality assessment.

# CHAPTER II

# THEORETICAL CONSIDERATIONS

## 2.1 Basic Definitions

This research considers the propagation of sonic waves through rock materials. A sonic wave is generated by a forced oscillation on a part of a rock sample or mass. This oscillation is propagated from one rock particle to another and results in an unstable stress condition, depending on the material properties. As a result, the phrase "sonic waves" will include, in this research, all such waveforms, regardless of frequency range or oscillation-propagation mode.

With regard to the frequency range, sonic waves can be classified into three categories:

(i) Seismic frequency range: 50-1000 Hz. Are generated by small explosions or hammer blows and used for field work.

(ii) Acoustic or audio frequency range: 1-10 kHz. Are not used frequently for rock testing and their generation is difficult.

(iii) Ultrasonic frequency range: 10-100 kHz. Are generated by magnetorestrictive, crystal or ceramic devices.

Sonic waves show several modes of particle vibration, along the direction of propagation. For different modes of oscillation, sonic waves can be described as follows:

(i) Compressional waves (also mentioned as Primary or P-waves): The rock particles oscillate on a straight line, parallel to

the direction of propagation. The medium undergoes tension and compression alternately.

(ii) Shear waves (also mentioned as Secondary or S-waves): The rock particles oscillate on a plane orthogonal to the direction of wave propagation. The elements of the medium change in shape but not in volume. If the waves are polarized on a horizontal plane they are known as SH-waves, whereas if the polarization is on a vertical plane they are known as SV-waves.

(iii) Rayleigh waves (R-waves): These are surface waves and produce a particle oscillation described by two motions with a phase difference of $90^{o}$. The first motion is perpendicular to the free surface and the second is parallel to it and to the direction of propagation.

(iv) Love waves (Q-waves): These are surface waves and are similar to shear waves, polarized on an axis parallel to the free surface.

Two more types of surface waves are mentioned in the literature but are not discussed here, Hydrodynamic waves and Coupled waves (Farmer, 1968)

## 2.2. Wave Propagation Through Rock Materials

A theoretical analysis of wave propagation through rock will be presented in order to determine which parameters of the sonic waves, measured in the lab or in the field, can be correlated to static mechanical properties of rocks.

2.2.1. The Elastic Model

The Elastic Model is the one most commonly used in rock mechanics. Because of its simplicity it does not require measurement of a large number of parameters and it can be used to approximate real conditions in most cases.

Figure 2.1 shows an element of a continuous body (Desai and Christian, 1977). $\sigma_{xx}$, $\sigma_{xy}$, etc., denote the stresses exerted through the six faces of the element to neighboring elements. These stresses will respectively cause strains:

$$\varepsilon_{xx} = \frac{\partial u}{\partial x} \qquad \varepsilon_{yy} = \frac{\partial v}{\partial y} \qquad \varepsilon_{zz} = \frac{\partial w}{\partial z}$$

$$\gamma_{xy} = \frac{\partial u}{\partial y} + \frac{\partial v}{\partial x}\ ,\ \gamma_{xz} = \frac{\partial u}{\partial z} + \frac{\partial w}{\partial x}\ ,\ \gamma_{yz} = \frac{\partial v}{\partial z} + \frac{\partial w}{\partial y}$$

where u, v, w are the displacements in the x, y, z directions respectively.

It can be proved that:

$$\sigma_{xy} = \sigma_{yx}$$

$$\sigma_{xz} = \sigma_{zx}$$

$$\sigma_{yz} = \sigma_{zy}$$

Strains and stresses, for an elastic isotropic model, under simple tension or compression, are related as follows:

$$\sigma_{xx} = E\ \varepsilon_{xx} \tag{2.1}$$

where E: Young's Modulus

$$\varepsilon_{yy} = \varepsilon_{zz} = -\nu\ \varepsilon_{xy} \tag{2.2}$$

where $\nu$ is Poisson's ratio

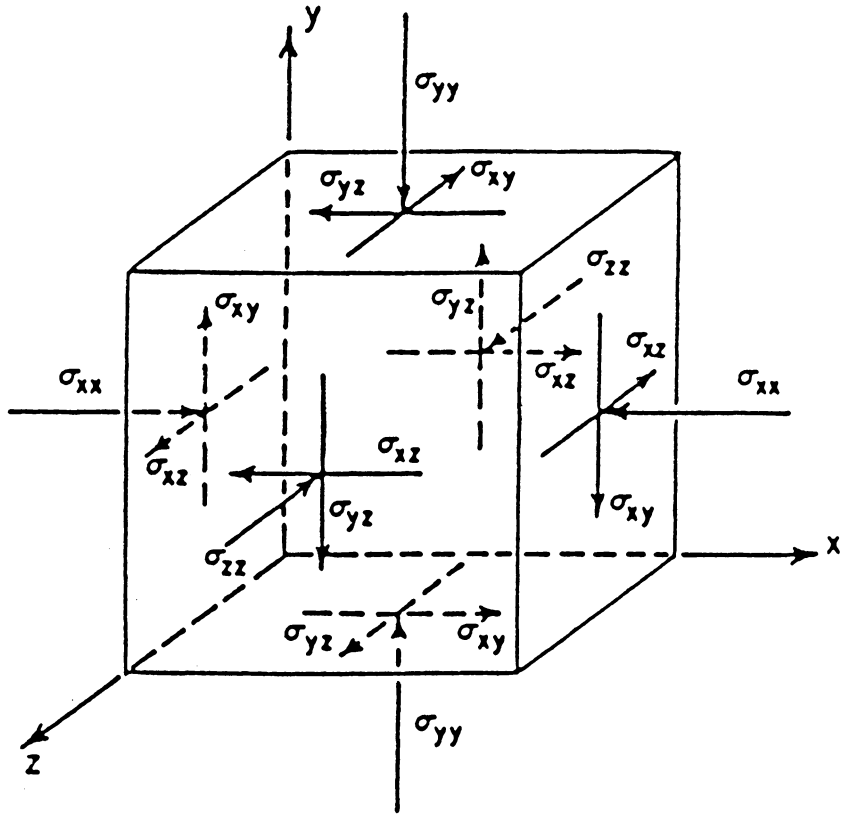


Figure 2.1 Sign convention for stress, compression positive (Desai and Christian, 1977)

$$\sigma_{xy} = 2G\,\varepsilon_{xy} = G\,\gamma_{xy} \tag{2.3}$$

where G is the shear modulus.

Stresses and strains can also be related with the use of Lamme's constants:

$$\varepsilon_{vol} = \varepsilon_{xx} + \varepsilon_{yy} + \varepsilon_{zz} \tag{2.4}$$

$$\sigma_{xx} = \lambda\,\varepsilon_{vol} + 2\mu\,\varepsilon_{xx} \tag{2.5}$$

(and similarly for $\sigma_{yy}$ and $\sigma_{zz}$)

$$\sigma_{xy} = 2\mu\,\varepsilon_{xy} \tag{2.6}$$

(and similarly for the other shears)

$$G = \mu = \frac{E}{2(1+\nu)} \tag{2.7}$$

$$\lambda = \frac{\nu E}{(1+\nu)\,(1-2\nu)} \tag{2.8}$$

For a propagating wave, the equilibrium equations, for a three dimensional case are:

$$\begin{aligned}
&\frac{\partial\sigma_{xx}}{\partial x} + \frac{\partial\sigma_{xy}}{\partial y} + \frac{\partial\sigma_{xz}}{\partial z} = \rho\,\frac{\partial^2 u_x}{\partial t^2} = \rho\ddot{u}_x \\
&\frac{\partial\sigma_{xy}}{\partial x} + \frac{\partial\sigma_{yy}}{\partial y} + \frac{\partial\sigma_{yz}}{\partial z} = \rho\,\frac{\partial^2 u_y}{\partial t^2} = \rho\ddot{u}_y \\
&\frac{\partial\sigma_{xz}}{\partial x} + \frac{\partial\sigma_{yz}}{\partial y} + \frac{\partial\sigma_{zz}}{\partial z} = \rho\,\frac{\partial^2 u_z}{\partial t^2} = \rho\ddot{u}_z
\end{aligned} \tag{2.9}$$

where $u_x$, $u_y$, $u_z$ are the displacements on the x, y, z axes respectively.

If $\{\Omega\}$ is a rotation vector with components $\Omega_x$, $\Omega_y$, $\Omega_z$ the result is:

$$\Omega_x = \frac{1}{2}\left(\frac{\partial u_z}{\partial y} - \frac{\partial u_y}{\partial z}\right)$$

$$\Omega_y = \frac{1}{2}\left(\frac{\partial u_x}{\partial z} - \frac{\partial u_z}{\partial x}\right) \qquad (2.10)$$

$$\Omega_z = \frac{1}{2}\left(\frac{\partial u_y}{\partial x} - \frac{\partial u_x}{\partial y}\right)$$

and by substituting from the relation of the elastic model, the result is:

$$(\lambda + 2\mu)\,\nabla^2\,\varepsilon_{vol} = \rho^2\,\frac{\partial^2 \varepsilon_{vol}}{\partial t^2}$$

$$\mu\nabla^2\Omega_x = \rho\,\frac{\partial^2\Omega_x}{\partial t^2} \qquad (2.11)$$

$$\mu\nabla^2\Omega_y = \rho\,\frac{\partial^2\Omega_y}{\partial t^2}$$

$$\mu\nabla^2\Omega_z = \rho\,\frac{\partial^2\Omega_z}{\partial z^2}$$

with the condition

$$\frac{\partial\Omega_x}{\partial x} + \frac{\partial\Omega_y}{\partial y} + \frac{\partial\Omega_z}{\partial z} = 0$$

where: $\dfrac{\lambda + 2\mu}{\rho} = V_p^2$

$$\frac{\mu}{\rho} = V_s^2$$

and $V_p$, $V_s$ are the velocities of propagation of the compressive and shear wave respectively.

By substituting for E, $\nu$ the result is:

$$E = V_s^2 \rho \frac{3(V_p/V_s)^2 - 4}{(V_p/V_s)^2 - 1}$$

$$\nu = \frac{1}{2} \cdot \frac{(V_p/V_s)^2 - 2}{(V_p/V_s)^2 - 1} \qquad (2.12)$$

So far it has been shown that there is a relation between E and $\nu$, the most significant mechanical properties in rock engineering, and $V_p$ and $V_s$. Other important parameters are the degree of fracturing, the number of joints, the surface characteristics of the fractures, and the filling materials. Assuming a homogeneous model, with n the number of similar joints. For n = 0, the travel time of a pulse would be:

$$t = \frac{L}{V}$$

where L is the traveled length and V is the propagating velocity. For n joints:

$$t_n = \frac{L}{V} + n\, t_c$$

where $t_c$ is the travel time through a joint. Assuming that the width of a joint is insignificant, compared to the total length:

$$L = L + n\, L_c$$

where $L_c$ is the width of a joint. Then:

$$V_n = \frac{L}{(L/V + n\, t_c)}$$

where $V_n$ is the average velocity through a rock mass with n joints. Solving for $\frac{n}{L}$ we get:

$$\frac{n}{L} = \frac{1}{t_c} \cdot \frac{1}{V_n} - \frac{1}{t_c V} = A \cdot \frac{1}{V_n} - B \qquad (2.13)$$

Relation (13) implies that we can use $V_p$ or $V_s$ as an index of the spacing and characteristics cracks and joints.

2.2.2. The Viscoelastic Model

Since rocks rarely behave like perfect elastic materials, other models have also been used to describe the mechanical behavior of rock materials. For wave propagation Roussel (1968) used a viscoelastic model, to adapt the experimental results given by Schneider (1967) with the "Petite-Sismique" method (Chapter 4).

Let us assume the Kelvin-Voight viscoelastic model on Figure 2. The equilibrium equation for an oscillating system would be

$$m \frac{d^2x}{dt^2} + \eta \frac{dx}{dt} + Ex = 0 \qquad (2.14)$$

where m: mass

$\eta$: viscosity coefficient

E: elastic constant of the spring

For a forced vibration, a simplified expression of the force generated by a hammer blow is given as follows:

$$P(t) = P_o e^{-at} \cos \omega t \qquad (2.15)$$

where a is the time attenuation constant. Equation (2.14) takes the form:

$$m \frac{d^2x}{dt^2} + \eta \frac{dx}{dt} + Ex = P_o e^{-at} \cos \omega t \qquad (2.16)$$

The stress-strain relationships for the viscoelastic isotropic medium are given by the equation:

$$\sigma_{ij} = \lambda\ \varepsilon_{vol} + 2\mu\ \varepsilon_{ij} + \lambda' \frac{d\varepsilon_{vol}}{dt}\ \sigma_{ij} + 2\mu' \frac{d\varepsilon_{ij}}{dt} \qquad (2.17)$$

where: $\lambda$, $\mu$: Lame's constants

$\lambda'$, $\mu'$: constants

$\sigma_{ij}$: Kronecker's $\sigma$

Assuming an elementary volume dV, with a mass of $\rho dV$, being displaced by $U_x$, parallel to axis x, under the force $dF_x$, the equation is:

$$\left(\frac{\partial \sigma_{xx}}{\partial x} + \frac{\partial \sigma_{xy}}{\partial y} \quad \frac{\partial \sigma_{xz}}{\partial z}\right)\ dV = dF_x$$

Its reaction would be $\rho dV \dfrac{\partial^2 u_x}{\partial t^2}$ .

Substituting and taking the derivative of both sides (over time), the equation that describes the propagation of compressional waves is:

$$\frac{\partial^2\ \varepsilon_{vol}}{\partial t^2} = \frac{\lambda + 2\mu}{\rho}\ \nabla^2\ \varepsilon_{vol} + \frac{\lambda' + 2\mu'}{\rho} \cdot \frac{\partial(\nabla^2 \varepsilon_{vol})}{\partial t} \qquad (2.18)$$

Substituting and taking the curl of both sides, the equation describing the propagation of shear waves is:

$$\frac{\partial^2\ W_i}{\partial t^2} = \frac{\mu}{\rho}\ \nabla^2\ W_i + \frac{\mu'}{\rho} \cdot \frac{\partial(\nabla^2\ W_i)}{\partial t} \qquad (2.19)$$

where: $W_i$ = curl $u_i$

It can be shown that Equations (2.18) and (2.19) can be written as follows:

$$\nabla^2\ \varepsilon_{vol} + \frac{\rho\eta}{\lambda + 2\mu} \cdot \frac{\partial(\nabla^2 \varepsilon_{vol})}{\partial t} - \frac{\rho}{\lambda + 2\mu} \cdot \frac{\partial^2 \varepsilon_{vol}}{\partial t^2} = 0 \qquad (2.20)$$

$$\nabla^2 W + \frac{\rho\eta}{\mu} \cdot \frac{\partial(\nabla^2 W)}{\partial t} - \frac{\rho}{\mu} \cdot \frac{\partial^2 W}{\partial t^2} = 0 \qquad (2.21)$$

In the case of plane waves, Equation (2.20) can be simplified as follows:

$$(\lambda + 2\mu) \frac{\partial^2 u}{\partial x^2} + \rho\eta \frac{\partial^3 u}{\partial x^2 \partial t} - \rho \frac{\partial^2 u}{\partial t^2} = 0 \qquad (2.22)$$

To explain the results presented by the "Petite Sismique" method a solution of Equation (2.22) should describe a vibration that attenuates exponentially with the distance, i.e.:

$$u = u_o \, e^{-bx} \, e^{-i\omega(t-x/c)} \qquad (2.23)$$

where b is the attenuation coefficient and c is the wave velocity. Substituting u in (2.22) gives:

$$(-b - i\omega/c)^2 \, u + A \, i\omega(-b - i\omega/c)^2 \, u - B(i\omega)^2 \, u = 0 \qquad (2.24)$$

where: $A = \frac{\rho\eta}{\lambda + 2\mu}$

$$B = \frac{\rho}{\lambda + 2\mu}$$

From (2.24), separating the real and imaginary parts gives the system:

real: $b^2 - \omega^2/c^2 - 2A \, \omega^2 \, b/c + B\omega^2 = 0$

imaginary: $2b \, \omega/c + A \, b^2 \, \omega - A\omega^3/c^2 = 0$

Finally, $\lambda + 2\mu$ is calculated:

$$\lambda + 2\mu = \rho \, c^2 \, \omega^2 \, \frac{\omega^2 - b^2 \, c^2}{\omega^2 + b^2}$$

By assuming that c is frequency independent the result is, from the theory of elasticity

$$\rho\, c^2 = \lambda + 2\mu = E_d \frac{1 - \nu_d}{(1 + \nu_d)(1 - 2\nu_d)} = E_d \cdot K_d$$

and finally:

$$\frac{E_s \cdot K_s}{E_s \quad K_d} = \frac{\omega^2 - b^2 c^2}{(\omega^2 + b^2 c^2)^2} \quad \omega^2 \tag{2.25}$$

By introducing $\lambda = \frac{2\pi c}{\omega}$, the result is:

$$\frac{E_d (1 + \nu_s)}{E_s (1 + \nu_d)} = \frac{1}{4\pi^2} \frac{(4\pi^2 + b^2 \lambda^2)}{(4\pi^2 - b^2 \lambda^2)}$$

where:

$E_d$, $\nu_d$: as defined in Equation (2.12)

$E_s$, $\nu_s$: the values of the static modulus of elasticity and Poisson's ratio.

$\lambda$: the wavelength

2.2.3. The Potential of Wave Propagation for Rock Classification

It has been shown that, according to theoretical analysis, the measurement of wave propagation parameters can be used for estimating static engineering properties of rocks. However, the static parameters, calculated from dynamic properties, may deviate from the actual values.

Using the theoretical relation, as well as experimental data and information obtained from literature, this research will attempt to determine the most appropriate dynamic properties for engineering rock purposes. Since the Young's Modulus, the compressive strength and the

spacing and nature of joints are the most important parameters of rock competency and behavior for engineering rock classification, it is important to correlate these parameters with dynamic properties which are easy to measure. In this case, it might be possible to develop experimental relations of the form:

$$E_{stat} = A \cdot E_{dyn} + B$$

where $E_{stat}$: Modulus of Elasticity or Deformation

$E_{dyn}$: calculated from (12)

A, B: coefficients, from experimental data

$$E_{stat} = A\, V_p^{\,2} + B$$

$$E_{stat} = A\, V_s^{\,2} + B \quad \text{etc.}$$

$$n/L = (\text{number of cracks per foot}) = A \frac{1}{V_n} - B$$

$$n/L = A - B \cdot V_n$$

# CHAPTER III

# ENGINEERING CLASSIFICATION OF ROCKS

## 3.1. The Purpose of Rock Testing and Classifications

The successful design, construction and operation of structures in rock requires a knowledge of the mechanical behavior of the rock in-situ. Therefore, an investigation of the properties determining the engineering rock quality is required. Such an investigation will produce a number of parameters, including compressive strength, tensile strength, modulus of elasticity or deformation, creep rate, anisotropy, water flow, in-situ stress, drillability, degree of jointing, filling material type, etc. In order to implement these parameters, they must be compared with data obtained from case studies, in order to predict the behavior of the rock and its response under stress.

Engineering rock classification systems are based on data determined from laboratory and field tests and which are used to classify and describe rock material or rock mass in a way that is useful and meaningful for the design of structures.

Bieniawski (1973) set the purposes and requirements of a rock mass classification system as follows:

(i) divide a rock mass into groups of similar behavior;

(ii) provide a good basis for understanding the characteristics of a rock mass;

(iii) facilitate the planning and design of structures in rock by yielding quantitative data for the solution of real engineer-

ing problems; and

(iv) provide a common basis for effective communication among all persons concerned with a geomechanics problem.

In order to fulfill this purpose, a classification system should be simple and meaningful and must be based on measurable parameters which can be easily determined.

Although Bieniawski mentions the above purposes and requirements for the classification of rock mass or discontinuous rocks, such criteria could also be considered for the classification of rock material (intact rocks).

## 3.2. Methods of Engineering Rock Classification

Engineering Rock Classification systems may refer to rock material or rock mass or both. Goodman (1976) has tabulated the major rock classification methods, specifying their object (rock material or rock mass) and application (Table 3.1). A representative selection of these methods, the parameters they incorporate and the final designation of rock quality by numerical values or categories are described below.

### 3.2.1. Intact Rock Classification (Deere and Miller, 1966)

This system classifies intact rock and takes into consideration the compressive strength ($C_o$) and the modulus of elasticity. Five classes (A through E) of compressive strength are defined, following a geometric progression. Class E includes weak samples, with $C_o$ less than 4,000 psi, and Class A includes very strong samples, with $C_o$ more than 32,000 psi. The second parameter taken into consideration is the

Table 3.1

References to Some Engineering Classification Systems for Rock

(Goodman, 1976)

| Object | For General Purpose | For a Special Purpose |
|---|---|---|
| Rock Material | Coates (1964) | Bergh-Christensen and Selmer-Olsen (1970) - resistance to blasting |
| | Coates and Parson (1966) | |
| | Deere and Miller (1966) and Deere et al. (1967) | Selmer-Olsen and Blindheim (1970) - drillability |
| | Underwood (1967) - shales | |
| Rock Mass | John (1962) | Terzaghi (1946) - tunnels |
| | Onodera (1970) | Lauffer (1958) - tunnels |
| | Iada et al. (1970) | Bieniawski (1974) - tunnels |
| | Muller and Hoffman (1970) | Barton et al. (1975) - tunnels |
| | Franklin et al. (1971)* | Kruse et al. (1969) - tunnel liner design |
| | | Ege (1968) - tunnels in granitic rocks |
| | | Obert and Duvall (1967) - mining |
| | | Goodman and Duncan (1971) - rock slopes |
| | | Caterpillar Tractor Co. (1966) - rippability |

* Best applied to rippability classification.

Modulus Ratio, which is defined as the ratio of Modulus of Elasticity/ Uniaxial Compressive Strength for the same rock. Rock material is classified into three categories, i.e., high (H), average or low (L), regarding this ratio. Finally a rock will be classified as B, BH, AL, etc. Table 3.2 gives the ranges for the values of $C_o$ and the Modulus Ratio for rock classification.

3.2.2. Franklin's Rock Quality Classification (Franklin et al., 1971)

This system classifies rock mass by taking into consideration an index for discontinuities in the rock mass as well as the strength of the rock material.

The compressive strength of the rock material can be determined either by a uniaxial compressive test or by the point load index ($I_s$). As an index for fractures or discontinuities, the "Fracture Spacing Index" ($I_f$) is used. It is defined as "the average size of cored material within a recognizable geological unit." Fractures which result from drilling are not to be included. A graph, of $I_s$ versus $I_f$, with logarithmic scales, is used to determine the class of a given rock mass and assign it a general quality characterization, such as EH (Extremely High), VH (Very High), etc. (Figure 3.1.a).

Figure 3.1.b can be used when the fracture spacing is of no importance (e.g., for the production of crushed stone). Alternatively, another parameter can be considered, such as a durability or an anisotropy index.

In Figure 3.1.c another proposed classification is illustrated for application to rock excavation. The parameters used for the general-

Table 3.2

Engineering Classification for Intact Rock

(Deere and Miller, 1966)

I. On Basis of Strength

| Class | Description | Uniaxial Compressive Strength, $lb/in^2$ |
|---|---|---|
| A | Very High Strength | Over 32,000 |
| B | High Strength | 16,000-32,000 |
| C | Medium Strength | 8,000-16,000 |
| D | Low Strength | 4,000- 8,000 |
| E | Very Low Strength | Less than 4,000 |

II. On Basis of Modulus Ratio

| Class | Description | Modulus Ratio[1] |
|---|---|---|
| H | High Modulus Ratio | Over 500 |
| - | Average Modulus Ratio | 200-500 |
| L | Low Modulus Ratio | Less than 200 |

Classify rock as B, BH, BL, etc.

1) Modulus Ratio = $E_t/\sigma_a$(ult.)

where $E_t$ = tangent modulus at 50% ultimate strength;

$\sigma_a$ = uniaxial compressive strength

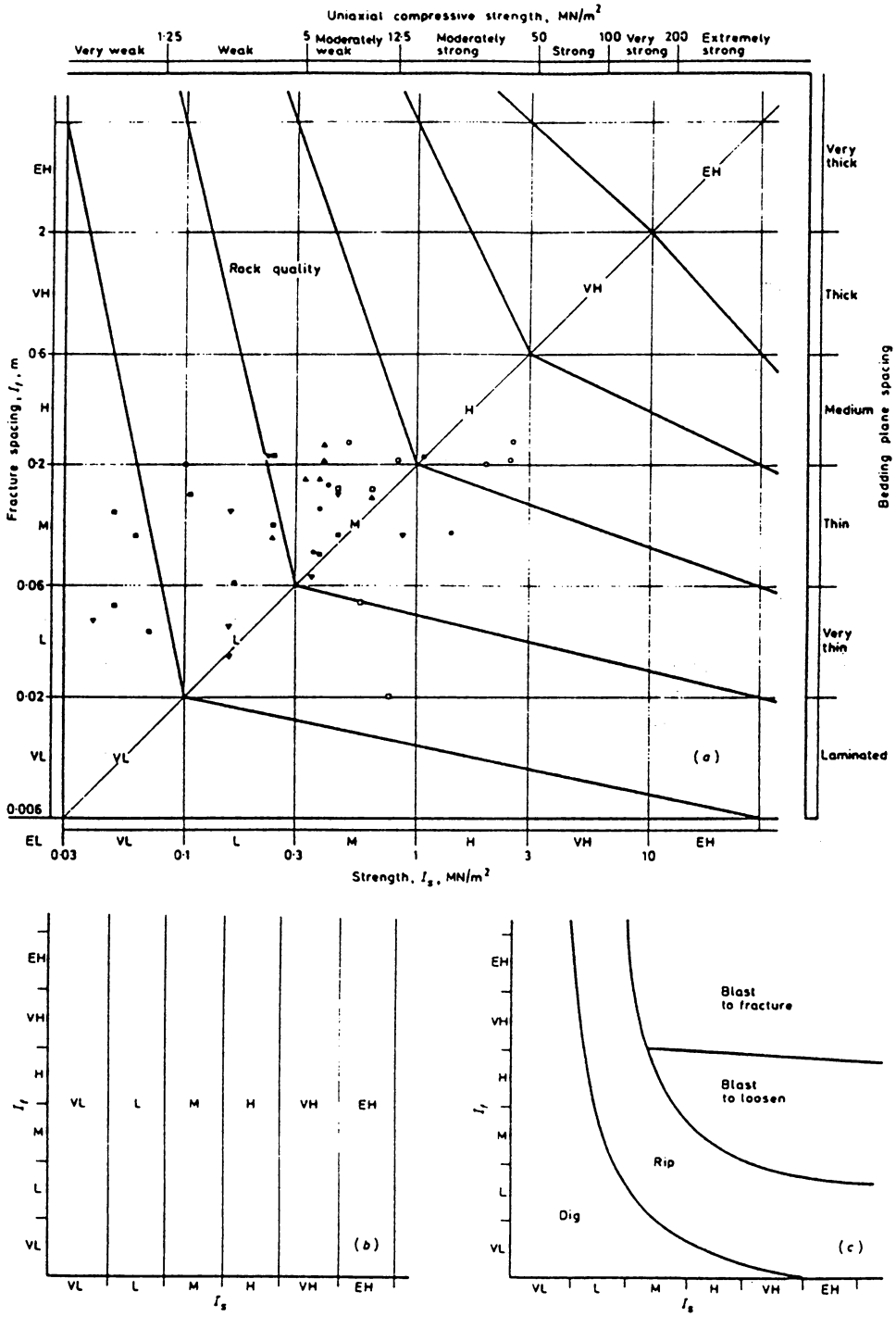


Figure 3.1 Rock quality classification diagrams. (a) general purpose classification, (b) and (c) alternative methods (Franklin et al. 1971)

purpose classification on Figure 3.1.a are used, i.e. an index of strength and an index of discontinuities.

3.2.3. Rock Quality Designation (RQD) (Deere et al., 1967)

This is a quantitative index used as an indication of the quality and probable engineering behavior of a rock mass. It is determined during core recovery. Barrels of NX or larger size must be used. RQD is defined as the total length of core pieces longer than 4 inches over the total drill run, i.e.:

$$\text{RQD } (\%) = 100 \frac{\text{Length of cores in pieces 4 inches or longer}}{\text{Length of borehole}}$$

Five rock quality classes were defined, depending on the RQD value, ranging from "very poor" to "very good", i.e. for RQD<25% rock quality is "very poor", 25%<RQD<50% rock quality is "poor" and so on.

It has been shown that a linear correlation exists between fracture frequency and RQD.

3.2.4. Rock Mass Quality (Q) (Barton et al., 1975)

This system is based on numerous case studies and correlates the amount and type of permanent support required for an underground opening depending on its Rock Mass Quality.

Rock Mass Quality (Q) is a numerical index of rock quality and incorporates six parameters referring to joint spacing and characteristics.

$$Q = \frac{RQD}{J_n} \cdot \frac{J_r}{J_a} \cdot \frac{J_w}{SRF}$$

where:

RQD: as mentioned in 3.2.3.

$J_r$, $J_w$, $J_n$, $J_a$, SRF: from Table 3.3.

Q is used in order to estimate the maximum safe span for an unsupported underground opening or to determine the required support method (by using a graph and a table).

$$D = 2.1\ (Q)^{0.387}$$

where D is the maximum safe unsupported span (in meters). Q ranges between 0.001 for extremely poor rock and 1,000 for exceptionally good quality rock.

3.2.5. The Geomechanics Classification (Bieniawski, 1973)

Bieniawski developed a classification system similar to that of Barton. The main difference is that the Geomechanics Classification takes into consideration the strength of the intact rock. The following parameters are used:

(i) Rock Quality Designation (RQD);

(ii) uniaxial compressive strength of intact rock;

(iii) spacing of joints or bedding;

(iv) strike and dip orientations;

(v) continuity of joints; and

(vi) ground water inflow.

With regard to each of these parameters the rock mass is classified into five categories (Tables 3.4 and 3.5). The sum of these values, for all eight parameters, is used to find the class of the rock mass which given an estimation of the average standup time of an

Table 3.3

Values of the Parameters
in Barton, Lien, and Lunde's Classification

(Goodman, 1976)

| A. Number of sets of discontinuities | Jn |
|---|---|
| massive | 0.5 |
| one set | 2.0 |
| two sets | 4.0 |
| three sets | 9.0 |
| four or more sets | 15.0 |
| crushed rock | 20.0 |

| B. Roughness of discontinuities | Jr* |
|---|---|
| non-continuous joints | 4.0 |
| rough, wavy | 3.0 |
| smooth, wavy | 2.0 |
| rough, planar | 1.5 |
| smooth, planar | 1.0 |
| slick, planar | 0.5 |
| "filled" discontinuities | 1.0 |

* add 1.0 if mean joint spacing exceeds 3 meters

| C. Filling and wall rock alteration | Ja |
|---|---|
| a) essentially unfilled | |
| healed | 0.75 |
| staining only; no alteration | 1.0 |
| silty or sandy coatings | 3.0 |
| clay coatings | 4.0 |
| b) filled | |
| sand or crushed rock filling | 4.0 |
| stiff clay filling <5 mm thick | 6.0 |
| soft clay filling <5 mm thick | 8.0 |
| swelling clay filling <5 mm thick | 12.0 |
| stiff clay filling >5 mm thick | 10.0 |
| soft clay filling >5 mm thick | 15.0 |
| swelling clay filling >5 mm thick | 20.0 |

Table 3.3 (continued)

| D. Water conditions | Jw |
|---|---|
| dry | 1.0 |
| medium water inflow | 0.66 |
| large inflow with unfilled joints | 0.5 |
| large inflow with filled joints which wash out | 0.33 |
| high transient inflow | 0.2 - 0.1 |
| high continuous inflow | 0.1 - 0.05 |

| E. Stress reduction class | SRF* |
|---|---|
| loose rock with clay-filled discontinuities | 10.0 |
| loose rock with open discontinuities | 5.0 |
| rock at shallow depth (<50 m) with clay-filled discontinuities | 2.5 |
| rock with tight, unfilled discontinuities under medium stress | 1.0 |

* Barton et al. also define SRF values corresponding to degrees of bursting, squeezing, and swelling rock conditions.

unsupported span (Table 3.4) or alternative support systems.

## 3.3. Comparison of the Classification Methods

An engineering classification system should take into consideration the properties of the rock material and the discontinuities of the rock mass.

The classification of rock material (as in sub-section 3.2.1.) does not provide enough information for engineering design purposes unless the rock mass is homogeneous and free of discontinuities, or there is large spacing between discontinuities compared to dimensions of the structure.

Classification systems emphasizing the characteristics of discontinuities (e.g., RQD) give a better understanding of the behavior of a rock mass. However, they need to be complemented by intact rock properties, particularly when the spacing of discontinuities is large with respect to the dimensions of the openings, in order to establish their structural competency.

## Table 3.4

### Geomechanics Classification of Rock Masses (Bieniawski, 1981)

**A. CLASSIFICATION PARAMETERS AND THEIR RATINGS**

| PARAMETER | | | RANGES OF VALUES | | | | | | |
|---|---|---|---|---|---|---|---|---|---|
| 1 | Strength of intact rock material | Point-load strength index | > 10 MPa | 4 - 10 MPa | 2 - 4 MPa | 1 - 2 MPa | For this low range - uniaxial compressive test is preferred | | |
| | | Uniaxial compressive strength | >250 MPa | 100 - 250 MPa | 50 - 100 MPa | 25 - 50 MPa | 5-25 MPa | 1-5 MPa | <1 MPa |
| | Rating | | 15 | 12 | 7 | 4 | 2 | 1 | 0 |
| 2 | Drill core quality RQD | | 90% - 100% | 75% - 90% | 50% - 75% | 25% - 50% | < 25% | | |
| | Rating | | 20 | 17 | 13 | 8 | 3 | | |
| 3 | Spacing of discontinuities | | >2 m | 0,6 - 2 m | 200 - 600 mm | 60 -200 mm | <60 mm | | |
| | Rating | | 20 | 15 | 10 | 8 | 5 | | |
| 4 | Condition of discontinuities | | Very rough surfaces. Not continuous No seperation Unweathered wall rock. | Slightly rough surfaces. Separation < 1 mm Slightly weathered walls | Slightly rough surfaces. Separation < 1 mm Highly weathered walls | Slickensided surfaces OR Gouge < 5 mm thick OR Separation 1-5 mm. Continuous | Soft gouge > 5 mm thick OR Separation > 5 mm. Continous | | |
| | Rating | | 30 | 25 | 20 | 10 | 0 | | |
| 5 | Ground water | Inflow per 10 m tunnel length | None | < 10 litres/min | 10-25 litres/min | 25 - 125 litres/min | > 125 | | |
| | | Ratio joint water pressure / major principal stress | 0 | 0,0-0,1 | 0,1-0,2 | 0,2-0,5 | > 0,5 | | |
| | | General conditions | Completely dry | Damp | Wet | Dripping | Flowing | | |
| | Rating | | 15 | 10 | 7 | 4 | 0 | | |

**B. RATING ADJUSTMENT FOR JOINT ORIENTATIONS**

| Strike and dip orientations of joints | | Very favourable | Favourable | Fair | Unfavourable | Very unfavourable |
|---|---|---|---|---|---|---|
| Ratings | Tunnels | 0 | -2 | -5 | -10 | -12 |
| | Foundations | 0 | -2 | -7 | -15 | -25 |
| | Slopes | 0 | -5 | -25 | -50 | -60 |

Table 3.4 (continued)

Geomechanics Classification of Rock Masses (Bieniawski, 1981)

C. ROCK MASS CLASSES DETERMINED FROM TOTAL RATINGS

| Rating | 100←81 | 80←61 | 60←41 | 40←21 | < 20 |
|---|---|---|---|---|---|
| Class No. | I | II | III | IV | V |
| Description | Very good rock | Good rock | Fair rock | Poor rock | Very poor rock |

D. MEANING OF ROCK MASS CLASSES

| Class No | I | II | III | IV | V |
|---|---|---|---|---|---|
| Average stand-up time | 10 years for 15 m span | 6 months for 8 m span | 1 week for 5 m span | 10 hours for 2,5 m span | 30 minutes for 1 m span |
| Cohesion of the rock mass | > 400 kPa | 300 - 400 kPa | 200 - 300 kPa | 100 - 200 kPa | < 100 kPa |
| Friction angle of the rock mass | < 45° | 35° - 45° | 25° - 35° | 15° - 25° | < 15° |

THE EFFECT OF DISCONTINUITY STRIKE AND DIP ORIENTATIONS IN TUNNELLING

| Strike perpendicular to tunnel axis | | | | Strike parallel to tunnel axis | | Dip $0^{o}$ - $20^{o}$ irrespective of strike |
|---|---|---|---|---|---|---|
| Drive with dip | | Drive against dip | | | | |
| Dip $45^{o}$-$90^{o}$ | Dip $20^{o}$-$45^{o}$ | Dip $45^{o}$-$90^{o}$ | Dip $20^{o}$-$45^{o}$ | Dip $45^{o}$-$90^{o}$ | Dip $20^{o}$-$45^{o}$ | |
| Very favourable | Favourable | Fair | Unfavourable | Very unfavourable | Fair | Unfavourable |

## Table 3.5

### Guide to the Selection of Primary Support in Horseshoe-Shaped Tunnels

### (Bieniawski, 1978)

| Rock mass class | Excavation | Primary support | | |
|---|---|---|---|---|
| | | Rockbolts* (length for tunnel of 10 m width) | Shotcrete | Steel sets |
| I | Full face 3 m advance | Generally no support required except for occasional spot bolting | | |
| II | Full face 1,0–1,5 m advance | Locally bolts in crown 2–3 m long, spaced 2–2,5 m with occasional wire mesh. Complete 20 m from face. | 50 mm in crown as basis for waterproof | None |
| III | Top heading and bench 1,5–3 m advances in top heading | Systematic bolts 3–4 m long, spaced 1,5–2 m in crown and walls with wire mesh in crown. Complete 10 m from face. | 50–100 mm in crown and 30 mm in sides | None |
| IV | Top heading and bench 1,0–1,5 m advance in top heading | Systematic bolts 4–5 m long, spaced 1–1,5 m in crown and walls with wire mesh. Complete 10 m from face | 100–150 mm in crown and 100 mm in sides. Support to be installed as excavation proceeds | Occasional light ribs spaced 1,5 m where required |
| V | Multiple drifts 0,5–1 m advance in top heading | Systematic bolts 5–6 m long, spaced 1–1,5 m in crown and walls with wire mesh. Bolt invert. Complete 5 m from face | 150–200 mm in crown, 150 mm in sides and 50 mm on face. Apply shotcrete as soon as possible after blasting | Heavy ribs spaced 0,75 m with steel lagging. Close invert |

* 20 mm diameter, fully resin bonded, length ½ tunnel width

# CHAPTER IV

# THE POTENTIAL OF SONIC METHODS FOR DETERMINING ROCK QUALITY

## 4.1. Advantages of the Sonic Methods

The measurement of parameters pertaining to rock classification requires sample collection, preparation and testing for determining the intact rock properties and extensive field work for identifying the frequency and nature of the discontinuities. The main advantages of using sonic methods for estimating rock quality are:

(i) minimal sample preparation for testing intact rock;

(ii) fast site preparation for field tests;

(iii) require non-destructive testing;

(iv) the tests are reproducible; and

(v) sonic methods can be used for large scale measurements in the field.

With the exception of transducers, a sonic measuring system can be developed from equipment readily available in most laboratories (a frequency generator, amplifiers, an oscilloscope). Samples can be prepared from rock pieces of any shape, with a portable grinding machine. The same grinding machine can also be used for field tests.

Seismic methods, based on the principles of reflection or refraction, are widely used in the exploration of mineral and hydrocarbon deposits.

Sonic methods have also been used to detect structural anomalies and geologic discontinuities in order to facilitate better planning of

mining operations.

## 4.2. Dynamic Properties Used for Estimating Rock Quality in the Laboratory and In-Situ

Sonic wave parameters that can be used for assessing rock material and rock mass quality include wave velocities, frequencies, amplitudes and wavelengths of both compressional and shear waves. Compressional waves are more widely used because they are commonly used for exploration purposes and are also easier to detect.

### 4.2.1. The Application of Wave Velocity

Stacy (1973) conducted a set of laboratory experiments for determining the correlation between wave velocities and the modulus of elasticity, the frequency of joints, the filling material in the joints and the confining stress. The results of the experiments including also work from other researchers are presented in Figures 4.1, 4.2, 4.3, 4.4. The "seismic modulus of elasticity" was defined as previously explained in Equation 2.12. A definite relation between the static and the dynamic modulus was not apparent. When determining the number of joints, it was observed that for a high confining stress wave velocities are not influenced by joint spacing. In general it was shown that wave velocities, of compressional and shear waves, can provide a quantitative index for the frequency of joints and the confining stress for values up to 3 MPa. It was also observed that under wet conditions and with clay in the joints, the degree of jointing had small impact on the compressional wave velocity.

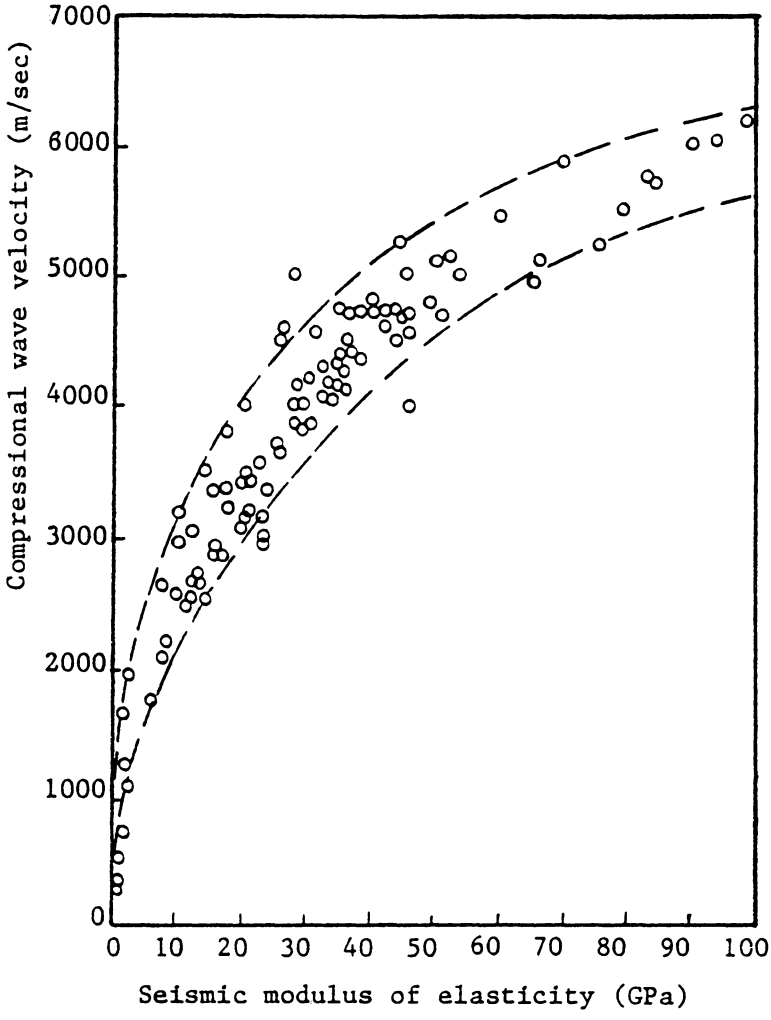


Figure 4.1 Empirical relationship between compressional wave velocity and modulus of elasticity (Stacy,1976)

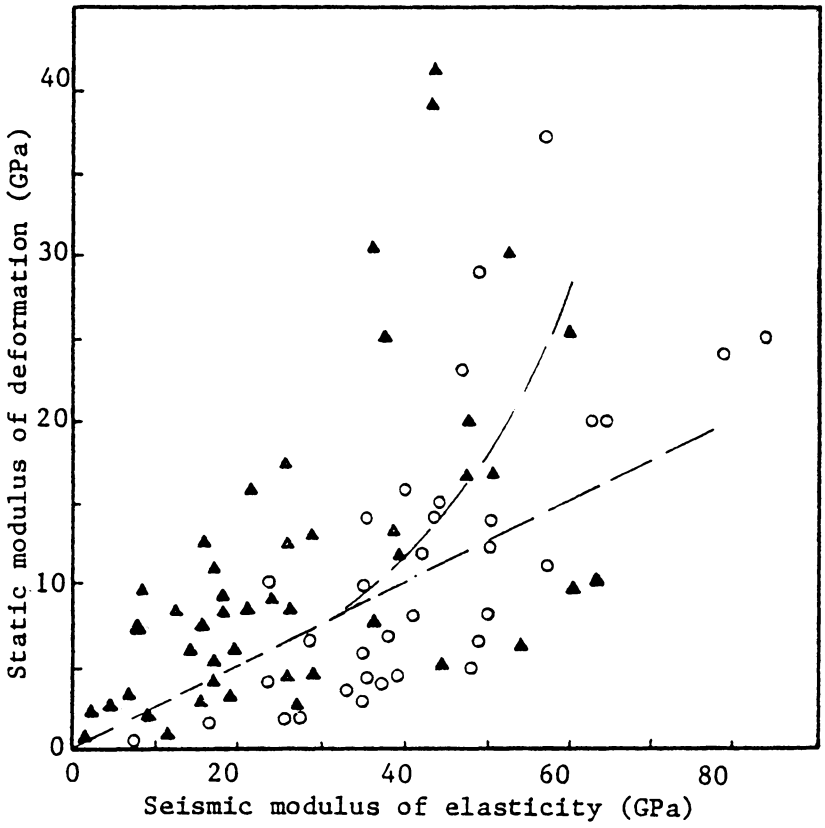


Figure 4.2 Relationship between static modulus of deformation and seismic elastic modulus (Stacy, 1976)

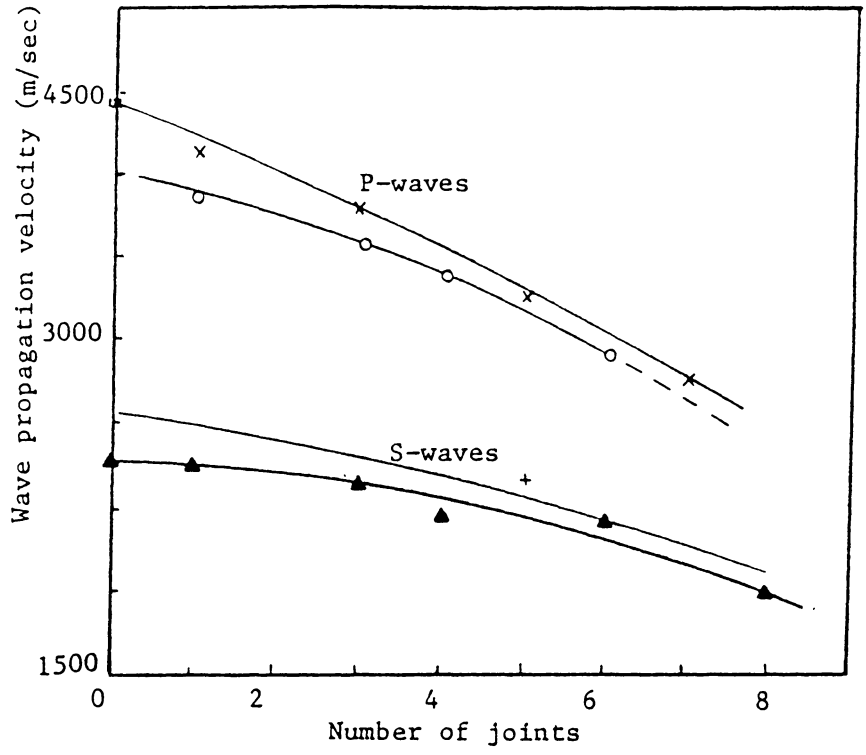


Figure 4.3 Effect of jointing on wave propagation velocity, with zero confining stress (Stacy, 1976)

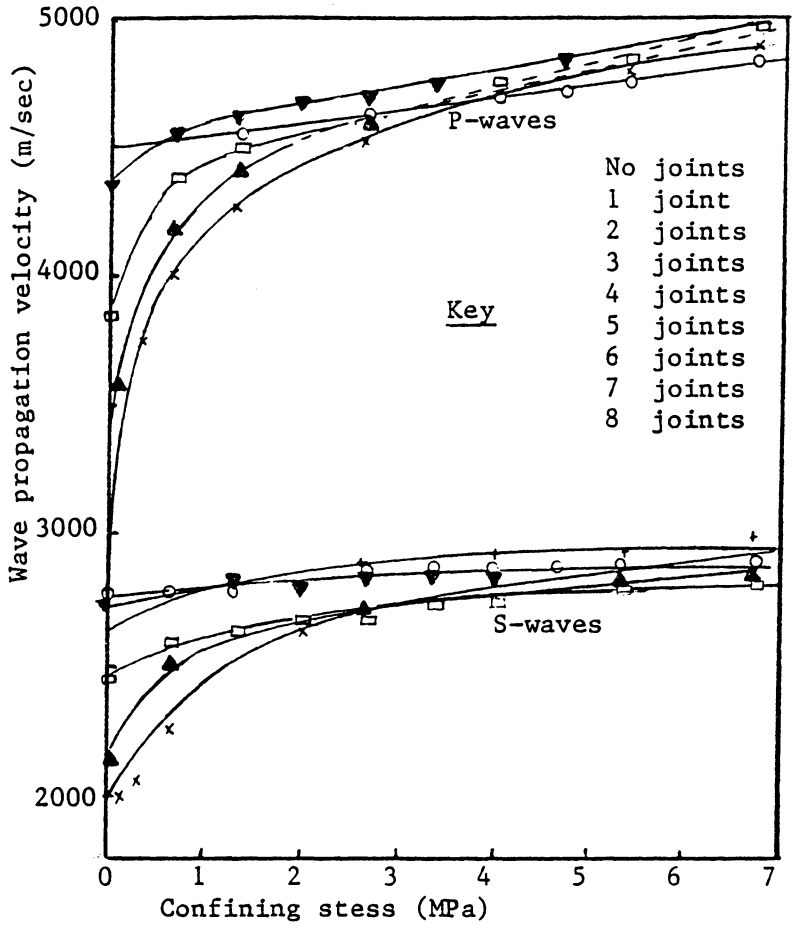


Figure 4.4 Variation of wave velocity with stress (dry conditions) (Stacy, 1976)

Coon and Merritt (1970) correlated RQD with the "velocity index" (Figure 4.5). The velocity index is defined as the square of the ratio of the compressional wave velocity in the field divided by the compressional wave velocity in the laboratory ($[V_F/V_L]^2$). Figure 4.6 shows a comparison of the square root of the velocity index to the Modulus Ratio. The Modulus Ratio is defined as the ratio of the field modulus of deformation over the laboratory modulus of elasticity (at 50% of the compressive strength).

Thill (1982) suggested a correlation between the compressional wave velocity of intact samples and the uniaxial compressive strength (Figure 4.7). The P-wave velocity, measured in the field, is compared to that measured in the laboratory in Figure 4.8. It is suggested that for most sandstones, shales, siltstones and mudstones the wave velocities in the field are higher than the corresponding velocities measured in the laboratory. This could be due to the higher stresses in the field. This condition was reversed for limestones.

Just and Walter (1978) presented a thorough review of applications of sonic waves for assessing rock quality. The following empirical relations were given:

(i) $$K \cdot n((V_{pl} - V_{po})/V_{pl}\, V_{po}) = \frac{1}{V_{pe}} - \frac{1}{V_{pl}}$$

where:

K: constant

n: number of cracks per meter

$V_{pl}$: P-wave velocity in intact rock

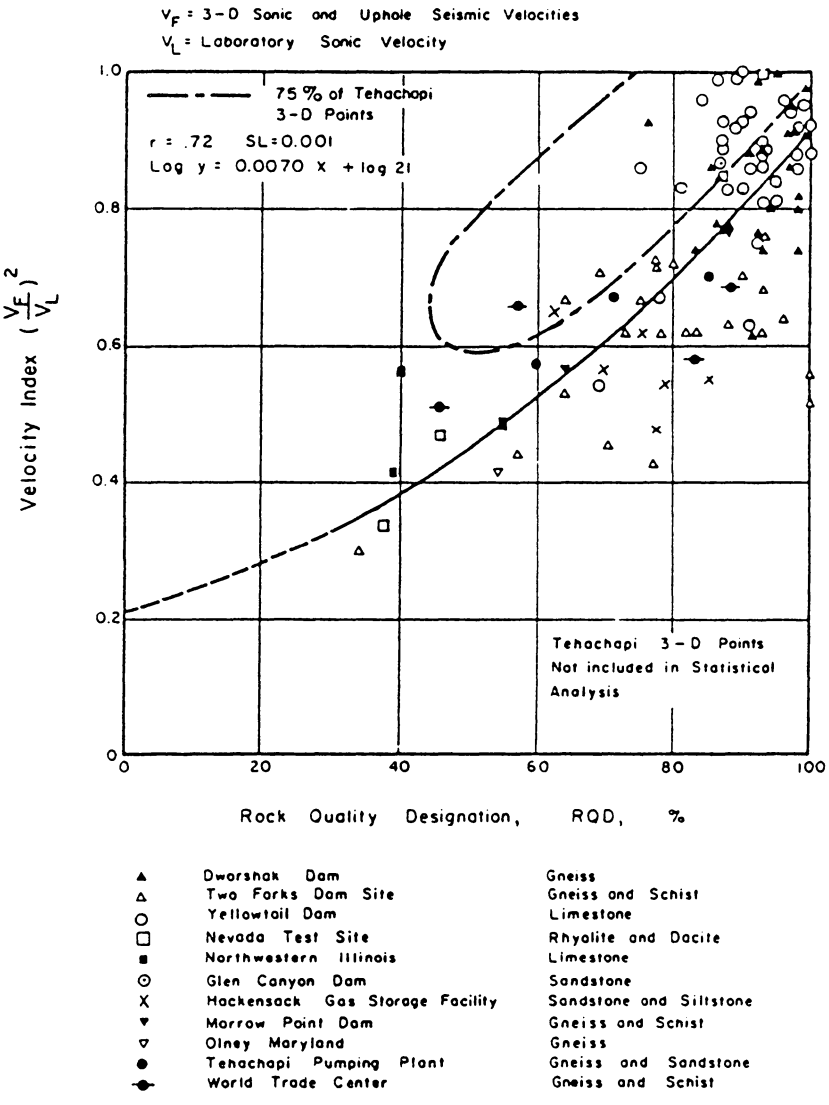


Figure 4.5 Relationship between RQD and Velocity Index (Coon and Merritt 1970)

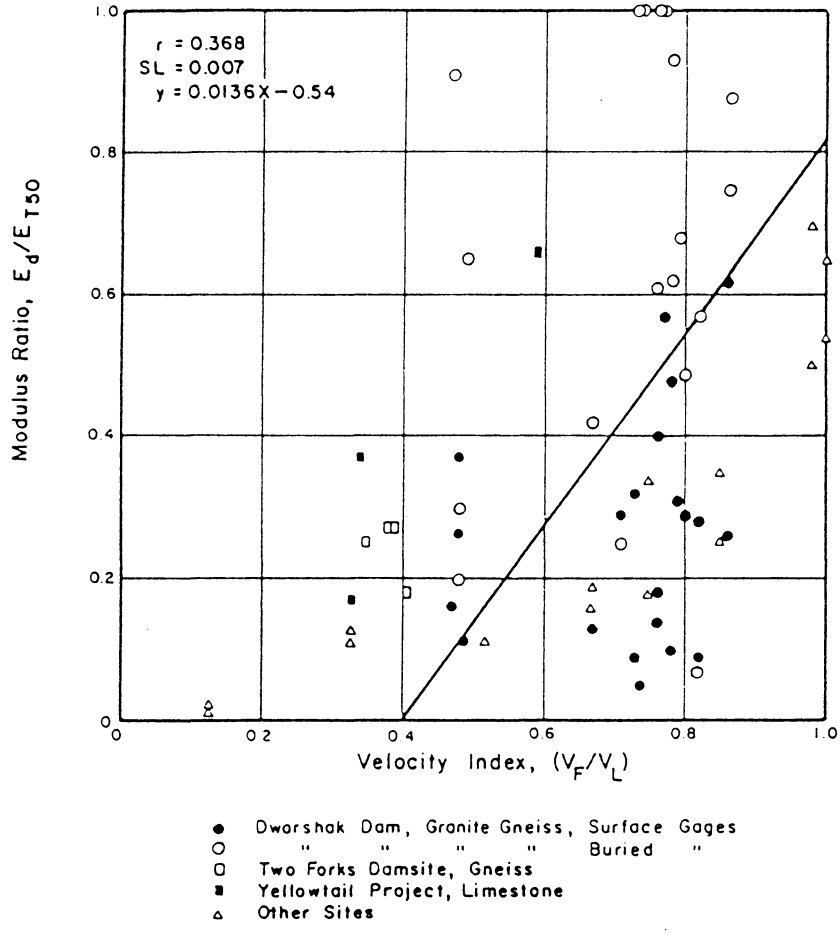


Figure 4.6 Comparison of Velocity Index and the Modulus Ratio $E_d/E_{t50}$ (Coon and Merritt, 1970)

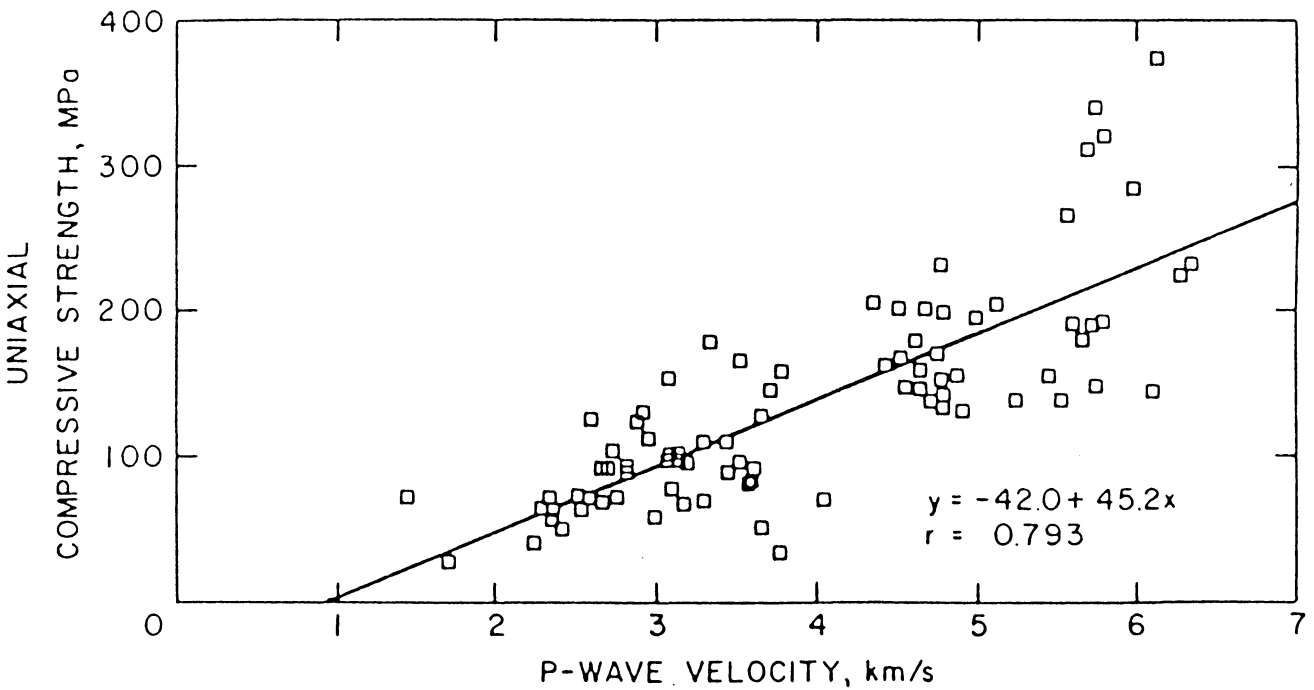


Figure 4.7 Crossplot of uniaxial compressive strength versus P-wave velocity (Thill 1982)

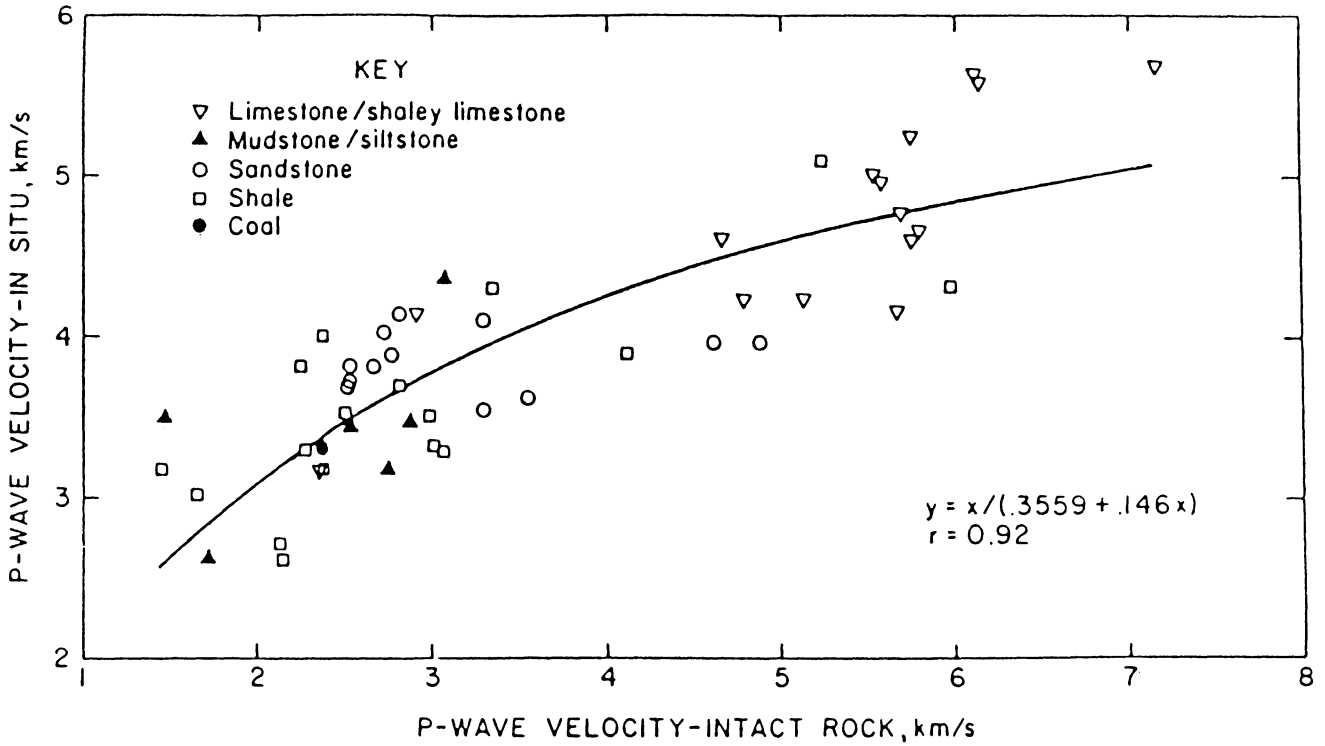


Figure 4.8 Crossplot of in-situ versus intact P-wave velocity (Thill 1982)

$V_{po}$: P-wave velocity in heavily fractured rock

$V_{pe}$: the measured P-wave velocity in a particular zone

(after Helfrich et al. 1970).

(ii) $n = V_m (V_{pl} - V_{pe})/[V_{pl}(V_{pe} - V_m)]$

for frequencies in the ultrasonic frequency range,

where:

$n$, $V_{pl}$, $V_{pe}$ as in (i)

$V_m$: P-wave velocity in the filling material. (After Lycoshin et al. 1970).

(iii) $n = V_m^2 \rho_2 (V_{pl}^2 \rho_1 - V_{pe}^2 \rho)/[V_{pl}^2 \rho_1 \rho(V_{pl}^2 \rho - V_m^2 \rho_2)]$

for seismic frequencies, where:

$n$, $V_m$, $V_{pl}$, $V_{pe}$: as in (i) and (ii)

$\rho$, $\rho_1$, $\rho_2$: the density of fractured rock, solid rock and joint filling material respectively. (After Lycoshin et al. 1970).

4.2.2. Wave Attenuation

A sonic wave radiates spherically from its source and the energy transmitted per unit area is reduced according to the inverse of the square of the distance. For a medium which is not perfectly elastic, energy is absorbed in its imperfection. For a sinusoidal wave, the attenuation process can be described by a quality factor Q as shown:

$$Q = 2\pi \left(\frac{\Delta E}{E}\right)^{-1}$$

where: $\Delta E$: the energy lost per cycle

$E$: the initial energy

(McKenzie et al. 1982).

The amplitude attenuation is described by the equation:

$$A = (A_o/r)e^{-\alpha(r-1)}$$

where: $A$: the amplitude at distance r from the source

$A_o$: the amplitude at unit distance from the source

$\alpha$: given by the following equation:

$$\alpha = \frac{\pi f}{QV}$$

where: $f$: the frequency

$V$: the wave velocity

(Jaeger and Cook, 1969)

Thus, if Q and V are frequency independent, the higher frequency waves will attenuate faster. In the previously mentioned equations, describing wave attenuation, all constants have to be determined experimentally.

Experiments have yielded encouraging results for the potential of wave amplitudes as means of assessing discontinuities. Stephenson (1978) observed that shear waves tend to be scattered by inhomogeneities (for example, aggregate particles) to a greater degree than compressional waves.

Stacy (1976) shows that the amplitude of compressional waves is sensitive to the degree of jointing, even under considerable confining stress. The tests were conducted with laboratory samples and with

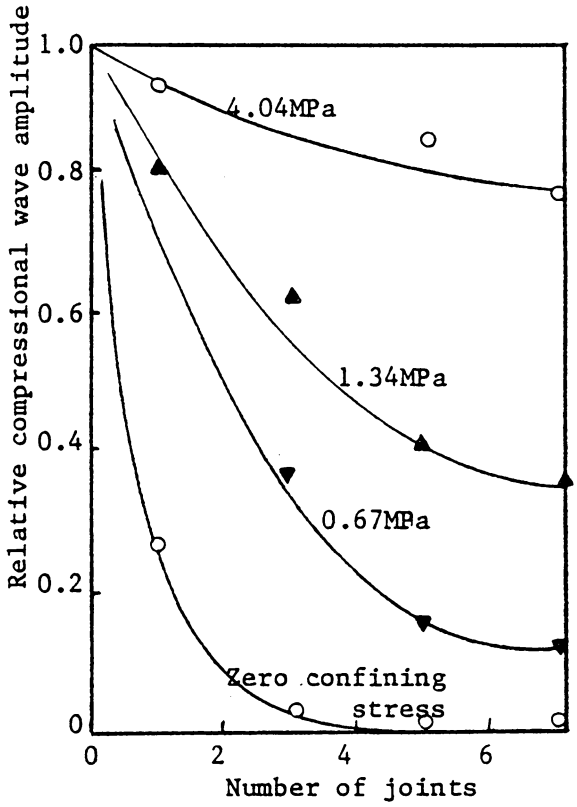


Figure 4.9 Relationship between compressional wave amplitude and number of joints (Stacy, 1976)

various conditions of joints: dry, wet and filled with mud as a filling material (Figure 4.9).

4.2.3. The Application of Wave Frequency or Wavelength

According to the theory of elasticity, wave frequency should be insensitive to rock mass characteristics. However, the equations describing wave attenuation in Section 4.2.2. suggest that attenuation depends on wave frequency, in the sense that when a waveform consisting of numerous frequencies is generated, the dominant frequency of the receiver will depend on rock quality (Q) as well as the distance.

Stacy (1976) observed that the number of joints and filling material have an effect on the frequency of shear waves, for a confining stress less than 2.5 MPa (Figure 4.10 and Figure 4.11).

Schneider (1967) observed a straight line relationship between the shear wave frequency and the static modulus of elasticity in the field. This lead to the development of the "Petite Sismique" method for indirect determination of static modulus of deformation in-situ. In this research a wave travel time measuring device was used for field testing. This instrument was designed to measure the time of the first arrival. By adjusting the sensitivity, the times corresponding to the first positive and negative peaks could be determined. The frequency was then calculated by the equation:

$$f = \frac{1}{2(t_b - t_a)}$$

where $(t_b - t_a)$ is the difference between the first positive and negative peaks (Figure 4.12).

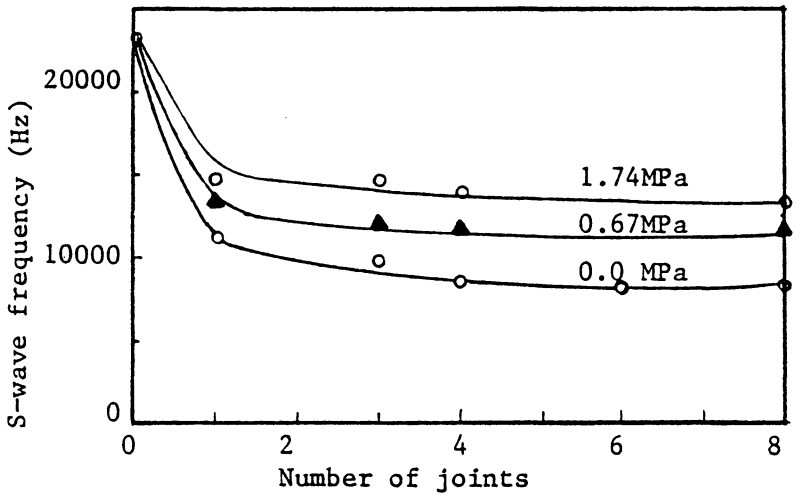


Figure 4.10 Dependence of shear wave frequency on number of joints (dry conditions) (Stacy, 1976)

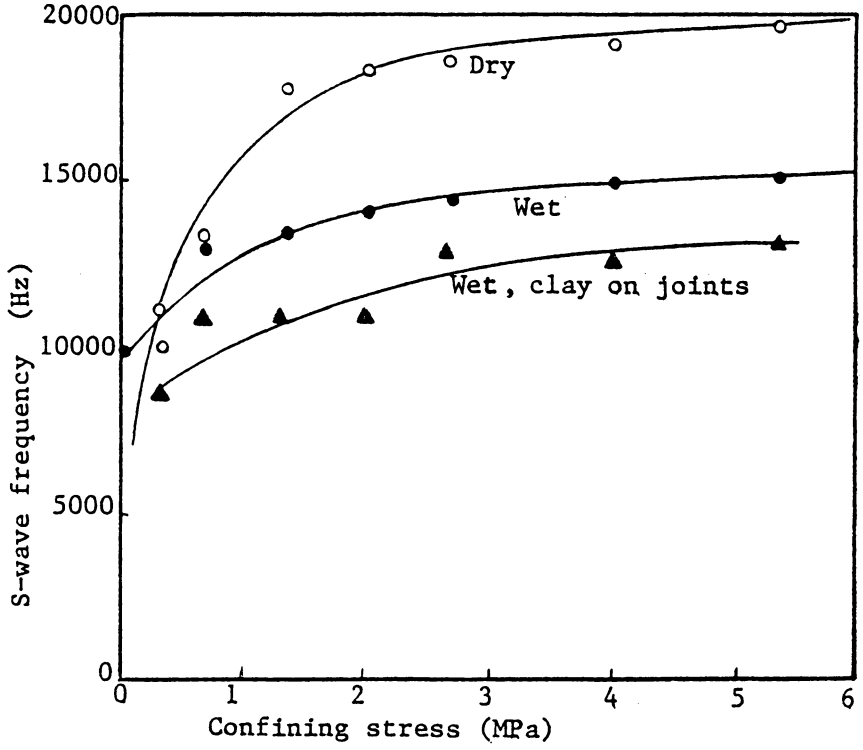


Figure 4.11 Variation of S-wave frequency with confining stress (Stacy, 1976)

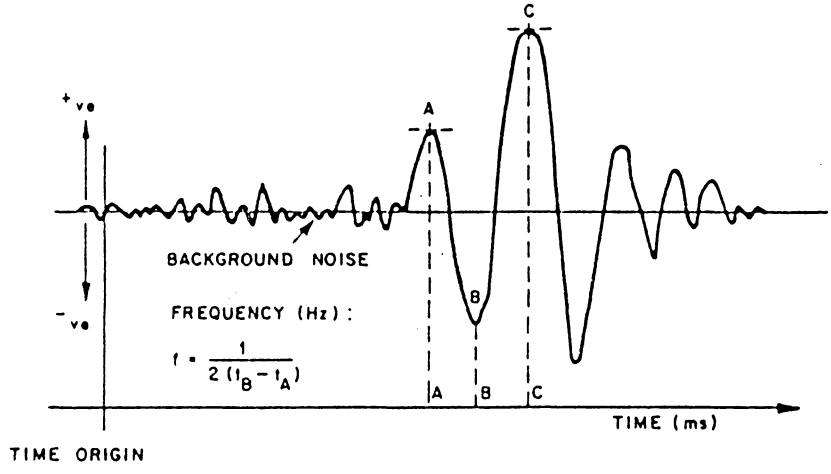


Figure 4.12 Calculation of the shear wave frequency (Bieniawski, 1978)

These tests were conducted in the field and within distances in the range of 100-200 feet. The source was a hammer which was hit perpendicularly to the rock surface and the receiver was aligned in such a way that it would detect vibrations orthogonal to the wave travel path. The problem with this technique is to decide whether S-waves were recorded or, instead, surface waves having almost the same velocity. However, the results suggested a good correlation between the frequency of the received waveform and the field static modulus of elasticity (Figure 4.13).

Roussel (1968) used a viscoelastic model, described in Section 2.2.2. to approximate these observations. The results are shown in Figure 4.14. Although the theoretical values differ greatly from the experimental data, there is a definite linear relation between the two parameters. Bieniawski (1978) conducted two sets of experiments and added more data on the graph, emphasizing its importance. He also presented an empirical relationship (Figure 4.15) in the form of:

$$E = 0.054f - 9.2$$

where: f: the frequency in Hz

E: in-situ modulus of deformation in GPa.

## 4.3. Other Applications of Sonic Methods

Bur et al. (1969) developed a method for determining the elastic symmetry of materials. He utilized ultrasonic pulse velocity measurements through spherical specimens and plotted the results on equal area polar projections.

Lama (1974) presented information on the wave velocity anisotropy

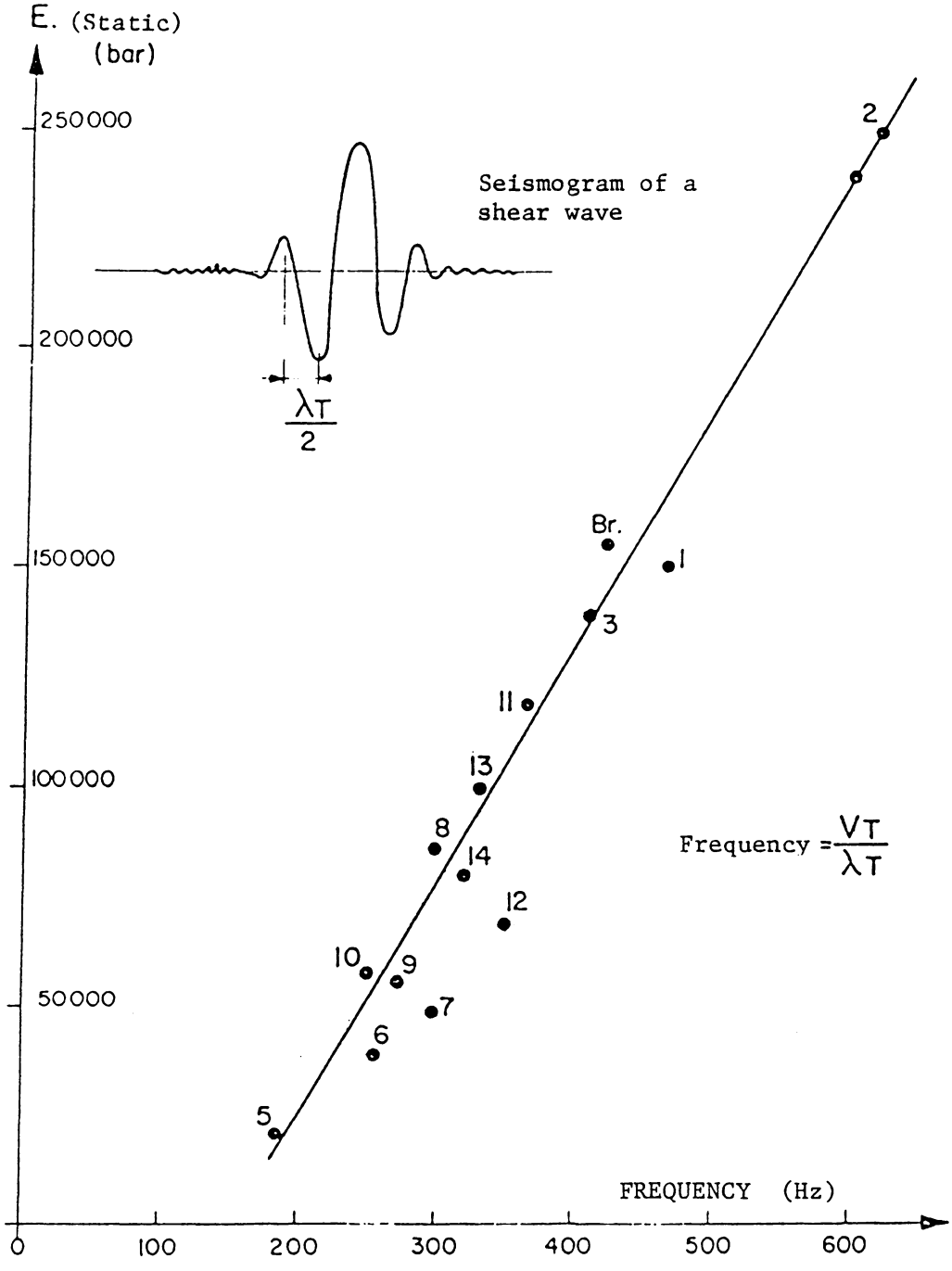


Figure 4.13 Relationship between static modulus and S-wave frequency (Schneider, 1967)

in-situ. He mentioned that the velocities of elastic waves differ along and across the layers or bedding planes. The velocity parallel to the layers ($V_L$) is always greater than the velocity perpendicular to the layers ($V_o$). The coefficient of anisotropy, defined as $V_L/V_o$, is given in Tables 4.1 and 4.2. for various rocks.

Thill (1972) suggested that stress level and deformation characteristics could be identified by monitoring acoustic emission in rock during loading. Deformation conditions that could be recognized were (1) crack closure, (2) linear elasticity, (3) fracture initiation and development, (4) accelerated fracture development, and (5) gross failure and post peak behavior.

## 4.4. Measuring Sonic Wave Parameters

### 4.4.1. Laboratory Experiments

The main problem when measuring sonic wave parameters is the identification of the various types of waves. This problem can be negotiated in the laboratory, where the generation of P-waves or S-waves can be achieved by utilizing the proper transducers. Possible reflections on the sides of specimens can be avoided by using specimens of proper dimensions and accurately determining the first arriving signal.

Measurement of the dominant received frequency can be used when the length of the sample is 5-10 times longer than the wave length of the received pulse. This condition can be satisfied with the use of high ultrasonic frequencies.

Table 4.1

Anisotropy Coefficients for Various Rocks
(Lama, 1978)

| Rock | Anisotropy coefficient | Reference |
|---|---|---|
| Austin chalk | 1.17 | TOCHER (1957) |
| Homogeneous anhydrite | 1.16 | DUNOYER de SEGONZAC and LAHERRERE (1959) |
| Anhydrite with intercalated limestones | 1.12 to 1.14 | DUNOYER de SEGONZAC and LAHERRERE (1959) |
| Limestone | 1.08 to 1.10 | DUNOYER de SEGONZAC and LAHERRERE (1959) |
| Arbuke limestone | 1.30 | UHRIG and VON MELLE (1955) |
| Salt | no anisotropy | DUNOYER de SEGONZAC and LAHERRERE(1959) |
| Sandstone | no anisotropy | DUNOYER de SEGONZAC and LAHERRERE (1959) |
| Eagle Ford shale | 1.33 | UHRIG and VON MELLE (1955) |
| Pierre shale (Limon, Colo.) | 1.18 | UHRIG and VON MELLE (1955) |
| Pierre shale (Last Chance, Colo.) | 1.14 | UHRIG and VON MELLE (1955) |
| Cambridge slate | 1.07 | TOCHER (1957) |
| Lorraine shale | 1.40 | TOCHER (1957) |
| Gneiss, Hell Gate, N.Y. | 1.20 | BIRCH (1960) |
| Micaschist, Woodsville, Vt. | 1.36 | BIRCH (1960) |
| Granodiorite gneiss, Bethlehem, N. H. | 1.33 | BIRCH (1960) |
| Gneiss, Pelham, Mass. | 1.27 | BIRCH (1960) |

Table 4.2

Velocity of P-waves in Layered Rocks
(Lama, 1978, after Rzhevski and Novic, 1971)

| Rock | Velocity of the longitidinal wave, m/s | | |
|---|---|---|---|
| | parallel to stratification $V_{II}$ | perpendicular to stratification $V_{\perp}$ | Coefficient of anisotropy $V_{II}/V_{\perp}$ |
| Limestone | 5300 | 5100 | 1.04 |
| Sandstone | 3800 | 3200 | 1.19 |
| Marl | 4300 | 3900 | 1.10 |
| Serpentinite | 4600 | 3800 | 1.18 |

4.4.2. Field Tests

During field testing the identification of different types of sonic waves is complicated because of the similar velocities of S-waves and surface waves as well as due to the many reflections on bedding planes and joints.

Mooney (1974) studied methods for the generation of shear waves, the principles of their propagation and measurement techniques. Almost any source of sonic waves will produce both P-waves and S-waves. If the source is located on the surface, surface waves will be produced as well. In addition, the reflection of sonic waves on the ground surface will produce significant and sometimes unanticipated effects (Figure 4.16). Figures 4.17.a and 4.17.b show the mode of propagation of P-waves and SV-waves, generated at the surface by a hammer blow. Figure 4.18 shows the mode of propagation of P-waves and SV-waves generated by a vertical impact in a drill hole. For a positive detection of shear waves in the field, three steps have to be taken: (i) use a source that yields the maximum energy in S-waves; (ii) take advantage of the mode of propagation (as in Figures 4.17 and 4.18) in selecting measuring locations; and (iii) appropriately orient the receiver, to take advantage of the expected polarization of the shear waves. However, when the test site is on a bedded formation or within jointed mass, the propagation path will not follow a straight line and the waveforms can change in nature (from P- to S-) or produce complicated images on the measuring instruments.

Hoar and Stokoe (1978) described a method for generating a tor-

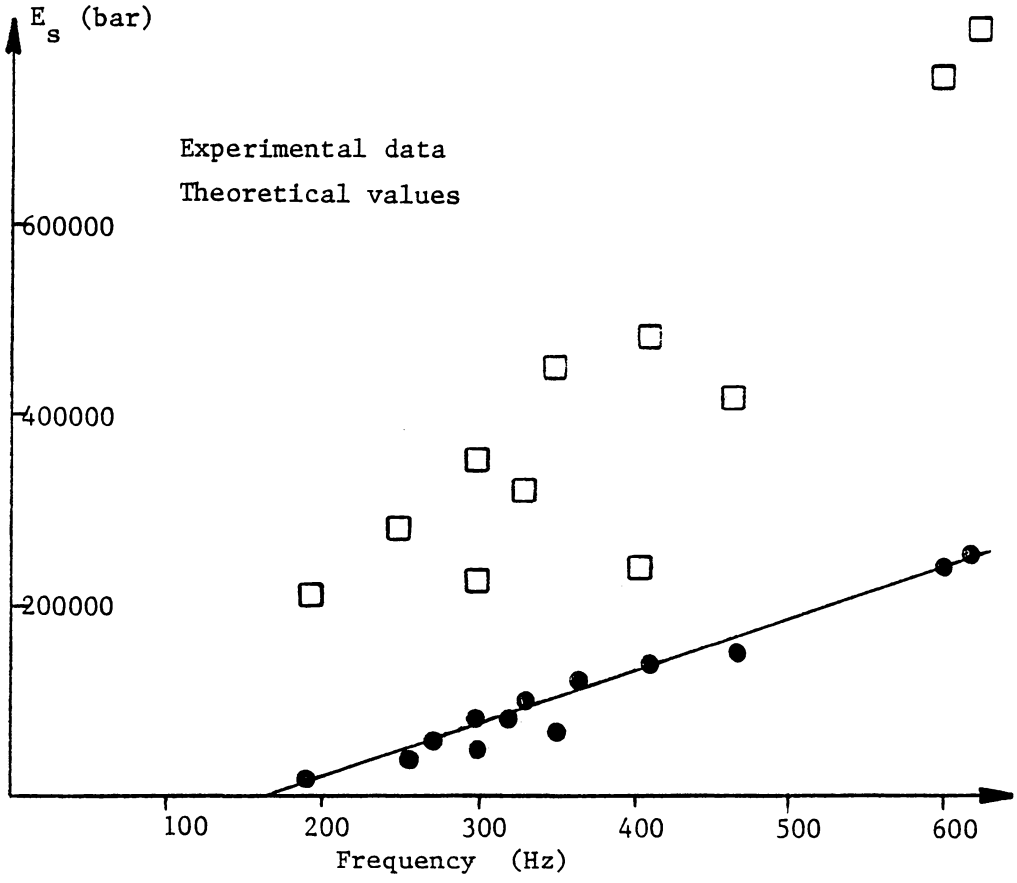


Figure 4.14 Comparison of the theoretical and exparimental data for the "Petite Sismique" method (Roussel, 1968)

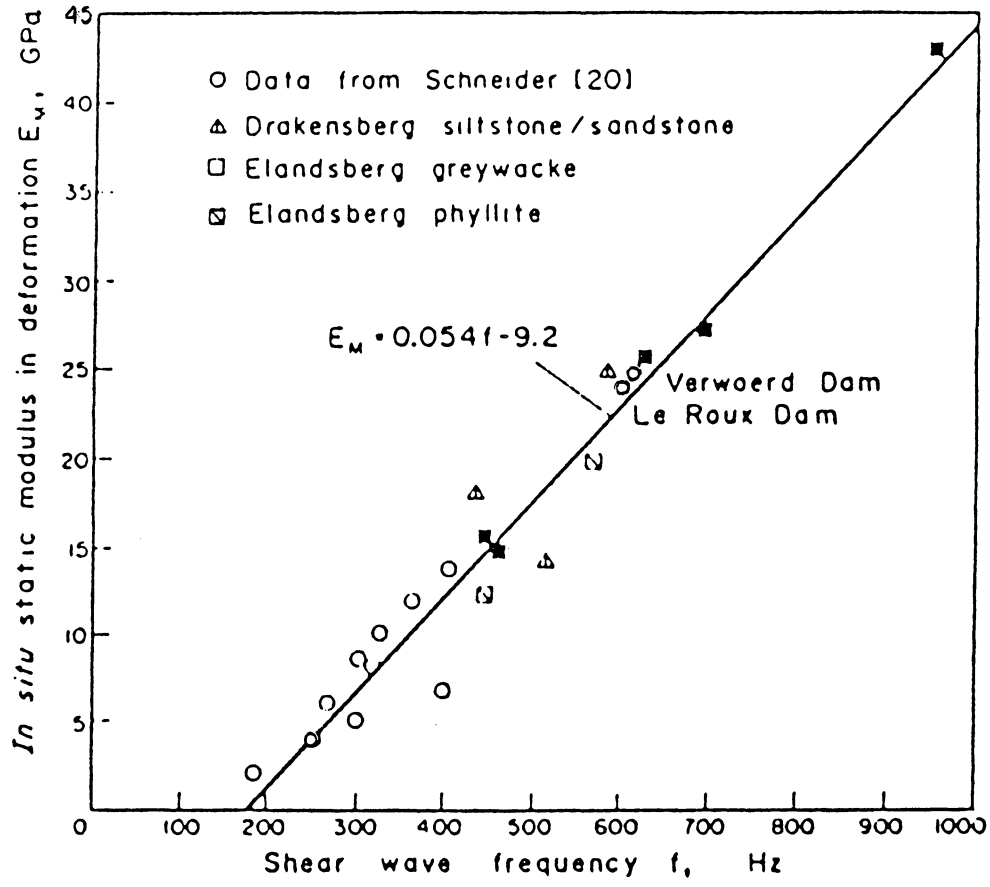


Figure 4.15 Correlation between static modulus of deformation and shear wave frequency (Bieniawski, 1978)

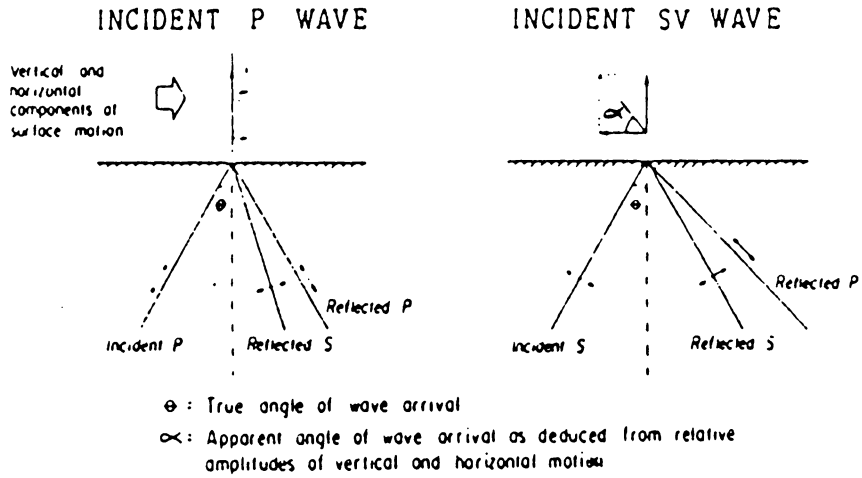


Figure 4.16 Effect of free surface on arriving sonic waves (Mooney,1974)

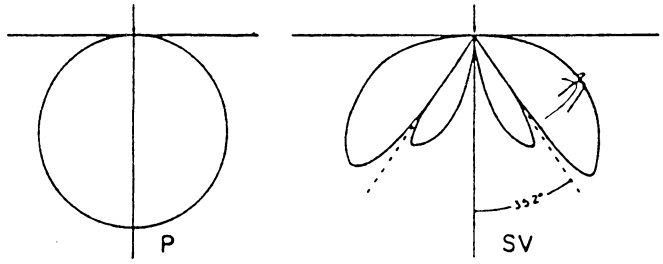


a. Radiation pattern from vertical point force as viewed in vertical plane

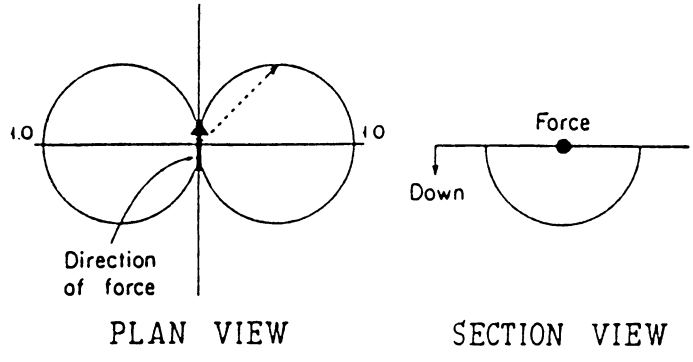


b. Radiation pattern for SH-waves from horizontal surface force

Figure 4.17 Radiation patterns from surface forces (Mooney, 1974)

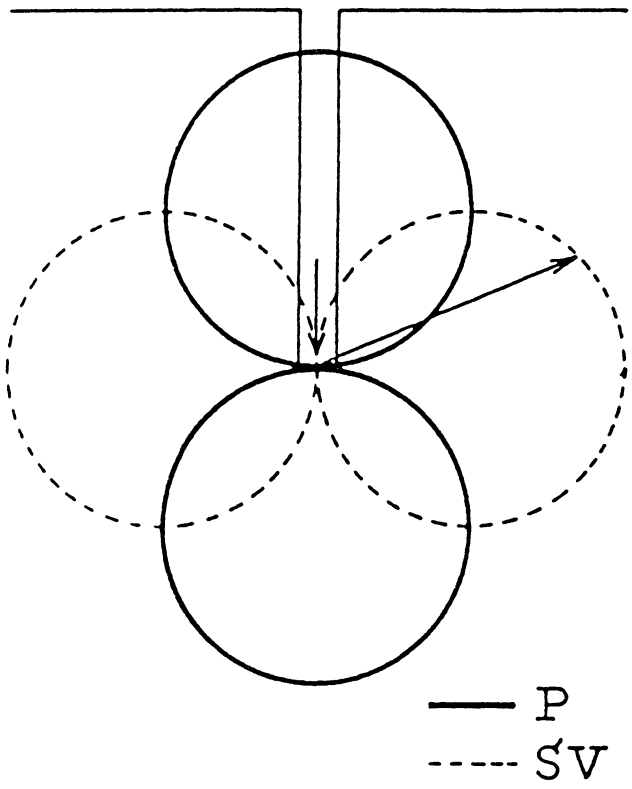


Figure 4.18 Radiation pattern for vertical impact in drill hole (Mooney, 1974)

sional impulse in the bottom of a borehole. This type of source is rich in SH-waves while generating very little P-wave energy. The main advantage of the method is that the direction of the pulse can be inverted, which will invert the polarity of the received shear wave. As a result, S-waves generated by this technique are easier to identify. Three different cross sections are used for the source: a tube, a vane or a plate (Figure 4.19). The tube source has the disadvantage of producing a stronger P-wave than the others. The method is used for cross-borehole testing.

Stratton et al. (1978) used a "shear-wave hammer" to produce SV-waves from a borehole. The objective of the method to apply upward and downward hammer blows, which will result to received waveforms with a different polarity for shear waves.

Thill (1978) developed an inflatable piezoelectric borehole probe which can be used for distances of up to ten feet. This method has the advantage of using high frequencies (around 20 kHz), which give a fast-rising first arrival pulse at the receiver, thus permitting greater accuracy for wave velocity measurements.

### 4.4.3. Determination of the Frequency of the Received Waveform

Most investigators used some empirical method for determining the frequency of the received waveform (e.g., Figure 4.13). However, a measured waveform contains a number of frequencies:

(i) the spectrum of the source;

(ii) the resonance frequency of the receiver; and

(iii) the resonance frequency of the (elastic or viscoelastic) model

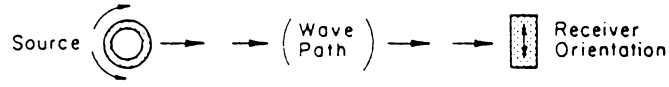


a.-TUBE SOURCE


b.-VANE SOURCE

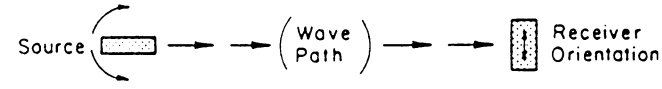


c.-PLATE SOURCE

Figure 4.19 Plan view of crossborehole shooting with torsional sources (Hoar and Stokoe 1978)

describing the rock, or in other words, the dominant frequency traced by the receiver if it is located more than several wavelengths away from the source.

As a result a more elaborate analysis of the spectrum of the received waveform should be preferred. The Fourier transform is a useful tool for determining the spectrum of the wave. The Fourier transform transforms a function (e.g., the amplitude or particle velocity versus time) from the time domain to the frequency domain:

$$X(f) = \int_{-\infty}^{\infty} x(t)\, e^{-i\pi ft} dt$$

$$x(t) = \int_{-\infty}^{\infty} X(f)\, e^{i2\pi ft} df$$

where: $-\infty<f<\infty$, $-\infty<t<\infty$, $i = \sqrt{-1}$

$X(f)$: the frequency-domain function

$x(t)$: the time-domain function.

However, when the waveform is sampled, or when the system is to be analyzed in a digital computer, the discrete Fourier transform has to be used. Bergland (1969) presented a detailed review of the Fourier transform as well as the fast Fourier transform algorithm. The International Mathematics and Statistics Library (IMSL) computer subroutine library provides such an algorithm in a subroutine, the FFTSC.

## 4.5. The Application of Sonic Methods to Engineering Rock Classification

As mentioned in Chapter III, engineering rock classification systems utilize one or more of the following parameters:

(i) modulus of elasticity;

(ii) compressive strength;

(iii) RQD;

(iv) spacing of discontinuities; and

(v) the characteristics of discontinuities.

In Section 4.3. most of the parameters were correlated to measureable parameters of sonic waves. Since the latter are easier to measure, it is suggested that a classification system based on this information would be of considerable value.

Coon and Merritt (1970) propose a classification system utilizing the Velocity Index (velocity of P-wave in the field over velocity of P-wave in the laboratory) (Table 4.3). It is actually a modification of the RQD method, based on the correlation between RQD and the Velocity Index (Figure 4.5).

In this research, a correlation between the dynamic and static properties of intact rock and rock mass was undertaken. The objective of this effort was to implement the sonic wave parameters for the development of improved rock classification systems.

Table 4.3

Engineering Classification of the In Situ Rock

(after Coon and Merritt, 1970)

| Classification | Velocity Index | RQD |
|---|---|---|
| Very Poor | 0 - 0.20 | 0 - 25 |
| Poor | 0.20 - 0.40 | 25 - 50 |
| Fair | 0.40 - 0.60 | 50 - 75 |
| Good | 0.60 - 0.80 | 75 - 90 |
| Excellent | 0.80 - 1.00 | 90 - 100 |

# CHAPTER V

# DYNAMIC TESTING OF ROCKS

## 5.1. Sample Preparation

The specimens used for this research were prepared from rock samples, collected from several quarries. A drill press, manufactured by Structural Behavior Engineering Laboratories Inc., equipped with a water swivel and diamond coring bits was used to obtain cores of BX and NX diameters (Figure 5.1). The cores were cut using an automatic feed diamond disk saw, manufactured by Highland Park Manufacturing (Figure 5.2). Core samples to be tested in the stiff loading machine were accurately ground on a Brown & Sharpe grinding machine (Figure 5.3) according to the specifications suggested by the International Society for Rock Mechanics.

## 5.2. Determination of Static Rock Properties

A MTS stiff testing machine was used to determine the static mechanical properties of the core samples (Figure 5.4). The loading frame has a capability of $10^6$ lbs in compression. A function generator, with a feedback signal, is used to control the loading rate. Post-failure behavior was ignored in this case. The load and deformation were displayed on digital display units and were recorded on an X-Y ink plotter.

## 5.3. Instrumentation for Sonic Tests

### 5.3.1. General

To measure the characteristic properties of sound waves, four

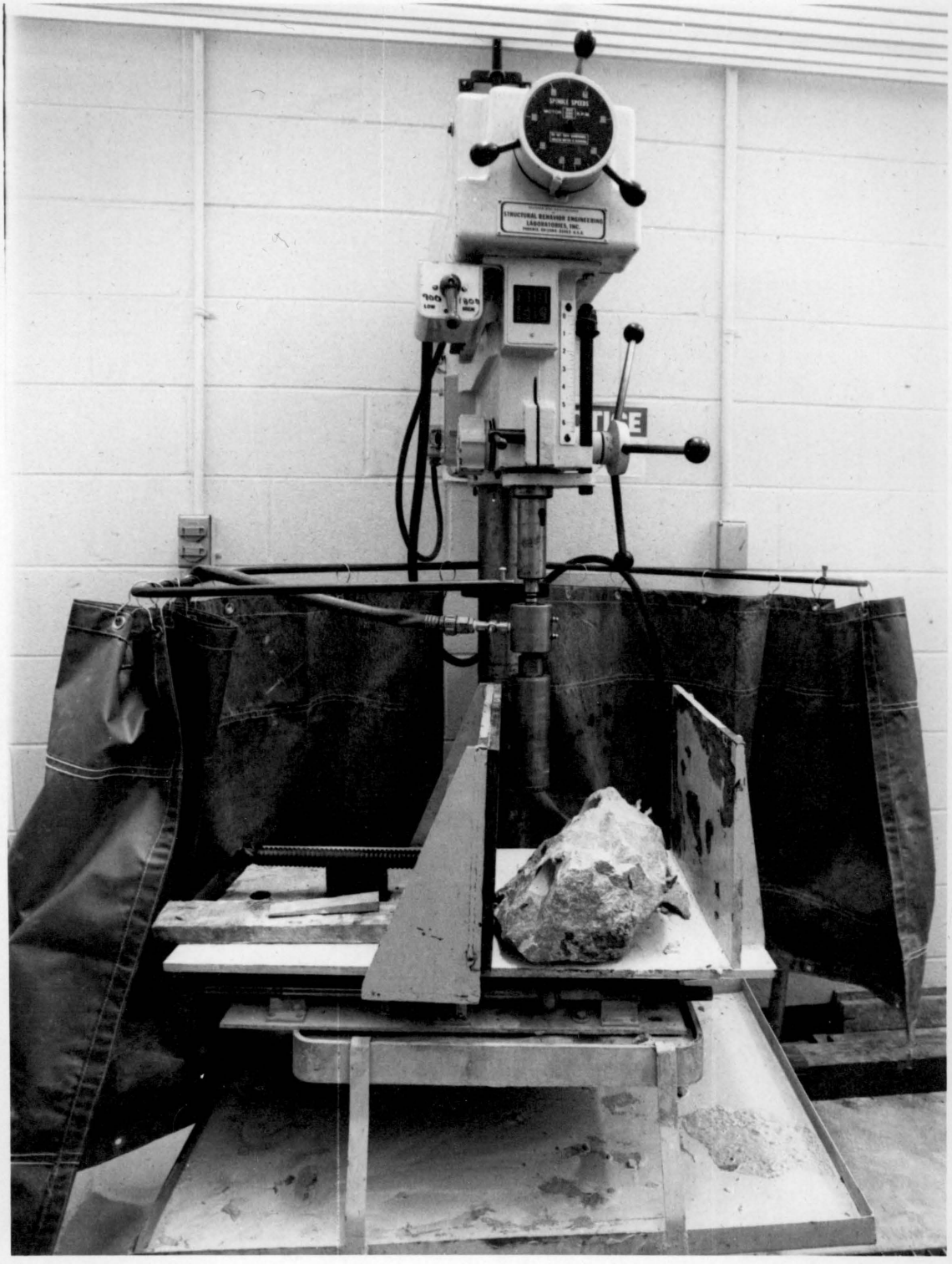


Figure 5.1 Coring Machine


Figure 5.2 Diamond Disk Saw

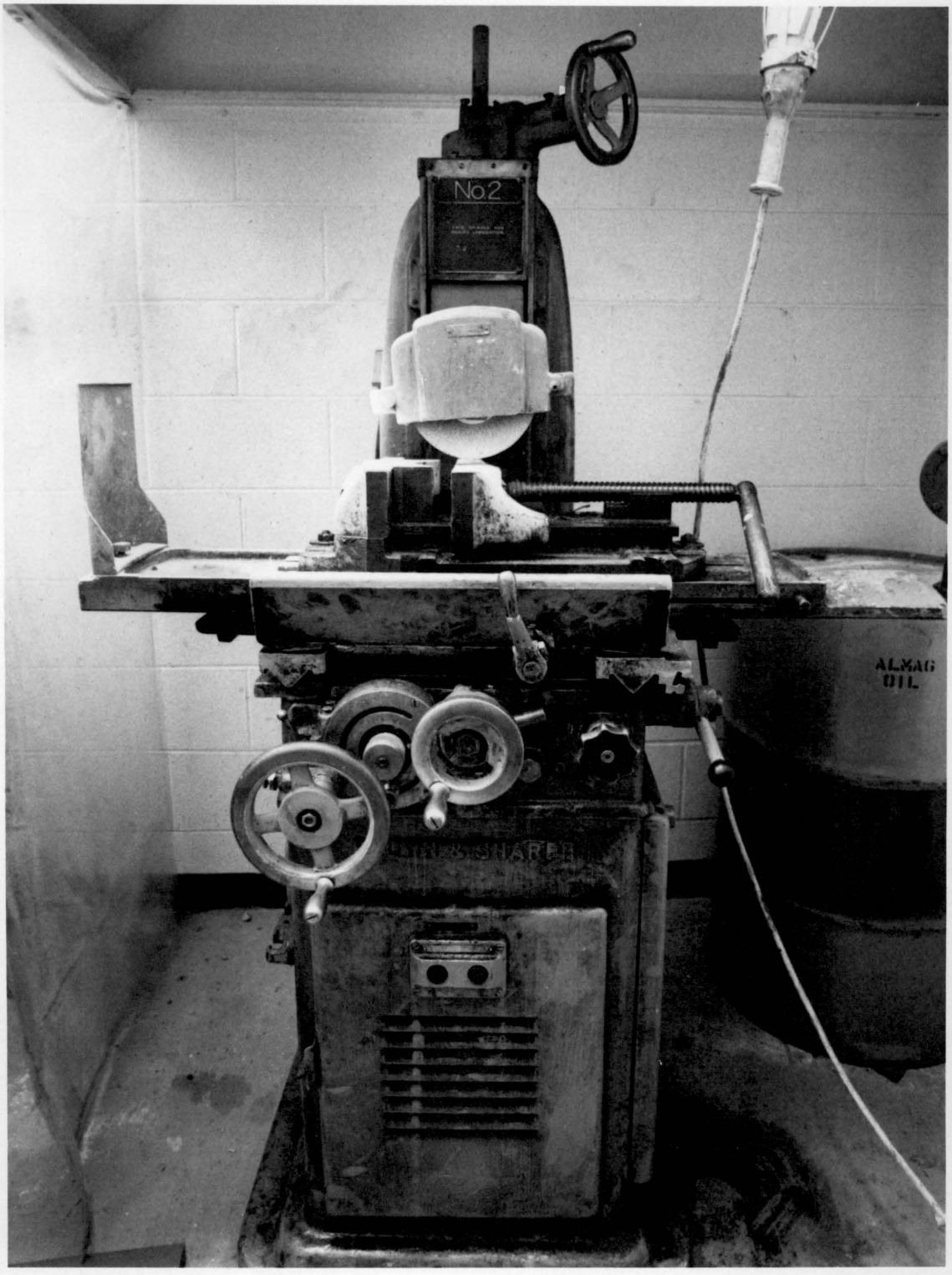


Figure 5.3 Grinding Machine


Figure 5.4 MTS Stiff Testing Machine and Control Console

instruments are required: a pulse generator, a transmitter, a receiver and a display unit, or recording unit.

A pulse generator generates electric pulses, usually at a frequency within the 50 Hz-100 kHz range. They can be sinusoidal, of a step or rectangular function, or δ-function (peak at a point). A sinusoidal pulse generator can only produce one frequency at a time, but usually has a wide range of available frequencies, using a basic circuit with a coil and a variable capacitor.

A step function or δ-function pulse consists, theoretically (from its Fourier transform), or an infinite number of frequencies. To generate a rectangular pulse a simple two transistor-two capacitor circuit is used.

The operation of the transmitter requires a pulse of voltage of 50-5,000 volts. A power amplifier is therefore required. When using a sinusoidal signal, a high power amplifier can be used. For rectangular or peak signals a DC to AC transformer using a special switch (SCR: silicon-controlled rectifier) is used (Cannaday and Leo, 1966). The SCR is a silicon diode with a control electrode (gate). It acts as an automatic switch with no moving parts, i.e., when a positive voltage from the pulse generator is applied on the gate, the SCR "close" and current flows. Otherwise the current stops flowing. Thus a high voltage pulse with only positive spikes is produced (Cannaday and Leo, 1966) (Figure 5.5).

The transmitter and the receiver are usually identical in design. They may differ at the connectors on the electrical leads. Their main

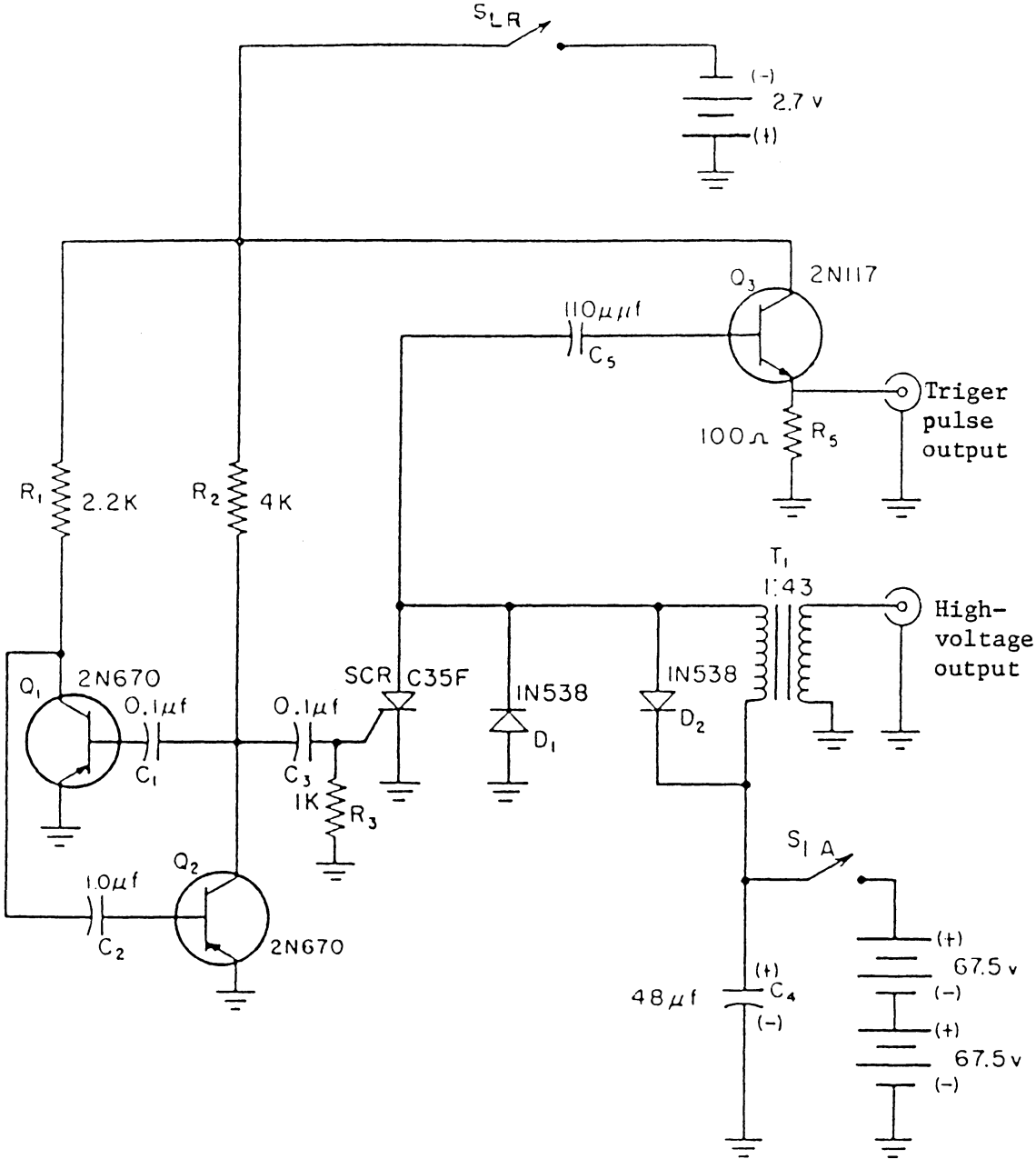


Figure 5.5 Pulse generator, schematic diagram
(Cannaday and Leo 1966)

component is a piezoelectric crystal or ceramic disk. An assembly around it provides electrical insulation, mechanical damping and, in some cases, it holds it in place for coupling to the sample under test.

A piezoelectric crystal or ceramic disk deforms or changes in shape when subjected to a voltage change on its sides or along a radius. By using the proper piezoelectric material, by giving it a suitable shape and by adjusting the voltage gradient we can control the mode of mechanical deformation. By applying a voltage gradient on the parallel sides of a disk we can create axial deformation, which can be used as a source of compressional waves. The generation of shear waves is more complicated. Cannaday (1968) mentions that, by positioning the edge of an axially electrically exited disk (as the one used for compressional waves) on a sample surface, we can produce shear waves. The S-waves thus produced travel close to the surface on a line perpendicular to the axis of the disk (Figure 5.6). Wattananikorn (1978) uses reflection on a free surface, at an angle of $30^{o}$ or $60^{o}$, in a material with Poisson's ratio of 0.25, to convert P-waves to S-waves (Figure 5.7). Another way to produce S-waves, but with circular polarization, is to use specially constructed sets of crystals, attached to each other, along the circumference of a circle.

The most common display unit is an oscilloscope. It should have vertical deflection and have a sweep range of between 0.1 μsec and 1 sec per division. The vertical band should have a range of 10-50 millivolts per division. External triggering is required in order to determine the

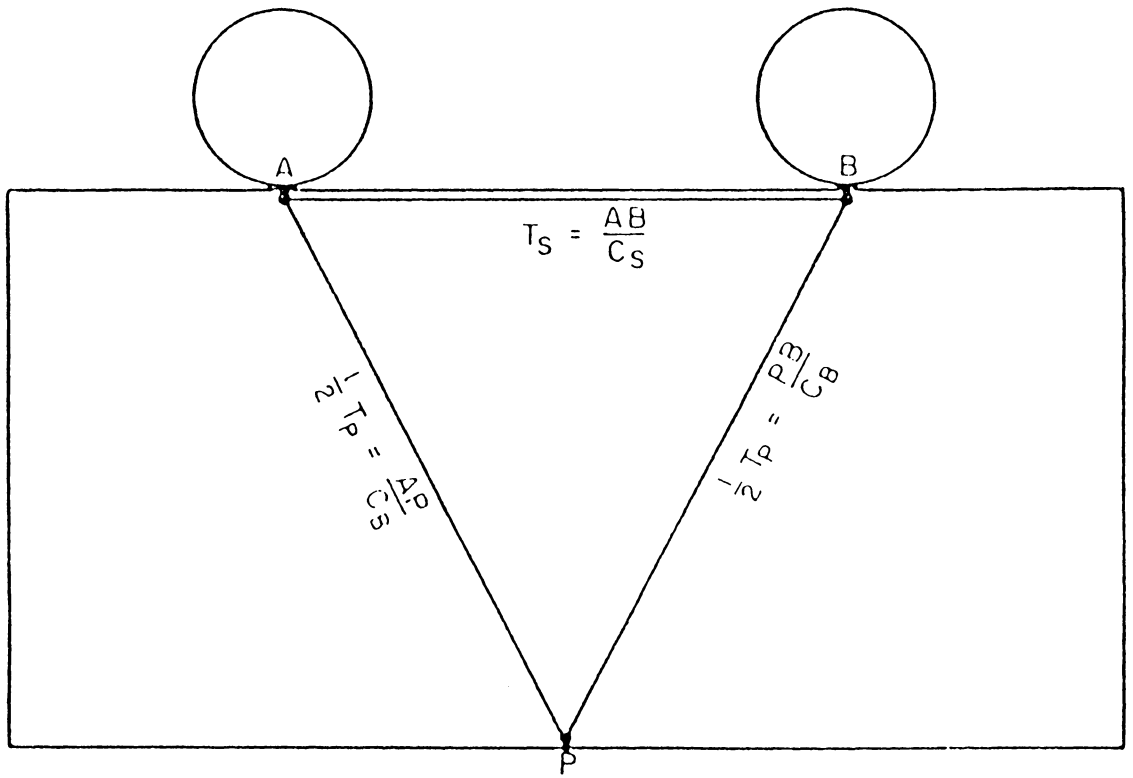


$C_B$ Compressional wave velocity (P wave)

$C_S$ Shear-wave velocity (S wave)

$T_P$ Travel time of P wave from A to P to B

$T_S$ Travel time of S wave from A to B

Figure 5.6 Diagram of wave paths (Cannaday, 1968)

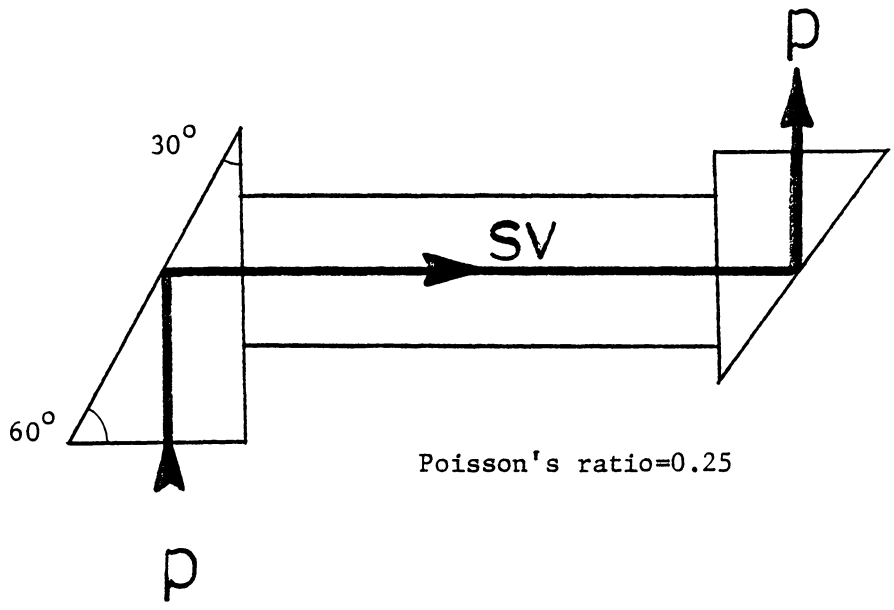


Figure 5.7 Conversion of a P-wave to an SV-wave (Wattananikorn, 1978)

time the pulse takes to travel through the specimen.

A simple block diagram of a sonic wave measuring system is shown on Figure 5.8. More details on such instrumentation can be found in Cannaday and Leo (1966), Cannaday (1968), Stephenson (1978), Hoar and Stokoe (1978).

Other components can also be added to the basic system. For field tests a hammer or drop weight can be used, to produce a stronger, but complicated (mathematically) and less accurate (i.e., not reproducable) pulse. A trigger switch has to be attached to the hammer, in order to trigger the oscilloscope or another recording device.

A preamplifier can be inserted between the receiver and the oscilloscope. Its purpose is to amplify the received signal as much as possible while keeping background noise insignificant. Background noise has several causes. External sounds may be reduced by using a soundproof laboratory, by inserting a high-pass (frequency) filter, or by pausing mining operations (for in situ measurements). The results of stray radio frequency can be avoided by using proper shielding and grounding of the electric components and circuitry. Internal electronic noise can be avoided by using low noise components and good amplifier design, especially in the circuitry from the receiver up to, and including, the first stage of amplification, since the received signal is very weak.

A memory unit, between the preamplifier and the display unit, can help in two ways. Firstly, for storing data, to be used for comparison or calculations. Secondly, to enhance a signal by repeating, one or

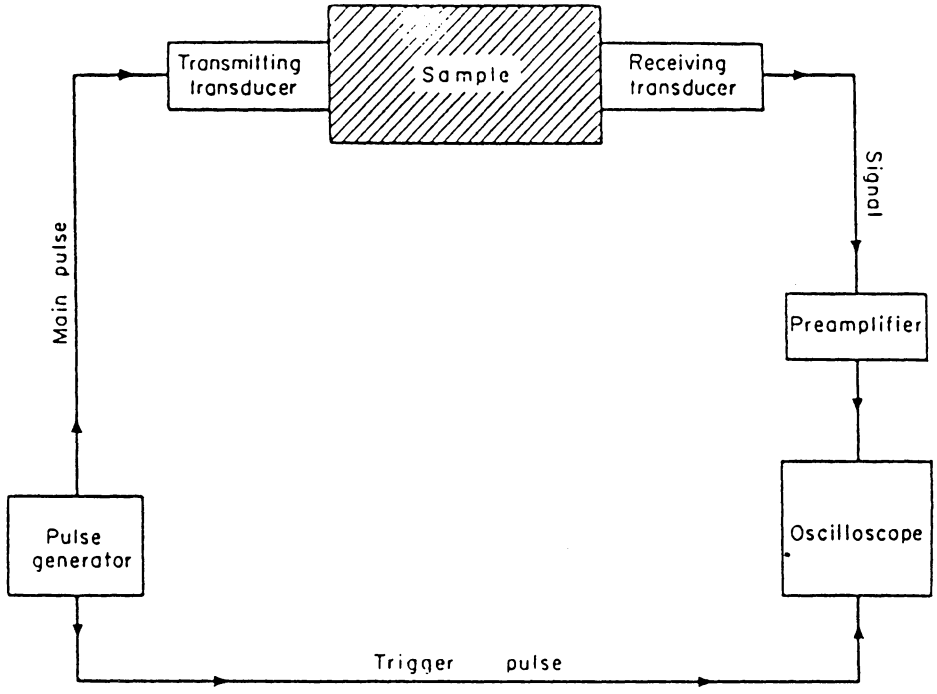


Figure 5.8 Block diagram of sonic testing apparatus (Cannaday and Leo 1966)

more times, the same experiment on a sample, or in the field, and adding the results algebraically. Using this method, a weak signal is enhanced in the memory and the display, whereas external noise is being canceled out gradually.

The use of a memory unit requires an analog to digital converter, in order that data can be stored in the memory. Figure 5.9 shows a block diagram of such a system.

### 5.3.2. Research Instrumentation

For measuring and recording waveforms transmitted through rock samples and in the field the "New Sonicviewer - Model 5217" was used. It is manufactured by OYO of Japan. It employs ultrasonic or acoustic frequency waves for measuring the travel time of waves through rock samples or the use of hammer blows for field tests. Other measurements (i.e., frequency or wavelength of a waveform) can be calculated using a hard copy of the waveform. The Sonicviewer has a two channel memory allowing the storage of two different waveforms at a time. A signal enhancement mode allows the stacking of any number of signals, so that even a weak input in a relatively noisy environment may yield easy to read data. The vibration source may be either a hammer or a piezoelectric transducer. A wide range of sweep time settings permits velocity measurements on samples a few inches long, as well as along distances of more than 200 feet in the field. The received waveforms can be observed on the cathode ray tube (CRT). A thermal printer produces a hard copy of the image on the screen.

All the above pieces of equipment, i.e., pulse generator, preampli-

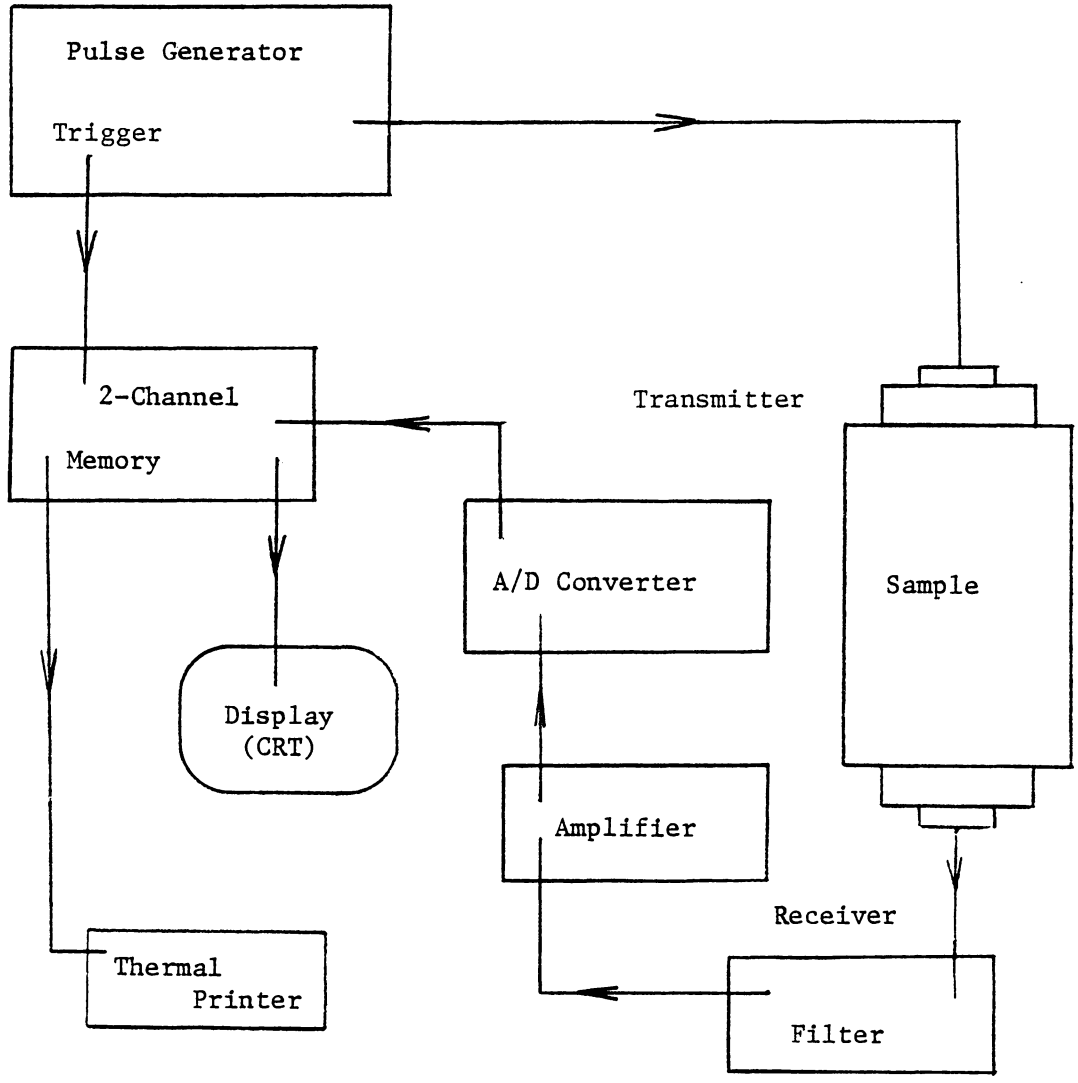


Figure 5.9 Schematic Diagram of Instrumentation

fier, analog to digital converter, memory unit, CRT, and printer are assembled in one compact unit which can be used in a laboratory or in the field (Figure 5.10).

Two pairs of transducers are supplied, one pair for P-waves (axial vibration mode) and the other pair for S-waves (torsional vibration mode) (Figures 5.11 and 5.12).

The pulse unit produces δ-function pulses (peaks) (Figures 5.13 and 5.14) at various rates (64, 128,256, 512 pulses per second).

The received signal can be enhanced from 10X to 10,000X in ten steps. The amplifier has a frequency range from 1 kHz to 100 kHz. The analog signal is then converted to digital, through an 8 bit A/D converter and stored in a 12 bit, 512 word, two channel memory. The A/D conversion sample time has a range from 20.48 μsec (256 word) or 40.49 μsec (512 word) to 40.96 msec (512 word), in ten steps.

Each memory channel can store a different waveform. To get a display or printout, the signal is converted to analog by a D/A converter with an output adjustor.

Figures 5.15 and 5.16 show a 512 word waveform with output gains of 2 and 5 respectively. Figures 5.17 and 5.18 respectively show the first and second 256 word parts of the same 512 word stored waveform. Figure 5.19 illustrates the method of getting a digital reading for the first arrival time, by moving the waveform to the left until the first arrival coincides with the zero time index. The digital display is in μsec or msec, depending on the selected time base.

The waveform is observed on a 5 inch CRT display. A 512 word

waveform, or a part of it (expanded) can be displayed. A thermal printer reproduces the image appearing on the screen, on 53 mm wide paper, with a choice of two time scales (1X or 2X). The unit also produces a 75 volt (75 Ohm, 1 volt peak to peak) video signal for use with a video recorder or video printer.

The unit weighs 20 lbs and is powered by a 12 volt, 8 Ah battery.

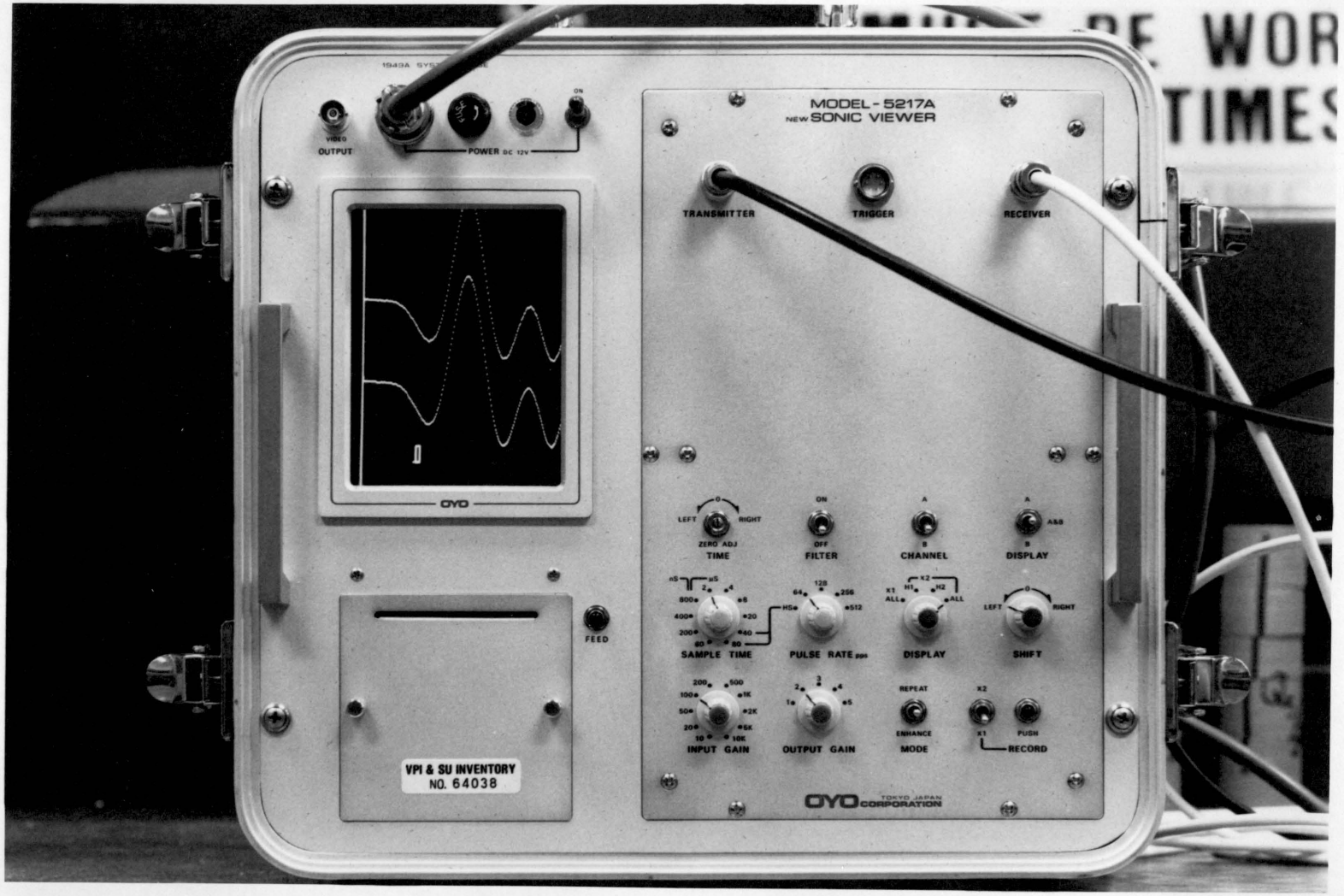


Figure 5.10 The "New Sonicviewer"

Figure 5.11 P-wave Transducers

Figure 5.12 S-wave Transducers

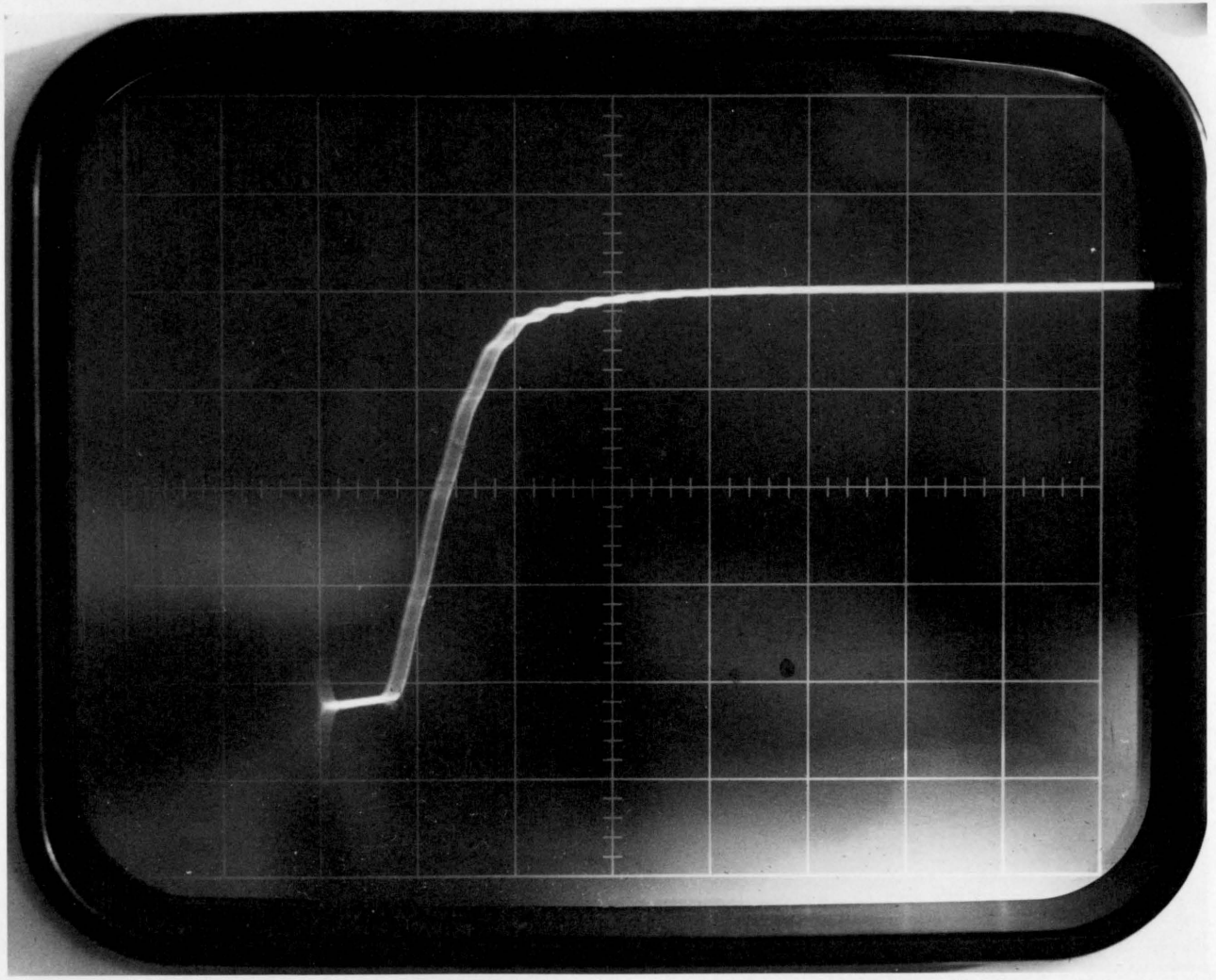

Figure 5.13 The Electric Pulse (Vertical Scale: 50 Volts per division, Horizontal Scale: 0.2 msec per division)

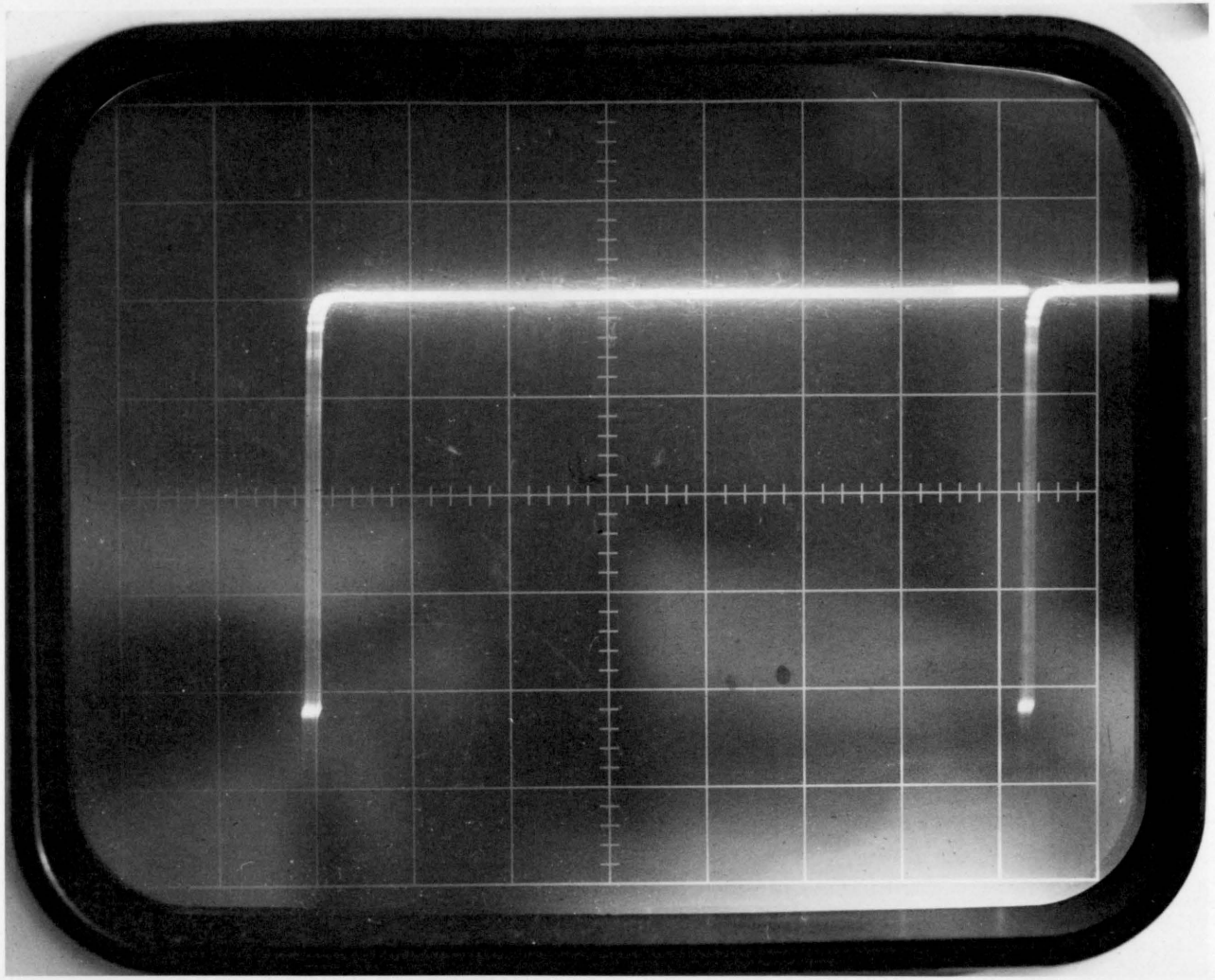

Figure 5.14 The Electric Pulse (Vertical Scale: 50 Volts per division, Horizontal Scale: 2 msec per division

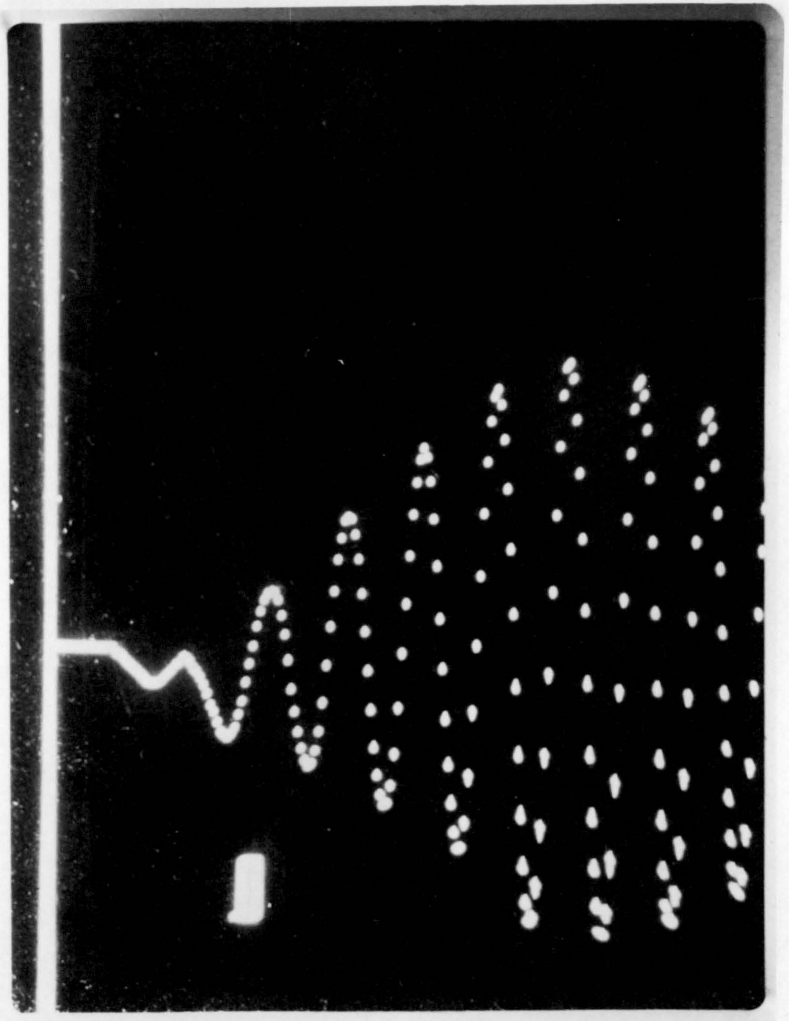

Figure 5.15 A 512 Word Waveform,
Output Gain: 2

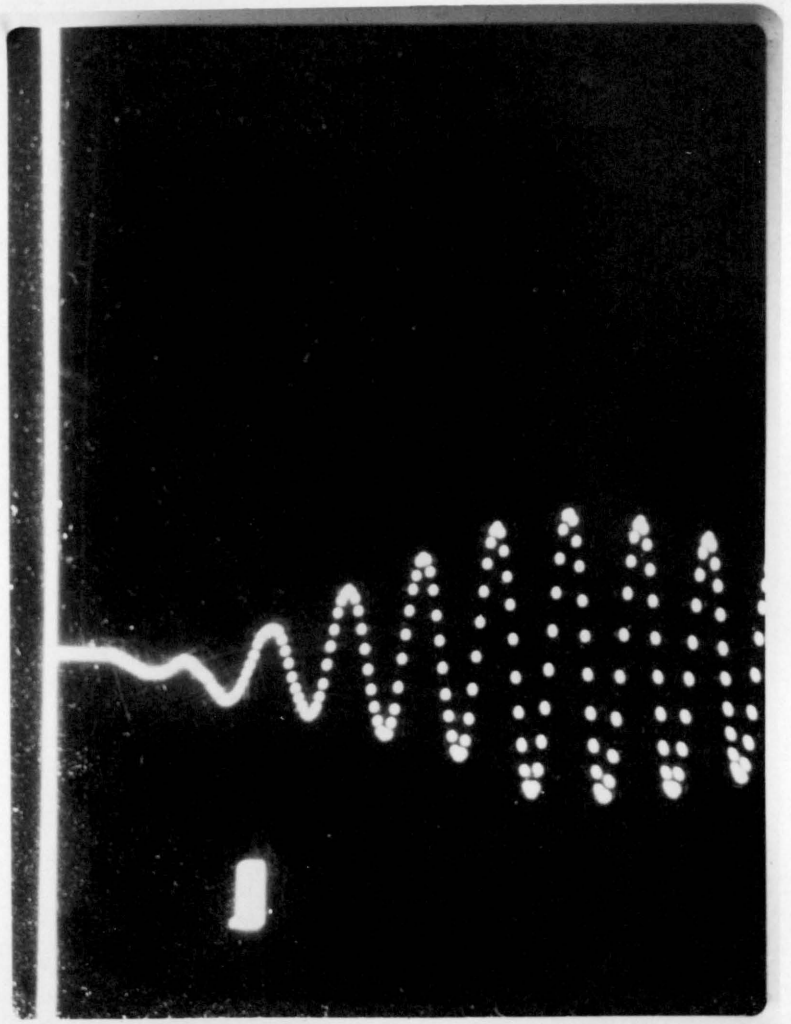

Figure 5.16 A 512 Word Waveform,
Output Gain: 5

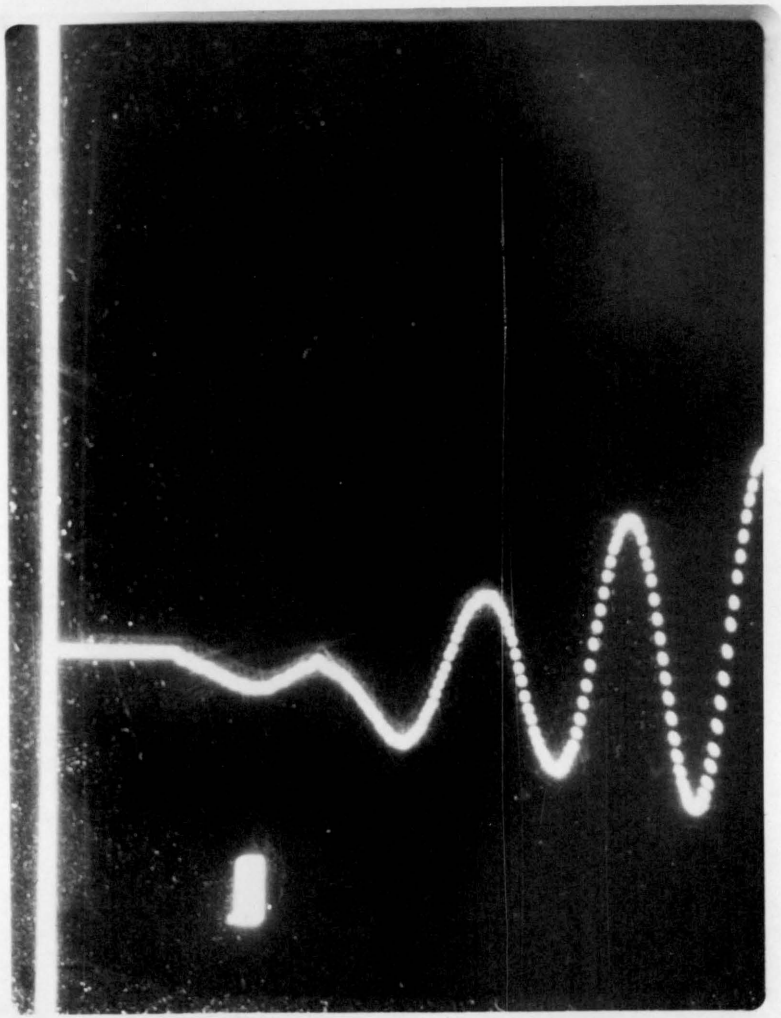

Figure 5.17 First Part of a Waveform

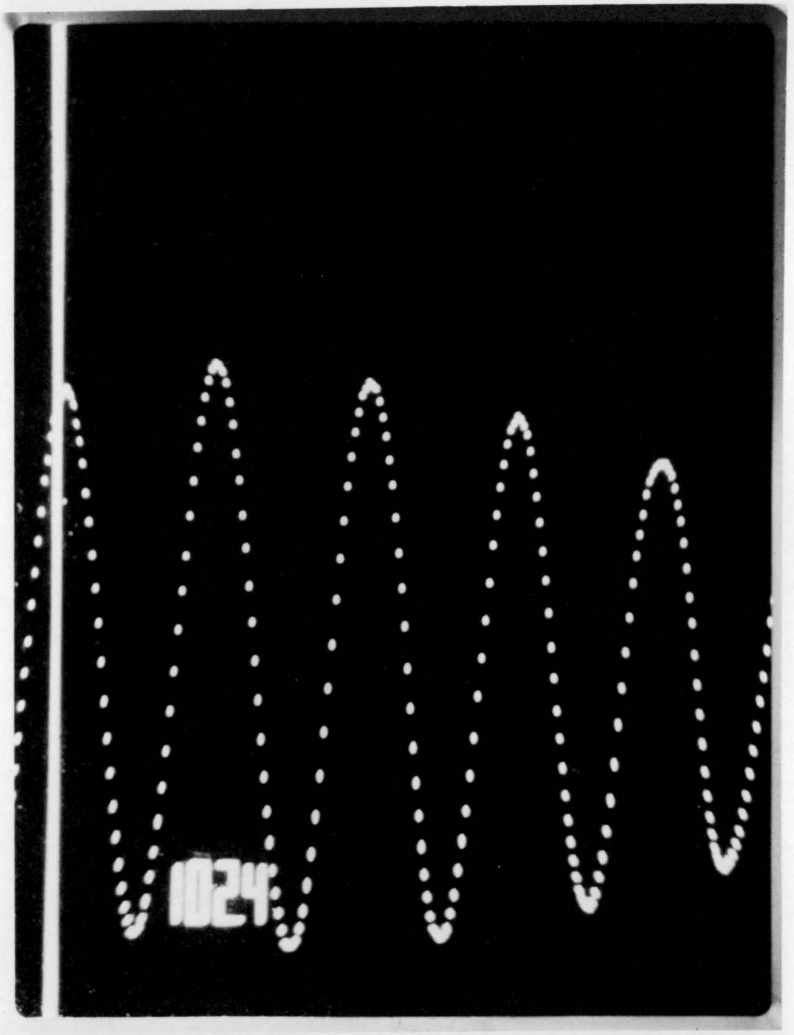


Figure 5.18 Second Part of a Waveform

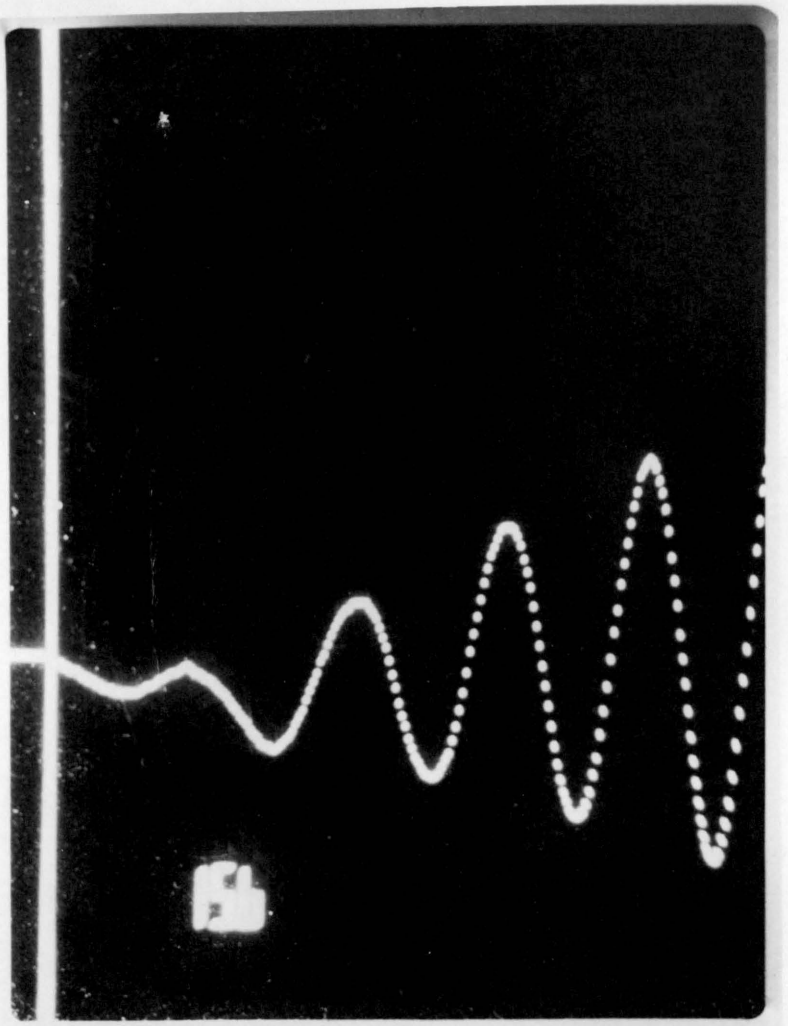

Figure 5.19 First-Arrival Digital Display

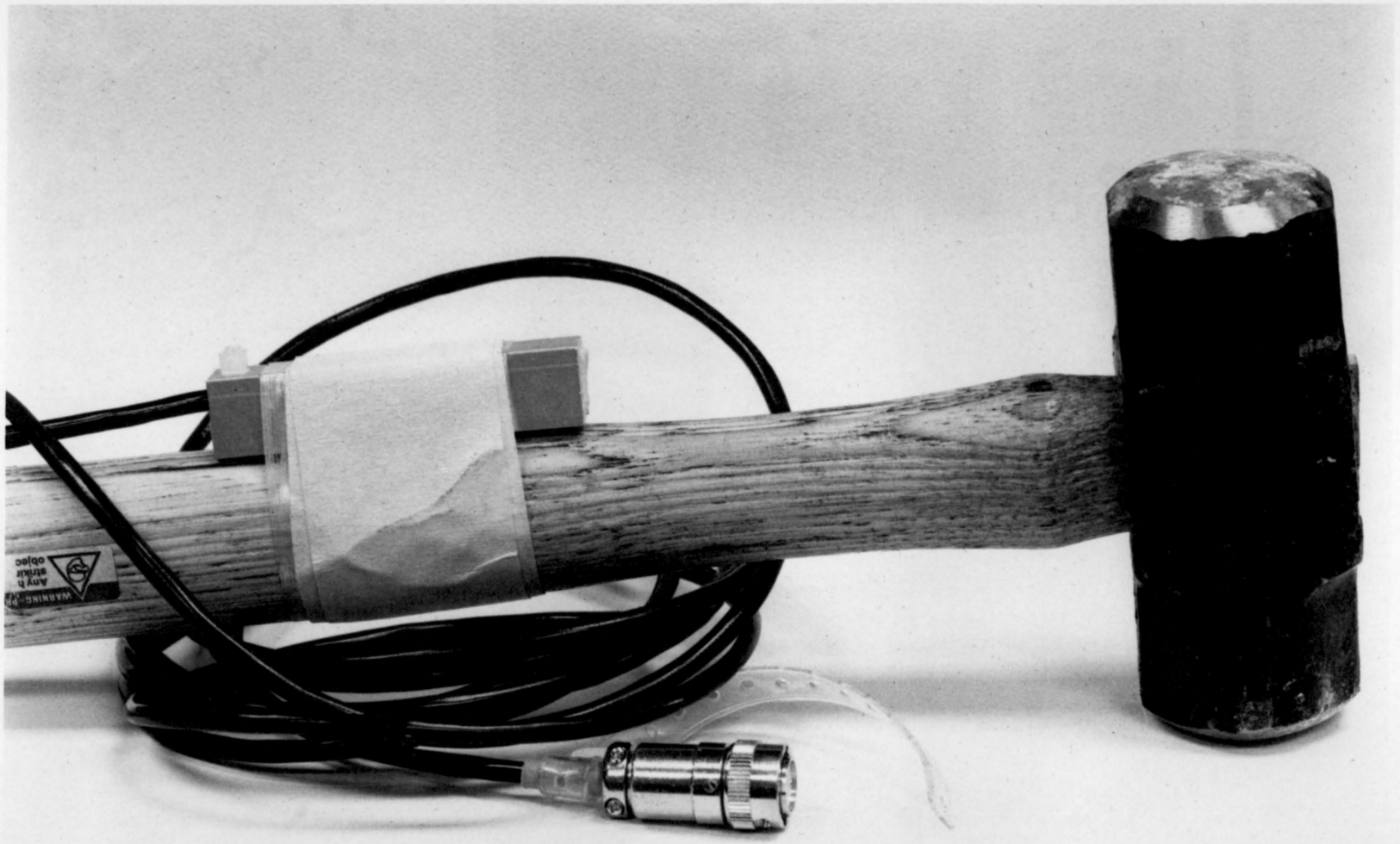

Figure 5.20 Trigger Switch Attached to the Hammer for Field Application

# CHAPTER VI

# EXPERIMENTAL PROCEDURE AND RESULTS

## 6.1. Description of Laboratory Rock Samples

The samples used for this research were collected from six quarries in southwestern Virginia. In addition, three other rock types that were available in the laboratory from previously conducted experiments were also used. Information about the geology of the areas was obtained from Gray et al. (1979), Furcron (1935) and Sweet (1981).

### (i) Quarry No. 1

This quarry is owned by the Radford Limestone Corporation and is located in Pulaski County, Virginia. The rock is Gray Limestone, fine grained with bands of calcite. The strike is east-west and the dip is $85^{o}$ to the south. Beds are approximately 3 inches thick. Three sets of joints can be identified. The first set is parallel to the bedding plane and the joints are filled with calcite. The second set of joints has the strike on $N45^{o}E$ and the dip is $70^{o}S$, the joints being 25" apart. The third set has a strike on $N25^{o}W$ and a dip of $25^{o}N$. Many random fractures are observed on the slope surface, without general orientation, probably caused by blasting.

### (ii) Quarry No. 2

This quarry is owned by Sisson and Ryan Incorporated and is located at Shawsville, Montgomery County, Virginia. The rock is a very fine grained, bedded limestone, with secondary calcite in small fractures, massive in place and belongs to the Copper Ridge Formation. The strike

is on N10°W and the dip is 25°NE. Three sets of joints are again present. The first has a strike on N-S and is dipping 60°W. The second set of joints has the strike N45°E and the dip is 80°NW. The third set of joints has the strike E-W and is dipping 88°S.

(iii) Quarry No. 3

This quarry is owned by James River Limestone Incorporated and is located near Buchanan, Botetourt County, Virginia. The rock is gray crystalline dolomite and belongs to the Shady Dolomite. The strike is N-S and the dip is almost vertical. Bedding planes are almost 15 feet apart and they are filled with mud. Numerous fractures are observed on the slope surface, probably caused by blasting.

(iv) Quarry No. 4

The quarry is owned by the Martinsville Stone Corporation. It is located at Fieldale, Henry County, Virginia. The rock is granite, containing abundant quartz, biotite mica, plagioclase, some muscovite and belongs to the Leatherwood Granite. There are many quartz filled fractures. Two sets of joints, both filled with quartz were observed. One set has the strike SE-NW and vertical dip. The other set of joints is horizontal. For both sets the joints were 4-6 inches apart.

(v) Quarry No. 5

The quarry is located at Arvonia, Buckingham County, Virginia. The rock is hard, dark slate and belongs to the Arvonia Slate. It is massive and compact, easily fractured along the plane of schistocity.

(vi) Rock Type No. 6

The rock samples in this case consist of rough grained yellow sandstone with numerous bedding planes (unknown origin).

(vii) Quarry No. 7

The quarry is owned by the Blue Ridge Stone Corporation and is located close to Lynchburg, Campbell County, Virginia. The rock is a mashed and slaty marble and belongs to the Cockeysville Marble. Numerous fractures without specific orientation were observed.

(viii) Rock Type No. 8

Samples are medium grained sandstone (unknown origin).

(ix) Rock Type No. 9

Laminated shale with many planes of weakness, easily fractured during preparation (unknown origin).

Core samples were prepared using the equipment described in paragraph 5.1. Wherever possible a length to diameter ratio of 2/1 was obtained, if the samples were to be tested in the MTS stiff loading machine. Table 6.1 gives the length, diameter, specific weight and the rock type of each sample (each sample is numbered and the first digit indicates the quarry from which it was collected or the rock type). These samples were tested in the sonic apparatus and subsequently on the MTS loading machine.

Table 6.2 gives the length and rock types for samples used to determine the influence of fractures on wave propagation velocities.

Several of these samples are shown in Figures 6.1 and 6.2.


Figure 6.1 Intact Samples


Figure 6.2 Fractured Samples

Table 6.1

Samples Used for Static and Sonic Testing

| Sample Number | Length (inches) | Diameter (inches) | Specific Weight ($lbs/in^3$) | Rock Type |
|---|---|---|---|---|
| 1/1 | 2.677 | 2.125 | 0.114 | Limestone |
| 1/2 | 2.185 | 1.615 | 0.105 | Limestone |
| 1/3 | 3.346 | 1.615 | 0.089 | Limestone |
| 1/4 | 1.622 | 2.125 | 0.091 | Limestone |
| 1/5 | 4.075 | 2.011 | 0.094 | Limestone |
| 1/6 | 3.269 | 1.615 | 0.101 | Limestone |
| 1/7 | 3.225 | 1.615 | 0.101 | Limestone |
| 1/8 | 3.240 | 1.615 | 0.102 | Limestone |
| 1/9 | 3.316 | 1.615 | 0.101 | Limestone |
| 2/1 | 3.339 | 2.011 | 0.101 | Limestone |
| 2/2 | 1.535 | 2.011 | ----- | Limestone |
| 2/3 | 1.870 | 2.011 | 0.098 | Limestone |
| 2/4 | 1.858 | 2.011 | 0.100 | Limestone |
| 3/1 | 3.354 | 2.011 | 0.099 | Dolomite |
| 3/2 | 2.949 | 2.011 | ----- | Dolomite |
| 3/3 | 2.945 | 2.011 | ----- | Dolomite |
| 3/4 | 2.717 | 2.011 | 0.104 | Dolomite |
| 3/5 | 2.587 | 2.011 | 0.098 | Dolomite |
| 3/6 | 3.197 | 1.615 | ----- | Dolomite |
| 3/7 | 2.854 | 1.615 | 0.097 | Dolomite |
| 3/8 | 2.354 | 1.615 | ----- | Dolomite |
| 4/1 | 3.969 | 2.011 | 0.096 | Granite |
| 4/2 | 4.016 | 2.011 | ----- | Granite |
| 4/3 | 3.984 | 2.011 | 0.096 | Granite |
| 4/4 | 3.260 | 1.615 | 0.099 | Granite |
| 4/5 | 3.228 | 1.615 | ----- | Granite |
| 4/6 | 3.244 | 1.615 | 0.099 | Granite |
| 4/7 | 3.236 | 1.615 | 0.100 | Granite |
| 4/8 | 3.217 | 1.615 | ----- | Granite |
| 4/9 | 1.543 | 1.615 | 0.096 | Granite |

Table 6.1 (continued)

Samples Used for Static and Sonic Testing

| Sample Number | Length (inches) | Diameter (inches) | Specific Weight ($lbs/in^3$) | Rock Type |
|---|---|---|---|---|
| 5/1 | 3.215 | 1.609 | 0.100 | Slate |
| 5/2 | 3.236 | 1.610 | 0.101 | Slate |
| 5/3 | 3.239 | 1.610 | 0.100 | Slate |
| 5/4 | 3.272 | 1.609 | 0.101 | Slate |
| 5/5 | 2.115 | 1.611 | 0.098 | Slate |
| 5/6 | 2.095 | 1.610 | 0.100 | Slate |
| 5/7 | 2.086 | 1.610 | 0.099 | Slate |
| 5/8 | 2.143 | 1.609 | 0.101 | Slate |
| 5/9 | 2.142 | 2.125 | 0.101 | Slate |
| 5/10 | 4.257 | 2.125 | 0.099 | Slate |
| 5/11 | 4.334 | 2.125 | 0.100 | Slate |
| 5/12 | 4.293 | 2.125 | 0.099 | Slate |
| 5/13 | 4.240 | 2.125 | 0.098 | Slate |
| 5/14 | 1.920 | 2.125 | 0.101 | Slate |
| 5/15 | 1.884 | 2.125 | 0.100 | Slate |
| 5/16 | 1.921 | 2.125 | 0.099 | Slate |
| 5/17 | 1.812 | 2.125 | 0.101 | Slate |
| 6/1 | 4.004 | 1.988 | 0.089 | Sandstone |
| 6/2 | 4.024 | 1.990 | 0.090 | Sandstone |
| 6/3 | 4.025 | 1.981 | 0.090 | Sandstone |
| 6/4 | 4.013 | 1.990 | 0.092 | Sandstone |
| 7/1 | 3.873 | 3.005 | 1.615 | Laminated Shale |
| 7/2 | 3.872 | 3.606 | 1.614 | Laminated Shale |
| 7/3 | 3.810 | 3.275 | 1.615 | Laminated Shale |
| 7/4 | 2.235 | 3.262 | 1.615 | Laminated Shale |
| 8/1 | 3.873 | 1.871 | 0.099 | Sandstone |
| 8/2 | 3.872 | 1.871 | 0.098 | Sandstone |
| 8/3 | 3.810 | 1.991 | 0.099 | Sandstone |
| 8/4 | 2.235 | 1.875 | 0.098 | Sandstone |
| 9/1 | 3.285 | 1.875 | 0.096 | Slaty Marble |
| 9/2 | 3.876 | 1.882 | 0.094 | Slaty Marble |
| 9/3 | 3.891 | 1.875 | 0.094 | Slaty Marble |
| 9/4 | 3.877 | 1.875 | 0.095 | Slaty Marble |
| 9/5 | 4.003 | 1.882 | 0.095 | Slaty Marble |

Table 6.2

Samples Used for Joint Determinations

| Sample Number | Number of Cracks | Length (inches) | Rock Type | Surface of Fractures |
|---|---|---|---|---|
| 5/21 | 1,2,3 | 3.701 | Slate | Smooth along the bedding planes |
| 5/22 | 0,1,2,3,4 | 5.434 | Slate | Smooth along the bedding planes |
| 5/23 | 0,1,2,3 | 5.291 | Slate | Smooth along the bedding planes |
| 6/21 | 0,1,2,3 | 7.801 | Sandstone | Rough |
| 6/22 | 0,1,2,3 | 7.805 | Sandstone | Rough |
| 6/23 | 0,1,2,3 | 7.835 | Sandstone | Rough |
| 6/24 | 0 | 8.206 | Sandstone | Smooth |
| 6/24 | 1 | 8.105 | Sandstone | Smooth |
| 6/24 | 2 | 7.995 | Sandstone | Smooth |
| 6/24 | 3 | 7.856 | Sandstone | Smooth |
| 6/25 | 0 | 8.191 | Sandstone | Smooth |
| 6/25 | 1 | 8.065 | Sandstone | Smooth |
| 6/25 | 2 | 7.965 | Sandstone | Smooth |
| 6/25 | 3 | 7.830 | Sandstone | Smooth |
| 6/26 | 0 | 7.999 | Sandstone | Smooth |
| 6/26 | 1 | 7.770 | Sandstone | Smooth |
| 6/26 | 2 | 7.648 | Sandstone | Smooth |
| 6/26 | 3 | 7.552 | Sandstone | Smooth |
| 6/31 | 0,1,2,3 | 7.688 | Sandstone | Smooth |
| 6/32 | 0,1,2,3 | 7.687 | Sandstone | Smooth |
| 6/33 | 0,1,2,3 | 7.478 | Sandstone | Smooth |
| 6/34 | 0,2,3 | 7.517 | Sandstone | Smooth |
| 9/21 | 0,1,2,3 | 6.073 | Shale | Rough along the bedding planes |
| 9/22 | 0,1,2,3 | 6.074 | Shale | Rough along the bedding planes |

## 6.2. Tests of Intact Samples

### 6.2.1. Sonic Wave Measurements

The instrumentation as described in Section 5.3.2 was used for these experiments. The accuracy of the equipment was assured by the comparison of the image on the CRT with a calibrated oscilloscope.

The samples were placed between the transmitter and the receiver. A weight of 13 lbs was placed on top to ensure good contact. For measuring P-waves the P-transducers were used. For a better contact between the sample and the transducers, it was suggested in the literature that a thin layer of petroleum jelly had to be applied on their contacting surfaces. It was found, instead, that a PVC tape (electrician's tape) had exactly the same effect and this technique was preferred. When using the S-wave transducers the surfaces had to be absolutely clean and dry. Before each test the delay time of the instrumentation was determined. To obtain accurate travel time measurements a low input gain was used in combination with the "enhancement mode". This procedure has two advantages: (i) it eliminates the effect of external noises and (ii) by continuous observation of the displayed waveform, the exact time of the first arrival could be determined.

All samples described on Table 6.1 were tested. Table 6.3 gives the values of the P-wave and S-wave velocities for these samples.

### 6.2.2. Measurement of the Static Properties

The MTS loading machine was used to determine the modulus of elas-

Table 6.3

Dynamic and Static Properties of Intact Samples

| Sample Number | $V_p$ ($\times 10^4$ in/sec) | $V_s$ ($\times 10^4$ in/sec) | $E_s$ ($\times 10^6$ psi) | $C_o$ ($\times 10^3$ psi) |
|---|---|---|---|---|
| 1/1 | 10.218 | 9.296 | 4.15 | 35.68 |
| 1/2 | 15.388 | 9.259 | 4.67 | 58.09 |
| 1/3 | 15.785 | 9.400 | 4.53 | 34.17 |
| 1/4 | 16.552 | 7.114 | 3.05 | 39.19 |
| 1/5 | 19.041 | 12.423 | 5.83 | 24.87 |
| 1/6 | 19.812 | 11.351 | 6.72 | 38.08 |
| 1/7 | 22.872 | 11.356 | 6.30 | 41.49 |
| 1/8 | 25.116 | 11.912 | 5.87 | 53.70 |
| 1/9 | 24.204 | 11.676 | 6.35 | 34.17 |
| 2/1 | 14.772 | 11.018 | 5.39 | 40.61 |
| 2/2 | 8.626 | 5.729 | 1.65 | 23.61 |
| 2/3 | 13.551 | 8.202 | 3.68 | 48.48 |
| 2/4 | 15.748 | 6.543 | ---- | 19.20 |
| 3/1 | 23.622 | 10.103 | 5.18 | 22.67 |
| 3/2 | 20.197 | 10.383 | 5.31 | 30.85 |
| 3/3 | 15.499 | 13.386 | 3.68 | 22.35 |
| 3/4 | 9.633 | 10.136 | 2.44 | 14.17 |
| 3/5 | 18.216 | 12.680 | 4.65 | 12.59 |
| 3/6 | 18.373 | 9.629 | 4.80 | 22.46 |
| 3/7 | 17.619 | 10.651 | 3.18 | 17.57 |
| 3/8 | 15.696 | 9.649 | 3.46 | 25.38 |
| 4/1 | 9.404 | 7.937 | 3.93 | 23.61 |
| 4/2 | 14.445 | 8.436 | 3.16 | 22.67 |
| 4/3 | 14.541 | 7.721 | 3.87 | 22.04 |
| 4/4 | 14.953 | 9.367 | 3.34 | 17.57 |
| 4/5 | 14.285 | 8.541 | 3.15 | 17.57 |
| 4/6 | 15.845 | 9.113 | 4.52 | 24.90 |
| 4/7 | 14.845 | 9.748 | 3.48 | 18.55 |
| 4/8 | 16.580 | 9.460 | 2.55 | 12.20 |
| 4/9 | 14.290 | 8.209 | 3.62 | 25.63 |
| 5/1 | 18.61 | 9.41 | 4.51 | 33.9 |
| 5/2 | 19.17 | 8.75 | 4.56 | 34.4 |
| 5/3 | 18.32 | 8.86 | 4.34 | 30.0 |
| 5/4 | 18.93 | 9.359 | 4.43 | 33.9 |

Table 6.3 (continued)

Dynamic and Static Properties of Intact Samples

| Sample Number | $V_p$ ($\times 10^4$ in/sec) | $V_s$ ($\times 10^4$ in/sec) | $E_s$ ($\times 10^6$ psi) | $C_o$ ($\times 10^3$ psi) |
|---|---|---|---|---|
| 5/5 | 17.50 | 8.75 | 3.58 | 36.3 |
| 5/6 | 14.88 | 8.46 | 3.54 | 33.4 |
| 5/7 | 13.65 | 8.22 | 3.53 | 29.5 |
| 5/8 | 14.80 | 8.58 | 3.43 | 27.0 |
| 5/9 | 17.16 | 8.58 | 3.63 | 33.6 |
| 5/10 | 18.61 | 9.22 | 4.47 | 29.9 |
| 5/11 | 16.62 | 9.15 | 4.55 | 33.8 |
| 5/12 | 17.54 | 8.84 | 4.54 | 33.6 |
| 5/13 | 19.38 | 8.73 | 4.57 | 34.7 |
| 5/14 | 14.46 | 7.51 | 2.98 | 33.6 |
| 5/15 | 12.658 | 8.06 | 2.87 | 30.7 |
| 5/16 | 15.39 | 7.82 | 2.95 | 32.1 |
| 5/17 | 16.06 | 6.62 | 2.86 | 33.3 |
| 6/1 | 10.62 | 7.12 | 1.81 | 11.27 |
| 6/2 | 10.19 | 7.01 | 1.83 | 12.86 |
| 6/3 | 10.57 | 6.87 | 1.28 | 10.06 |
| 6/4 | 10.65 | 6.99 | 1.74 | 10.77 |
| 7/1 | 12.70 | 8.00 | 1.55 | 16.55 |
| 7/2 | 9.65 | 6.77 | 1.36 | 15.46 |
| 7/3 | 13.56 | 8.66 | 1.61 | 15.74 |
| 7/4 | 12.08 | 7.87 | 1.91 | 22.10 |
| 8/1 | 17.37 | 9.28 | 3.89 | 27.58 |
| 8/2 | 16.03 | 9.69 | 3.67 | 20.99 |
| 8/3 | 18.09 | 9.99 | 4.24 | 29.29 |
| 8/4 | 15.61 | 9.06 | 3.62 | 23.43 |
| 9/1 | 15.72 | 8.05 | 2.29 | 17.02 |
| 9/2 | 12.08 | 7.94 | 2.55 | 10.06 |
| 9/3 | 13.65 | 8.11 | 2.88 | 21.73 |
| 9/4 | 17.54 | 8.01 | 3.24 | 25.71 |
| 9/5 | 17.18 | 8.94 | 2.94 | 14.74 |

ticity and the unconfined compressive strength. The results produced by the MTS machine are shown in the Appendix.

The modulus of elasticity was calculated at 50% of the unconfined compressive strength. Table 6.3 gives the values of the modulus of elasticity and the unconfined compressive strength.

### 6.2.3. Correlation Between Static and Dynamic Properties

The dynamic properties of intact samples include the velocity of the P-wave ($V_p$), the velocity of the S-wave ($V_s$) and the dynamic modulus of elasticity, as defined in Equation 2.12:

$$E_d = V_s^2 \rho \frac{3(V_p/V_s)^2 - 4}{(V_p/V_s)^2 - 1} \qquad (2.1)$$

For each sample $E_d$ was calculated. In addition, two similar parameters were defined:

$$E_{d\rho} = V_s^2 \rho_{av} \frac{3(V_p/V_s)^2 - 4}{(V_p/V_s)^2 - 1}$$

where $\rho_{av}$ is the average density of all samples from the same quarry of rock type, and:

$$E_\rho = E_d/\rho = V_s^2 \frac{3(V_p/V_s)^2 - 4}{(V_p/V_s)^2 - 1}$$

The Statistical Analysis System (SAS), available at the VPI & SU Computer Center, was utilized to determine the correlation between the static and dynamic properties. The results are shown on Figures 6.3 through 6.12 and are described by the following relations:

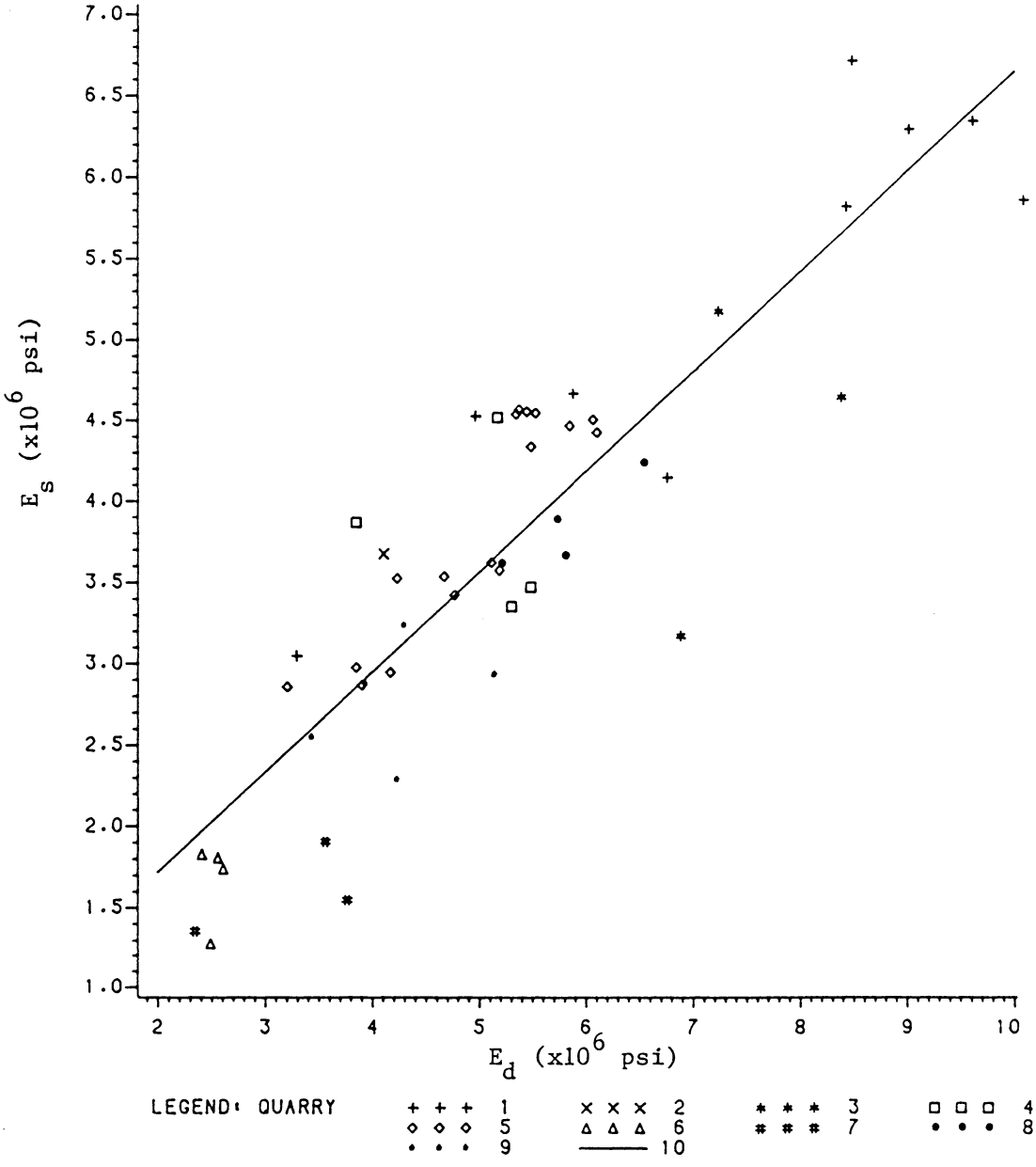


Figure 6.3 Relationship Between the Static and Dynamic Modulus of Elasticity

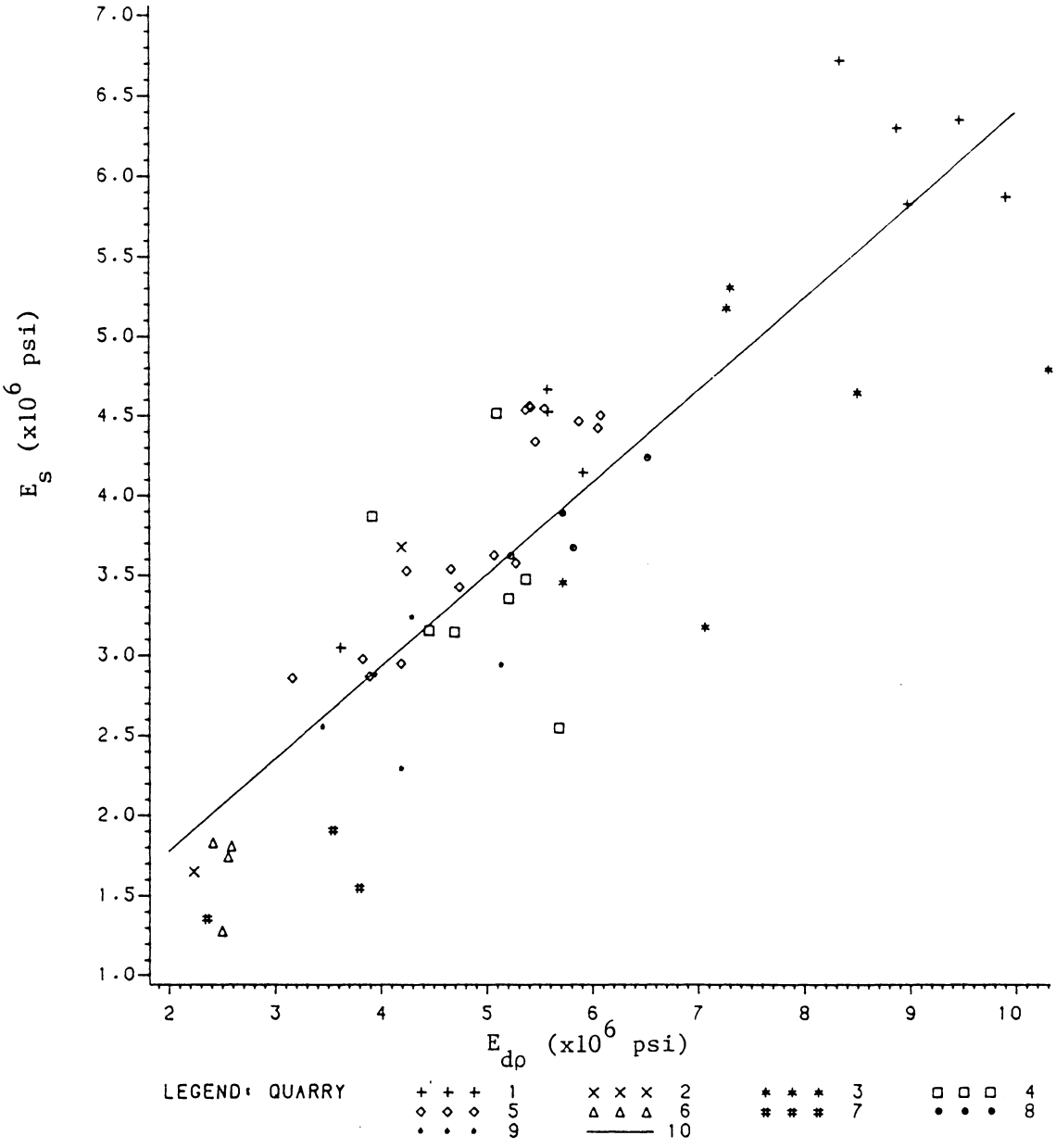


Figure 6.4 Relationship Between Static Modulus of Elasticity and the Dynamic Modulus (using the average density for each quarry)

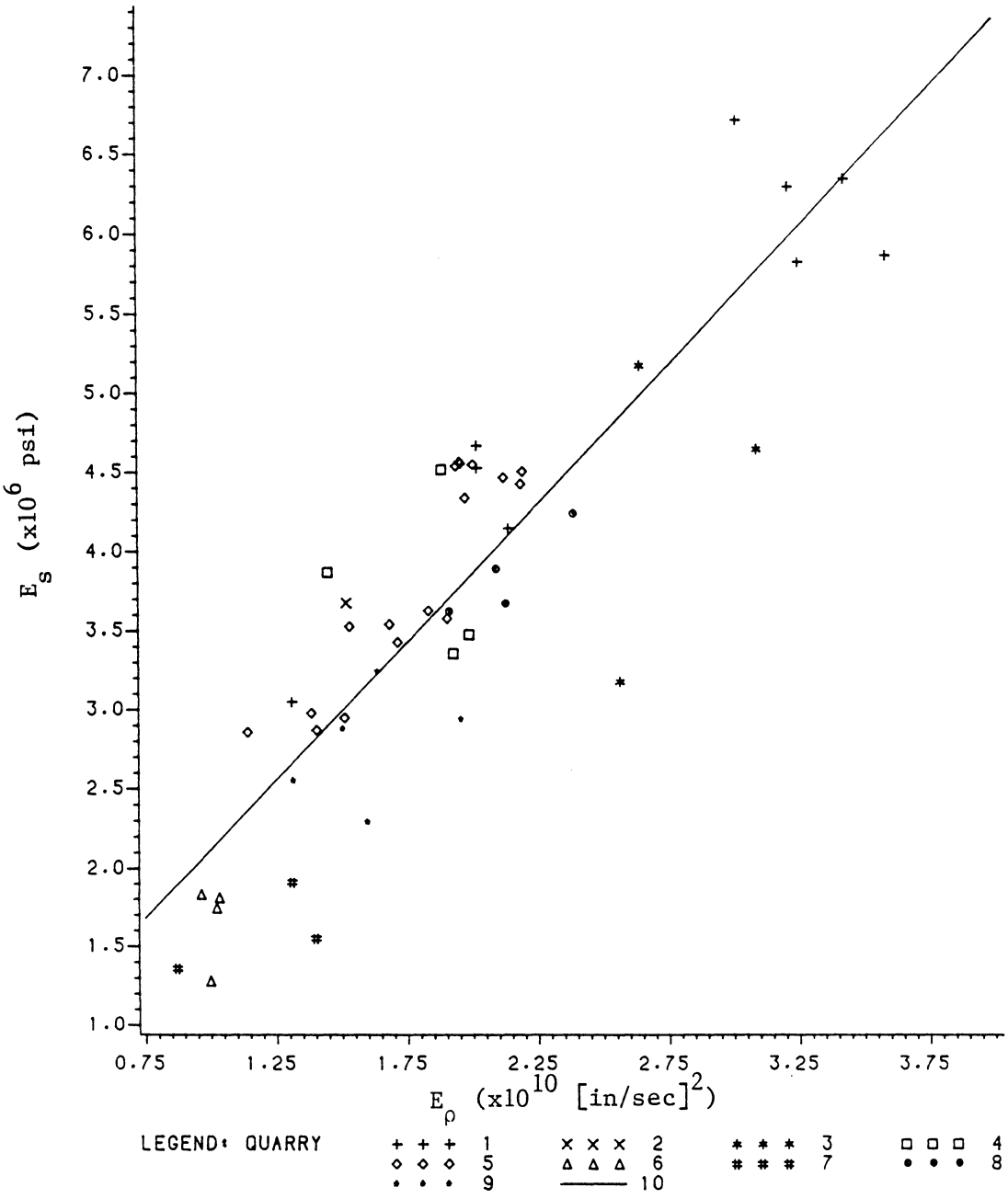


Figure 6.5 Relationship Between Static Modulus of Elasticity and the Ratio Dynamic Modulus/Density

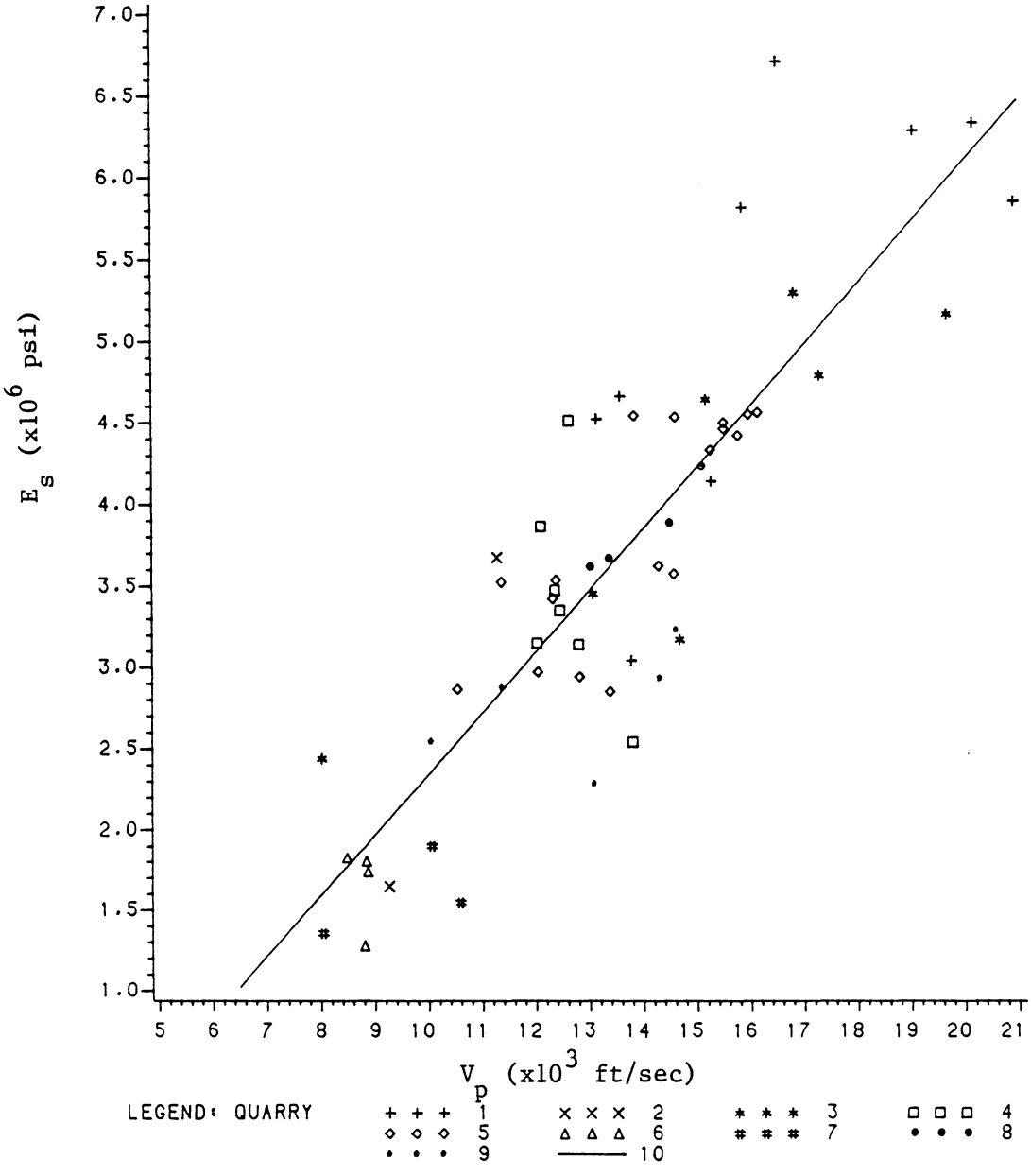


Figure 6.6 Relationship Between Static Modulus of Elasticity and the Velocity of the P-wave

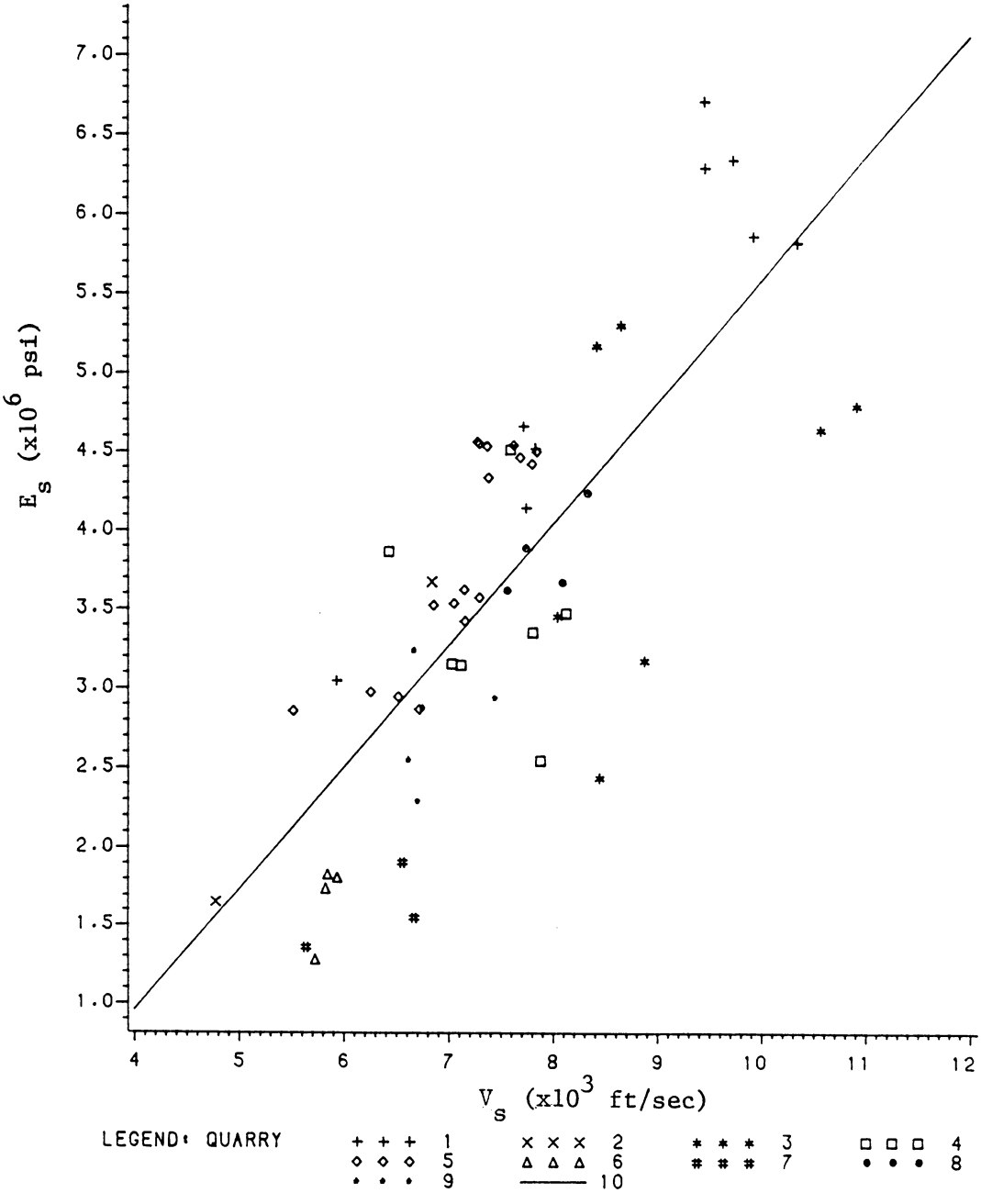


Figure 6.7 Relationship Between Static Modulus of Elasticity and the Velocity of the S-wave

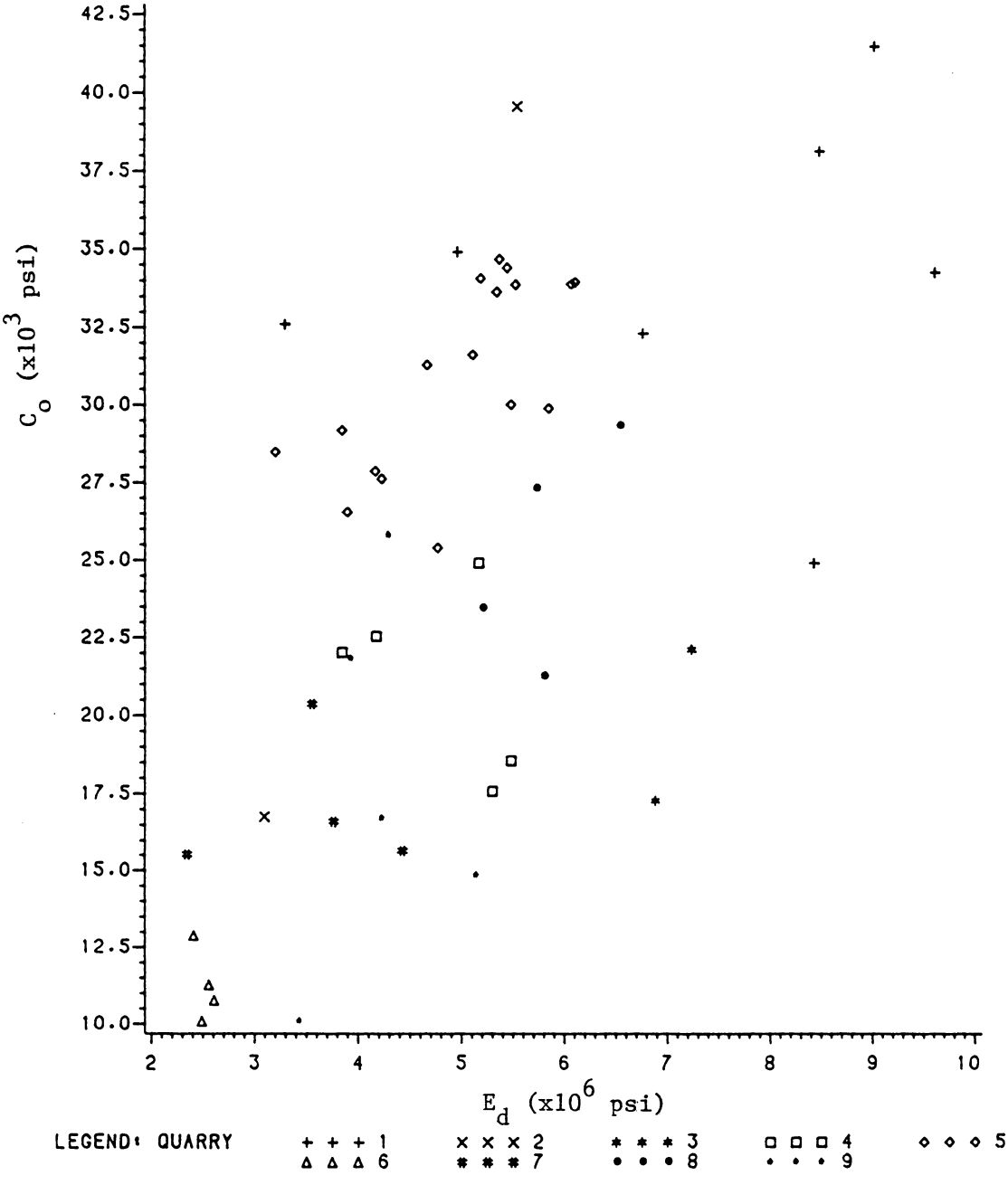


Figure 6,8 Unconfined Compressive Strength versus the Dynamic Modulus of Elasticity

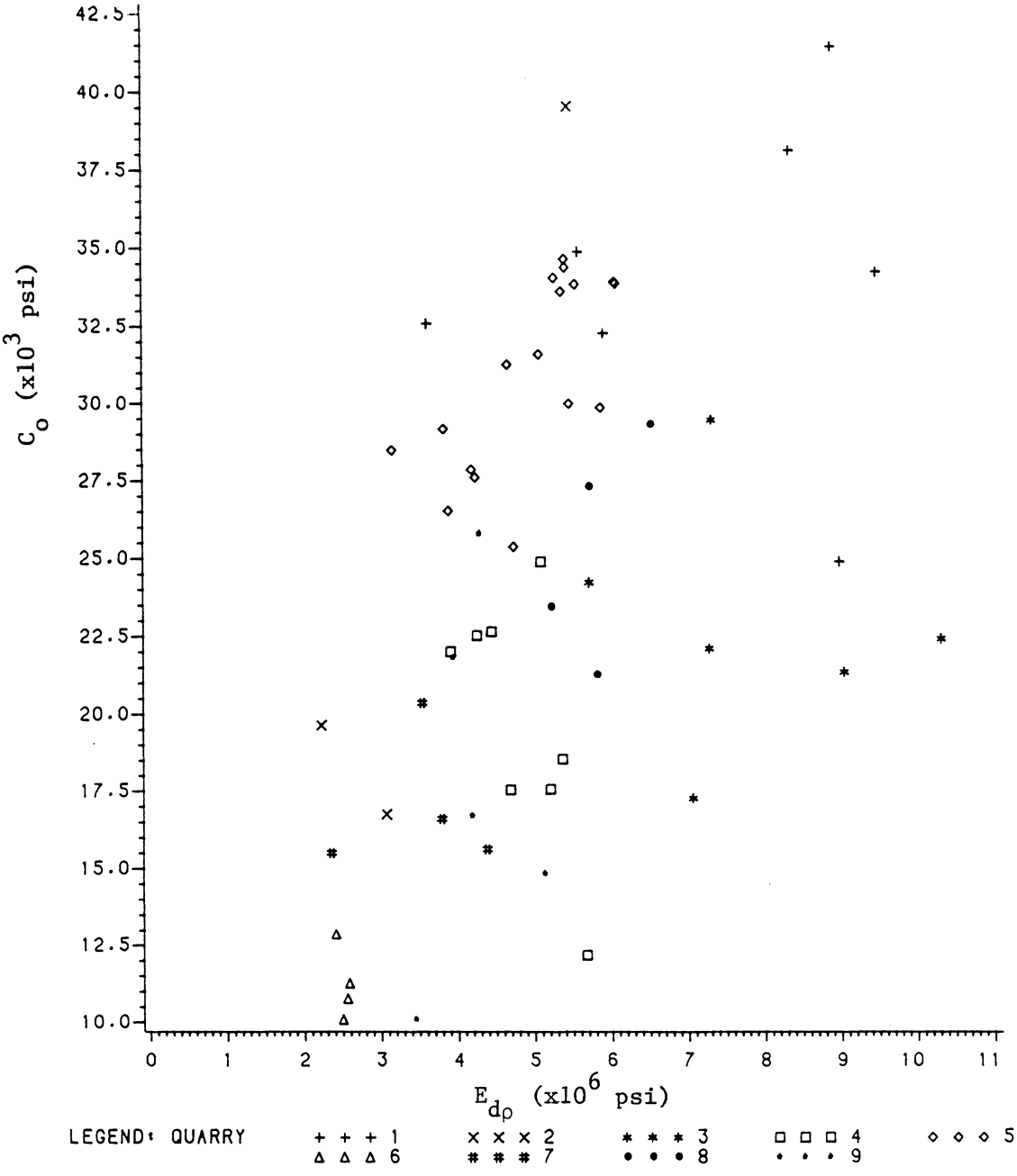


Figure 6.9 Unconfined Compressive Strength versus the Dynamic Modulus of Elasticity (using the average density for each quarry)

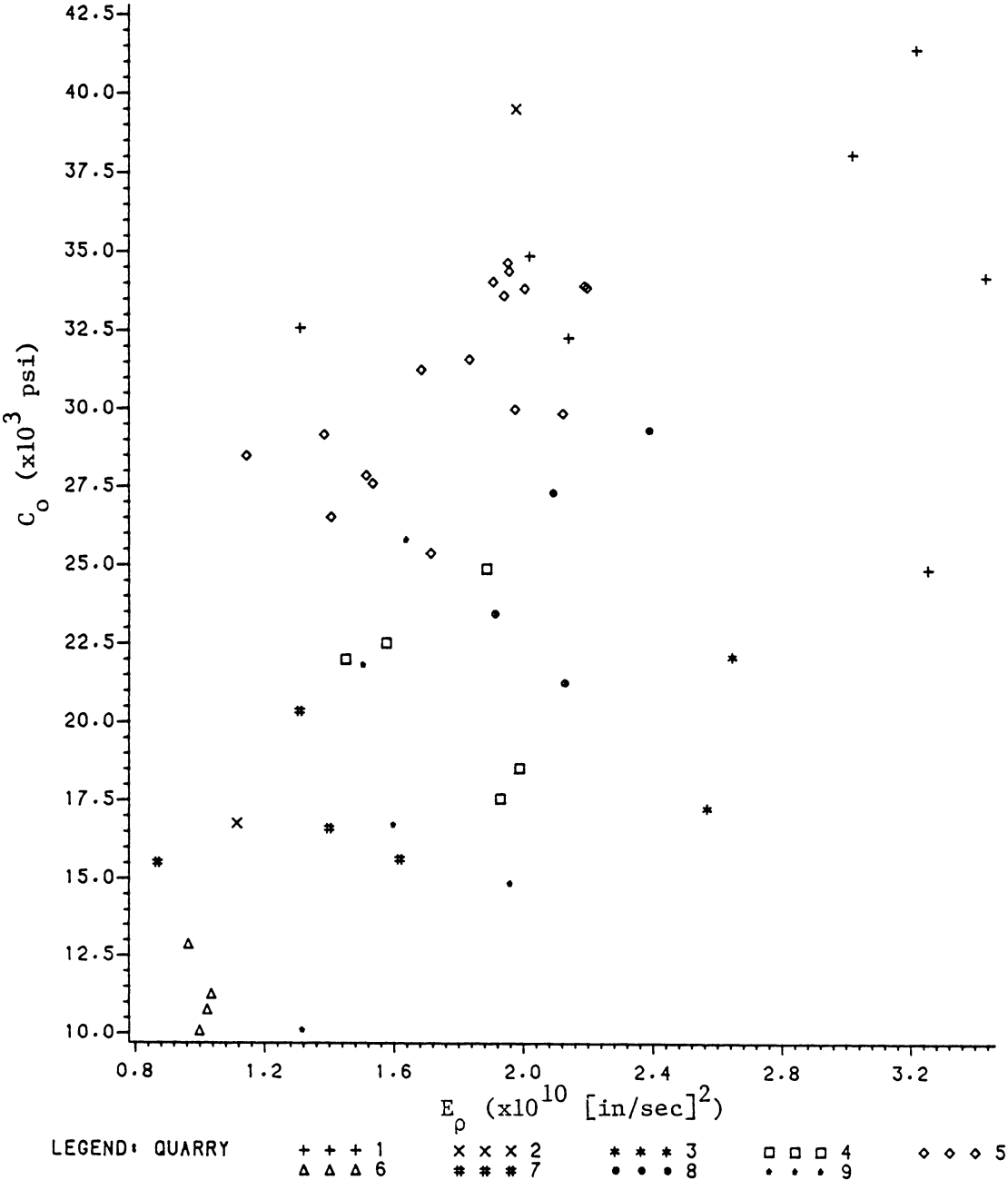


Figure 6.10 Unconfined Compressive Strength versus the Ratio Dynamic Modulus over Density

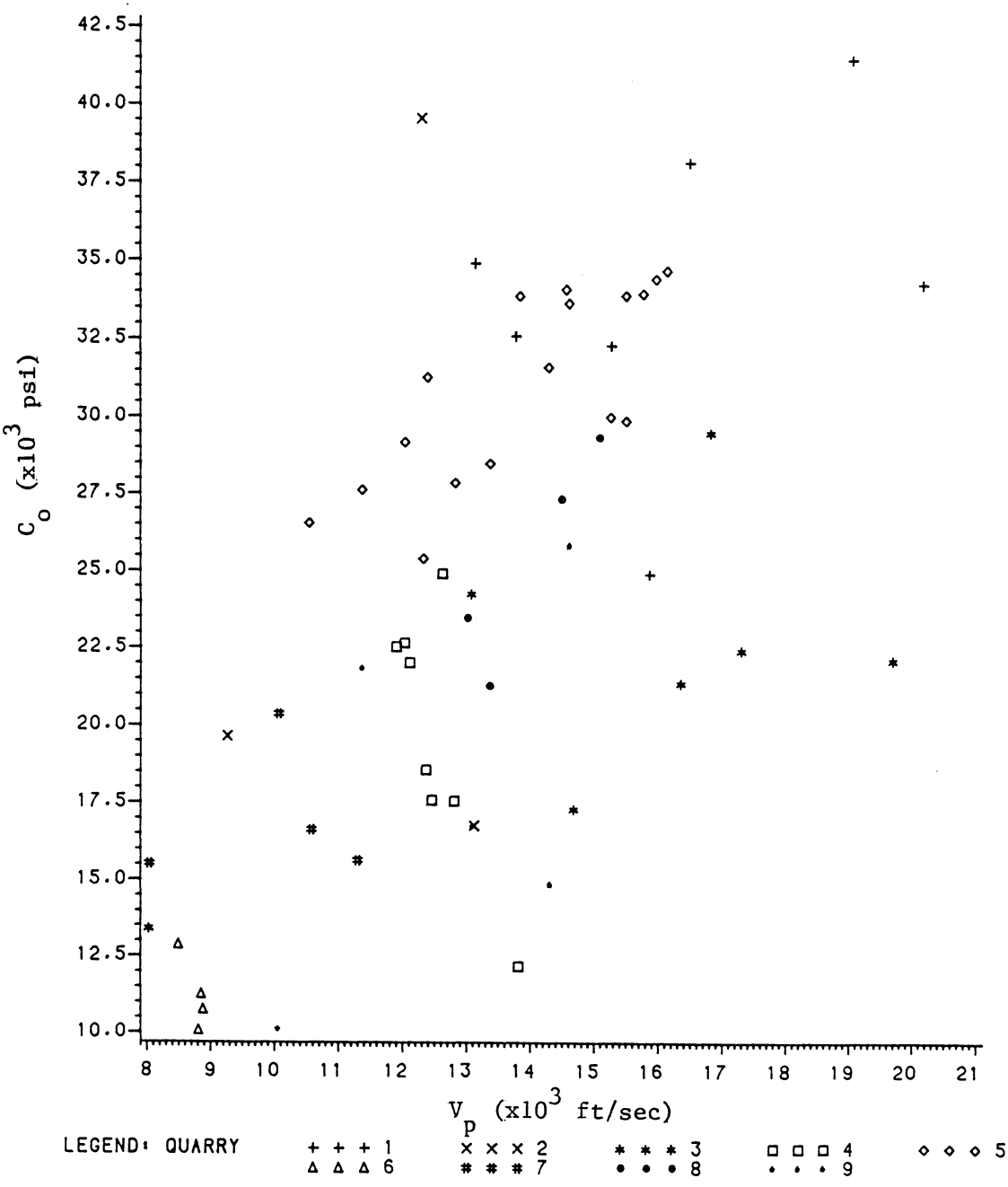


Figure 6.11 Unconfined Compressive Strength versus the Velocity of the P-wave

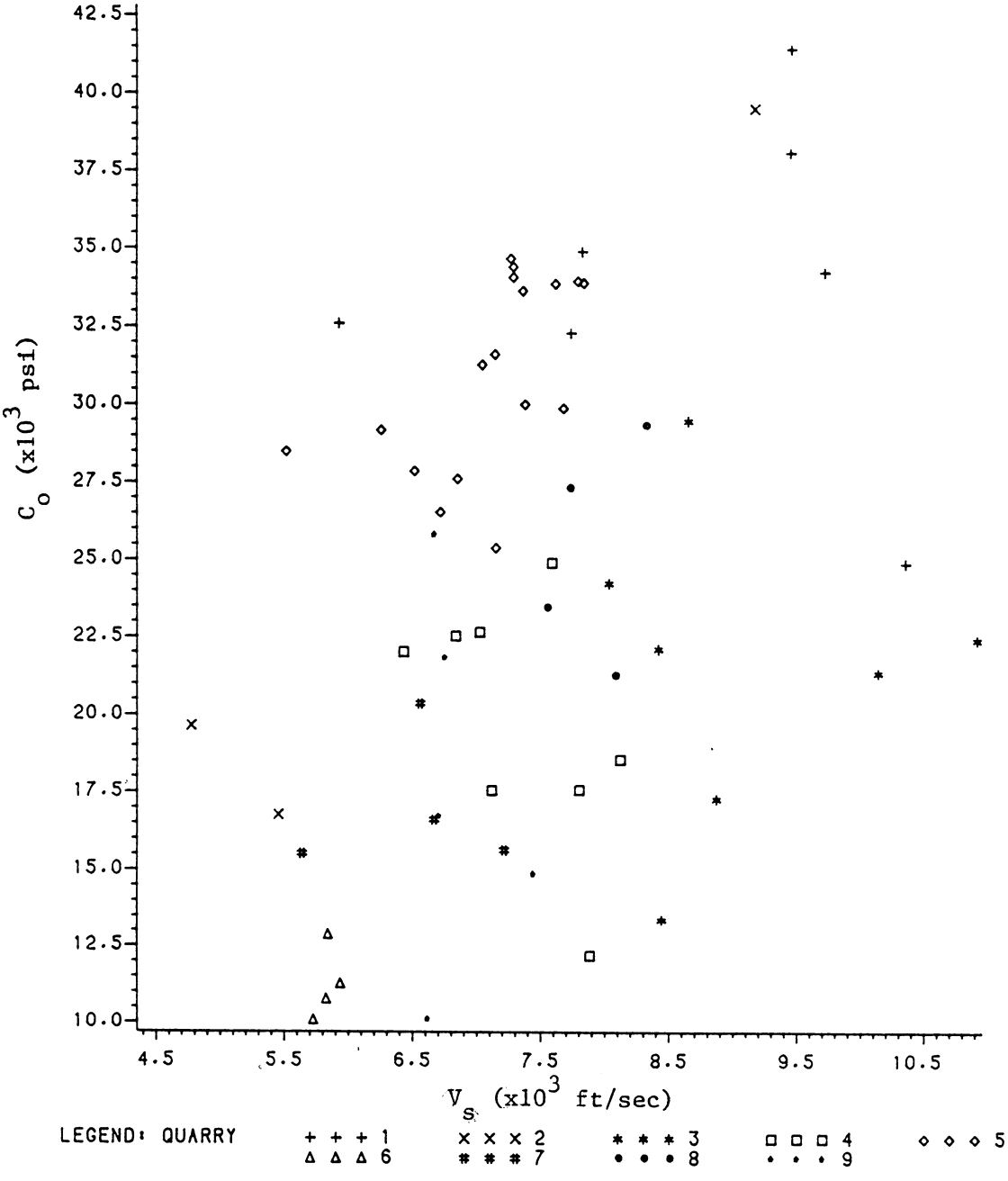


Figure 6.12 Compressive Strength versus the Velocity of the S-wave

(i) $E_s = 0.4858 + 0.6173\ E_d$

with $\rho^2 = 0.789$ and S.L. = 0.0001 (significance level)

(ii) $E_s = 0.6249 + 0.5769 \cdot E_{d\rho}$

with $\rho^2 = 0.749$ and S.L. = 0.0001

(iii) $E_s = 0.3693 + 1.747 \cdot E_{\rho}$

with $\rho^2 = 0.776$ and S.L. = 0.0001

(iv) $E_s = -1.4237 + 0.3770 \cdot 10^6\ V_p$

with $\rho^2 = 0.750$ and S.L. = 0.0001

(v) $E_s = -2.1292 + 0.7722 \cdot 10^6\ V_s$

In the above relations $E_s$ denotes the static modulus of elasticity and is expressed in psi. $V_p$ and $V_s$ are expressed in ft/sec. For $V_p$ and $V_s$ a quadratic model was also tested but $\rho^2$ was approximately 0.1 lower than for the linear model, as a result, the latter was preferred.

The statistical analysis for determining a relation between $C_o$ (compressive strength) and the dynamic parameters produced values for $\rho^2$ in the range of 0.3-0.35 which were not considered satisfactory to indicate any correlation.

### 6.2.4. Discussion of Results

In analyzing the results, it was found that some tests yielded irregular values (abnormally high or low), and as a result, for Figures 6.3 through 6.7 samples 2/1, 3/3, 4/1 and 7/3 were ignored.

For some of the quarries $E_s$ and $C_o$ varied considerably. This occurred because the samples represented different sites in the quarry, with differing joint frequencies and cementing materials.

The large number of samples (i.e., 64), the values of $\rho^2$ (0.75-0.8) and the significance level (0.0001) lead to the conclusion that the dynamic properties are a satisfactory method of estimating $E_s$. The best dynamic property for this purpose is $E_d$, however, $V_p$ can also be used with similar accuracy in cases where the measurement of $V_s$ is not possible.

The frequency of the P-waves and the S-waves appeared insensitive to the static properties. The frequencies received were almost equal to the resonance frequencies of the transducers (60 kHz for the P-wave and 33.3 kHz for the S-wave). As mentioned earlier, the frequencies are influenced by rock characteristics when the waves are traveling a distance several times their wavelength (the longest samples were approximately twice the length of the minimum measured wavelength).

The amplitudes were not measured because the instrumentation did not have the required accuracy for lateral measurements on the waveform.

It was observed that most received waveforms were sinusoidal. Some waveforms appeared to consist of two or more waves, with different first arrival times. They usually corresponded to jointed limestone or dolomite samples.

## 6.3. The Effects of Joints on Dynamic Properties

### 6.3.1. Sonic Wave Measurements on Dry Samples

The procedure described in Section 6.2.1. was followed for these experiments. Three different types of rock were tested, including a total of 15 samples (Table 6.2). After measuring $V_p$ and $V_s$ for all

samples, the samples were either cut in the diamond saw (samples 6/24, 6/25, 6/26) or broken manually. The effect of one crack on $V_p$ and $V_s$ was measured. The procedure was then repeated for as many cracks as the length of the sample would permit. The results are given in Table 6.4.

As described in Chapter II (elastic model), there should be a correlation between the frequency of fractures and the velocities of the P-wave and S-wave, in the form:

$$n/L = A - B \cdot \frac{1}{V_n}$$

The comparison of the theoretical model and the experimental data for samples from Quarry No. 5 (Arvonia Slate) is presented in Figures 6.13 and 6.14. The graphs corresponding to other samples are presented in Appendix B. The following relationships were derived, by using the Statistical Analysis System (SAS):

For Quarry No. 5:

$$n/L = 64.0/V_p - 3.83$$

$$\rho^2 = 0.851 \quad S.L. = 0.0001$$

$$n/L = 49.83/V_s - 5.09$$

$$\rho^2 = 0.784 \quad S.L. = 0.0001$$

For Rock Type No. 6:

$$n/L = 48.24/V_p - 4.78$$

$$\rho^2 = 0.826 \quad S.L. = 0.0001$$

$$n/L = 15.66/V_s - 1.927$$

$$\rho^2 = 0.853 \quad S.L. = 0.0001$$

Table 6.4

Values of $V_p$ and $V_s$ for Fractured Samples

| Sample Number | Number of Cracks | $V_p$ ($\times 10^4$ in/sec) | $V_s$ ($\times 10^4$ in/sec) |
|---|---|---|---|
| 5/21 | 1 | 13.17 | 8.19 |
| | 2 | 10.14 | 7.40 |
| | 3 | 6.62 | 5.41 |
| 5/22 | 0 | 19.07 | 10.70 |
| | 1 | 16.12 | 8.97 |
| | 2 | 10.19 | 6.15 |
| | 3 | 8.92 | 4.82 |
| | 4 | 5.18 | 3.63 |
| 5/23 | 0 | 15.43 | 9.66 |
| | 1 | 14.03 | 8.43 |
| | 2 | 8.92 | 5.99 |
| | 3 | 6.74 | 5.58 |
| 6/21 | 0 | 11.95 | 9.29 |
| | 1 | 9.84 | 7.04 |
| | 2 | 7.30 | 4.85 |
| | 3 | 5.27 | 2.97 |
| 6/22 | 0 | 11.81 | 8.99 |
| | 1 | 9.84 | 6.80 |
| | 2 | 8.59 | 4.57 |
| | 3 | 5.39 | 3.44 |
| 6/23 | 0 | 10.19 | 6.92 |
| | 1 | 9.59 | 6.08 |
| | 2 | 8.02 | 4.38 |
| | 3 | 6.08 | 3.23 |
| 6/24 | 0 | 11.01 | 8.37 |
| | 1 | 10.65 | 7.06 |
| | 2 | 8.83 | 4.19 |
| | 3 | 6.84 | 2.74 |
| 6/25 | 0 | 10.99 | 7.97 |
| | 1 | 10.37 | 7.28 |
| | 2 | 8.36 | 4.89 |
| | 3 | 6.81 | 2.43 |

Table 6.4 (continued)

Values of $V_p$ and $V_s$ for Fractured Samples

| Sample Number | Number of Cracks | $V_p$ ($\times 10^4$ in/sec) | $V_s$ ($\times 10^4$ in/sec) |
|---|---|---|---|
| 6/26 | 0 | 11.60 | 8.09 |
| | 1 | 11.02 | 7.28 |
| | 2 | 9.01 | 4.89 |
| | 3 | 7.00 | 2.32 |
| 6/31 | 0 | 11.49 | |
| (Wet) | 1 | 11.325 | |
| | 2 | 11.225 | |
| | 3 | 10.16 | |
| 6/32 | 0 | 12.07 | |
| (Wet) | 1 | 11.63 | |
| | 2 | 11.23 | |
| | 3 | 10.16 | |
| 6/33 | 0 | 12.36 | |
| (Wet) | 1 | 11.74 | |
| | 2 | 11.46 | |
| | 3 | 10.32 | |
| 6/34 | 0 | 17.21 | |
| (Wet) | 2 | 16.90 | |
| | 3 | 13.12 | |
| 9/21 | 0 | 13.41 | 8.83 |
| | 1 | 10.82 | 7.79 |
| | 2 | 8.61 | 6.27 |
| | 3 | 7.02 | 4.62 |
| 9/22 | 0 | 8.87 | 7.06 |
| | 1 | 7.22 | 6.41 |
| | 2 | 6.44 | 4.21 |
| | 3 | 5.48 | 4.08 |

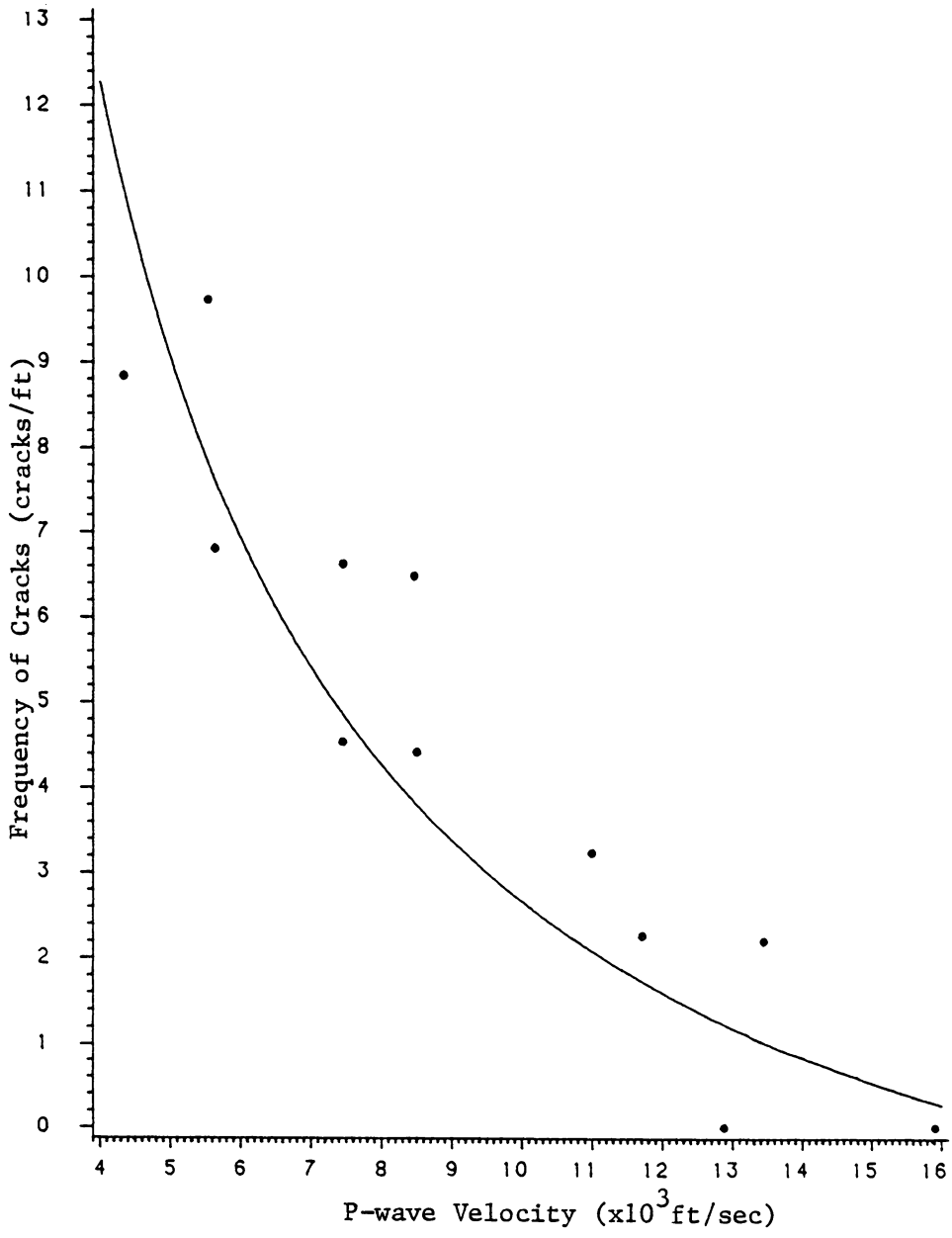


Figure 6.13 Effect of Cracks on P-wave Velocity, Quarry #5

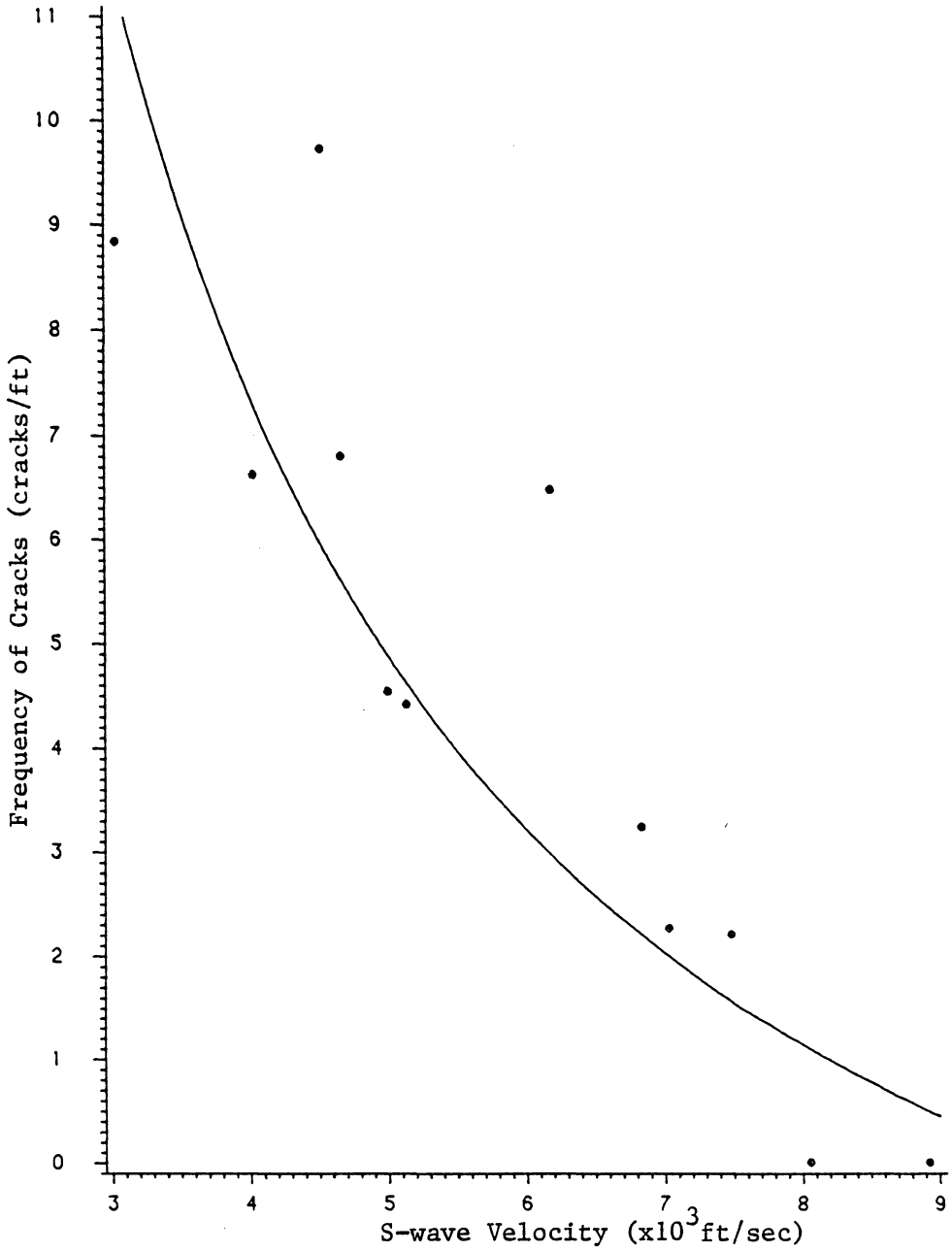


Figure 6.14 Effect of Cracks on S-wave Velocity, Quarry #5

For Rock Type No. 9:

$$n/L = 45.16/V_p - 4.41$$

$$\rho^2 = 0.615 \quad S.L. = 0.0212$$

$$n/L = 36.99/V_p - 5.16$$

$$\rho^2 = 0.773 \quad S.L. = 0.040$$

where $V_p$ and $V_s$ are expressed in thousands of ft/sec.

It can be observed from these graphs that a linear relationship may be valid for a certain range of joint spacing. Such a model is presented in Figures 6.15 and 6.16, for Quarry No. 5. The same model for the other samples is presented in Appendix B.

The relationships describing these models are given as follows:

For Quarry No. 5:

$$n/L = 12.32 - 0.83\ V_p$$

$$\rho^2 = 0.872 \quad S.L. = 0.0001$$

$$n/L = 14.09 - 1.61\ V_s$$

$$\rho^2 = 0.812 \quad S.L. = 0.0001$$

For Rock Type No. 6:

$$n/L = 9.62 - 0.97\ V_p$$

$$\rho^2 = 0.891 \quad S.L. = 0.0001$$

For Rock Type No. 9:

$$n/L = 8.75 - 0.82\ V_p$$

$$\rho^2 = 0.558 \quad S.L. = 0.0333$$

$$n/L = 10.23 - 1.42\ V_s$$

$$\rho^2 = 0.755 \quad S.L. = 0.0001$$

where $V_p$ and $V_s$ are expressed in thousands of ft/sec.

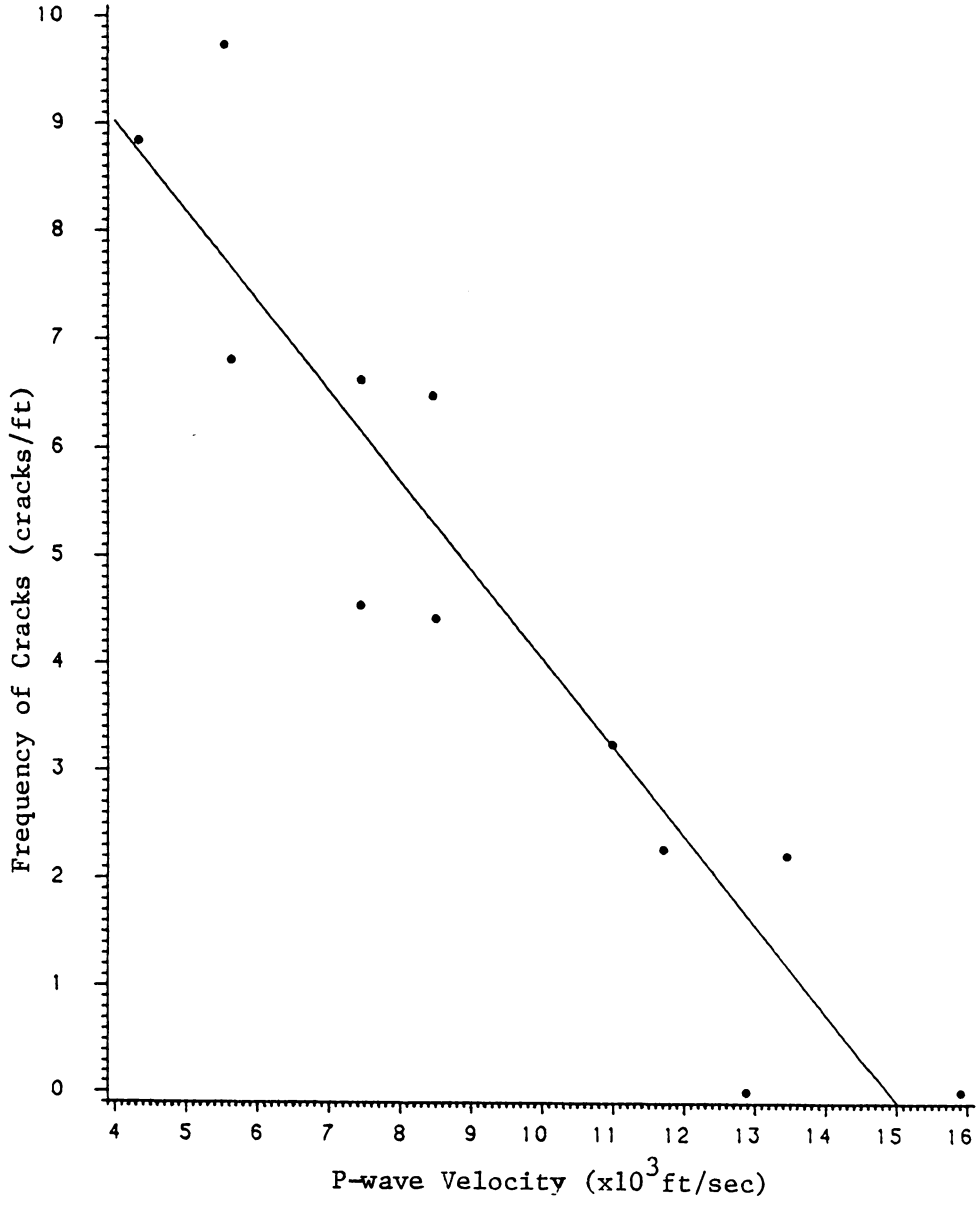


Figure 6.15 Effect of Cracks on P-wave Velocity, Quarry #5

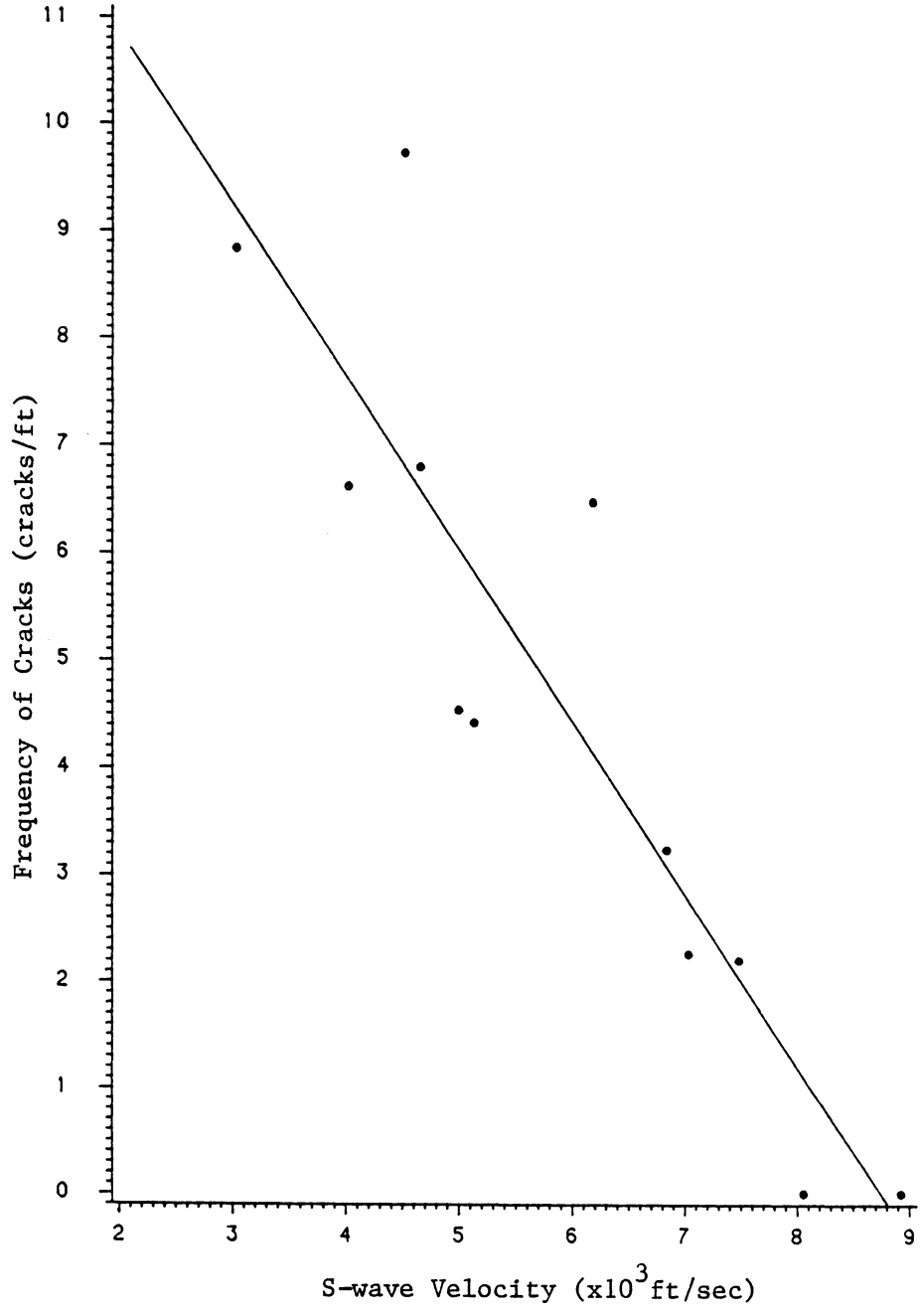


Figure 6.16 Effect of Cracks on S-wave Velocity, Quarry #5

The literature review has indicated that a correlation exists between RQD and the velocity index ($V_F/V_L$, where $V_F$ and $V_L$ are the velocities of P-wave in the field and in the laboratory, Coon and Merritt, 1970, Figure 4.5). The RQD mainly expresses the spacing of joints. This leads to the following relationships, by correlating the velocity index ($I_v = V/V_o$, where $V_o$ is the wave propagation velocity for intact samples) and the frequency of fractures (Figures 6.17 and 6.18):

For Quarry No. 5:

$$n/L = 12.95 - 12.95\ V_p/V_{po}$$
$$\rho^2 = 0.895 \quad S.L. = 0.0001$$

$$n/L = 14.64 - 14.64\ V_s/V_{so}$$
$$\rho^2 = 0.778 \quad S.L = 0.0001$$

For Rock Type No. 6:

$$n/L = 10.48 - 10.48\ V_p/V_{po}$$
$$\rho^2 = 0.837 \quad S.L.\ 0.0001$$

$$n/L = 7.06 - 7.06\ V_s/V_{so}$$
$$\rho^2 = 0.943 \quad S.L. = 0.0001$$

For Rock Type No. 9:

$$n/L = 12.87 - 12.87\ V_p/V_{po}$$
$$\rho^2 = 0.946 \quad S.L. = 0.0001$$

$$n/L = 12.56 - 12.56\ V_s/V_{so}$$
$$\rho^2 = 0.932 \quad S.L. = 0.0001$$

Finally, the above relations are combined, for all three rock types in the following:

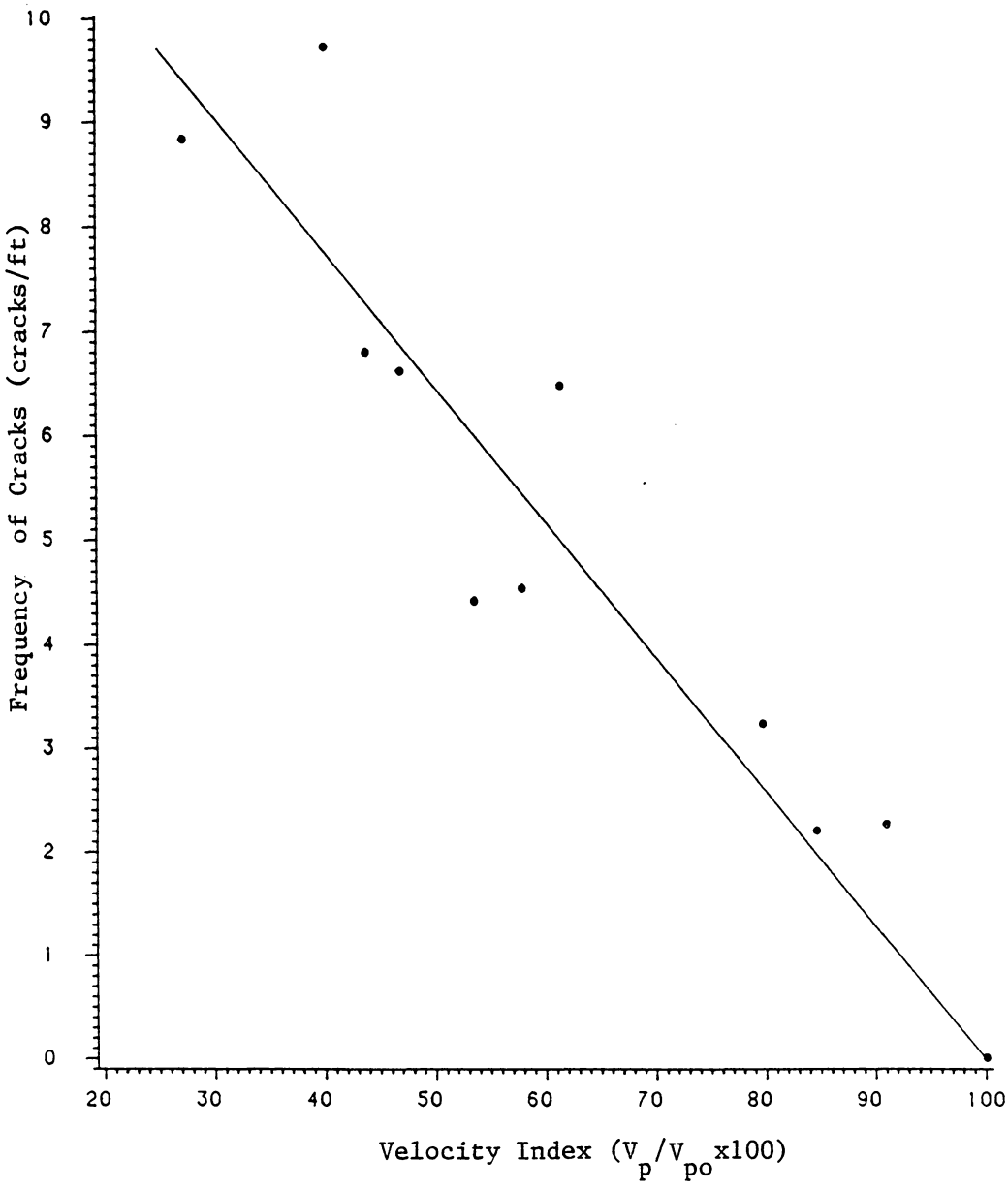


Figure 6.17 Effect of Cracks on the Velocity Index, Quarry #5

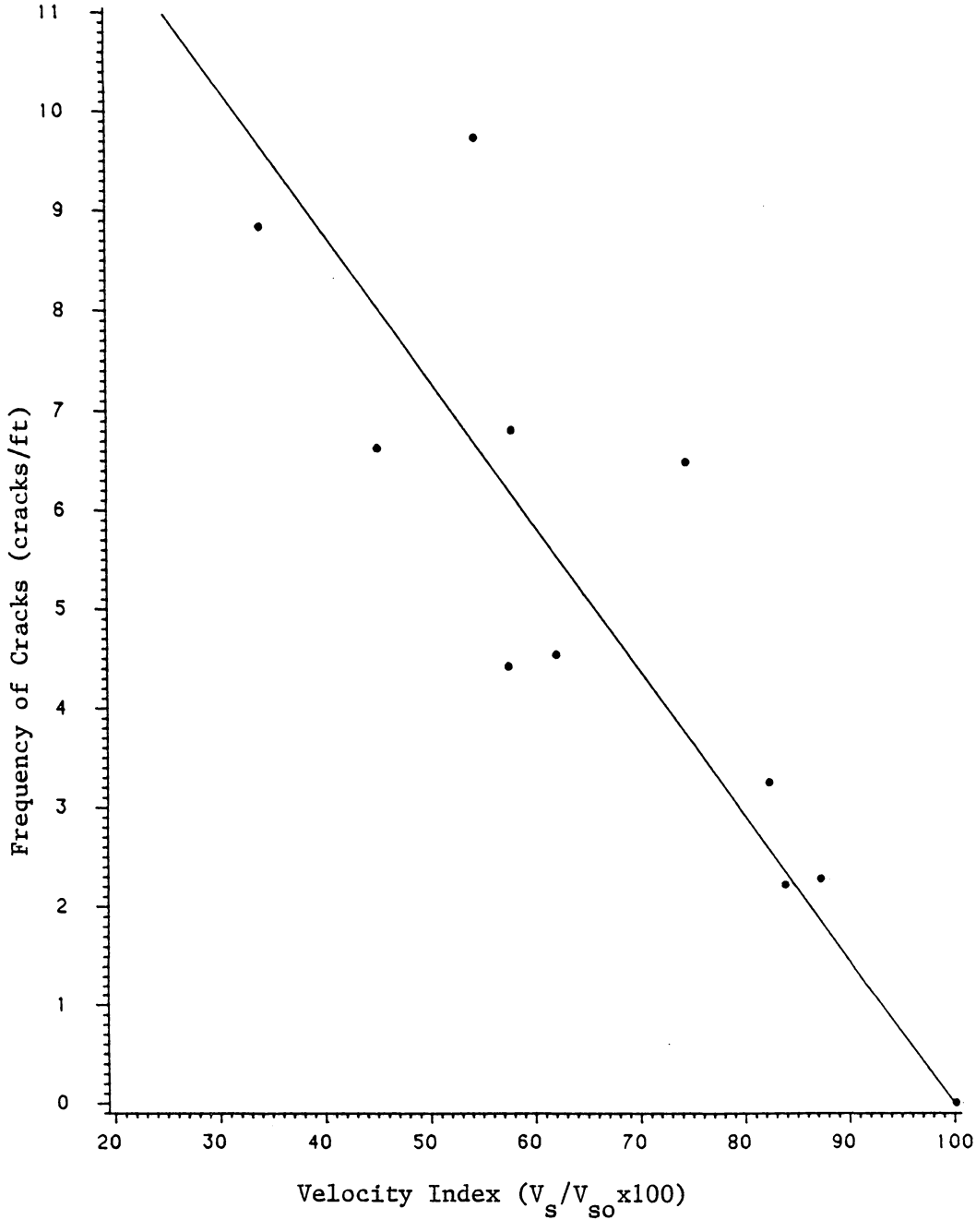


Figure 6.18 Effect of Cracks on the Velocity Index, Quarry #5

$$n/L = 11.321 - 11.32\ V_p/V_{po}$$

$$\rho^2 = 0.877 \quad S.L. = 0.0001$$

$$n/L = 8.68 - 8.68\ V_s/V_{so}$$

$$\rho^2 = 0.718 \quad S.L. = 0.0001$$

Figures 6.19 and 6.20 present a comparison of the above relationships and the experimental data.

6.3.2. Sonic Wave Measurements on Wet Samples

In order to determine the effect of fractures in saturated samples, on the velocities of P-waves and S-waves, four sandstone samples (Rock Type No. 6) were used. The procedure described in Section 6.3.1. was followed. The samples were considered to be saturated with water after being submerged for 48 hours. The tests were conducted in water and the transducers were protected by waterproof plastic. As a result, the S-wave transducers did not produce any results. The results of the experiments are presented in Table 6.4, in Figures 6.21, 6.22 and 6.23 and are described by the following relationships:

$$n/L = 28.4 - 2.77\ V_p \qquad (V_p: \text{ x 1000 ft/sec})$$

$$\rho^2 = 0.813 \quad S.L. = 0.0001$$

$$n/L = 235.3/V_p - 22.83$$

$$\rho^2 = 0.805 \quad S.L. = 0.0001$$

$$n/L = 34.24 - 34.24\ V_p/V_{po}$$

$$\rho^2 = 0.909 \quad S.L. = 0.0001$$

Figure 6.24 presents a comparison between the results for wet and dry conditions.

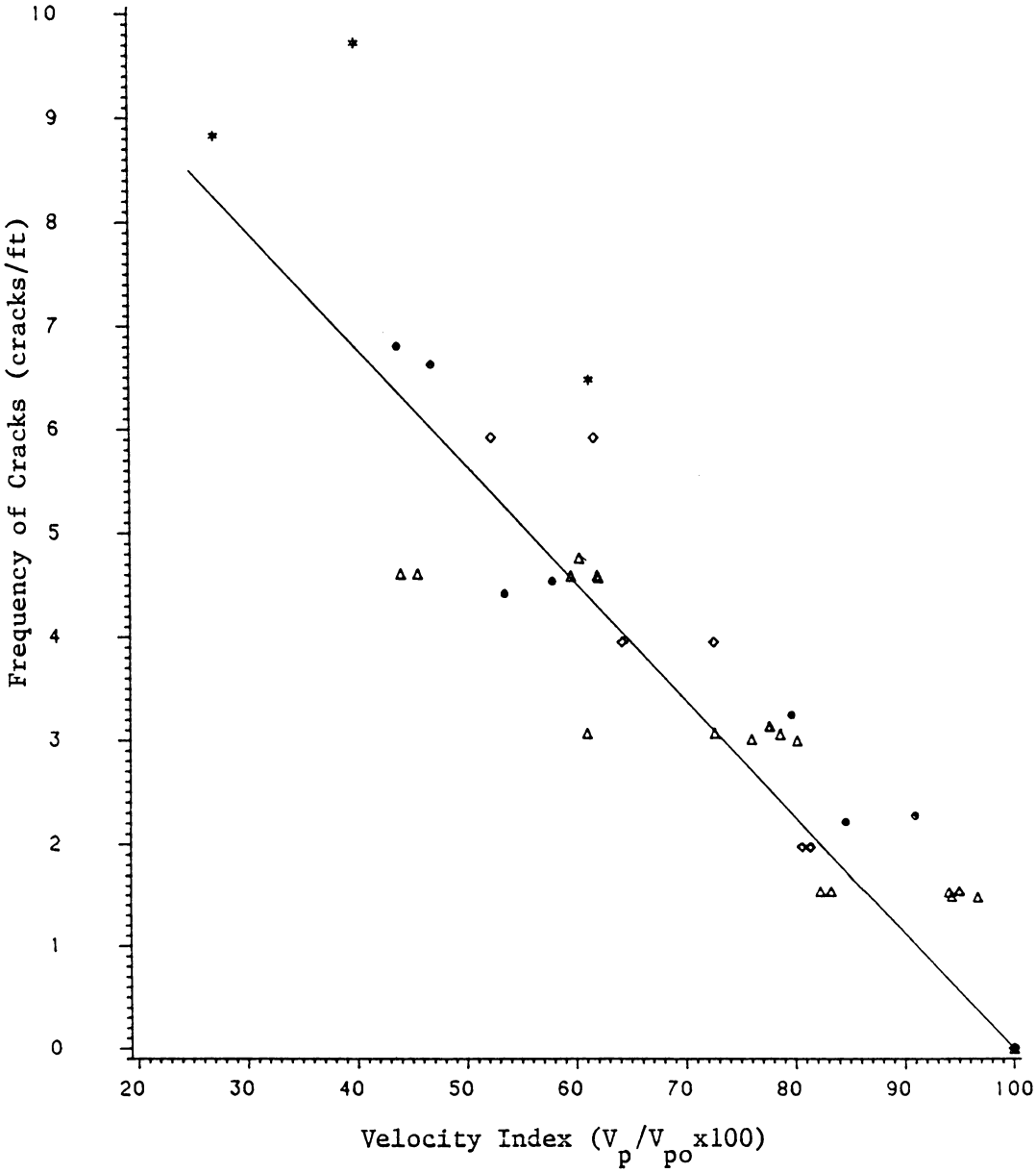


CIRCLED DOTS ARE SAMPLES FROM QUARRY 5
STARS ARE DELETED SAMPLES FROM QUARRY 5
TRIANGLES ARE SAMPLES FROM QUARRY 6
DIAMONDS ARE SAMPLES FROM QUARRY 9

FIgure 6.19 Effect of Cracks on the Velocity Index

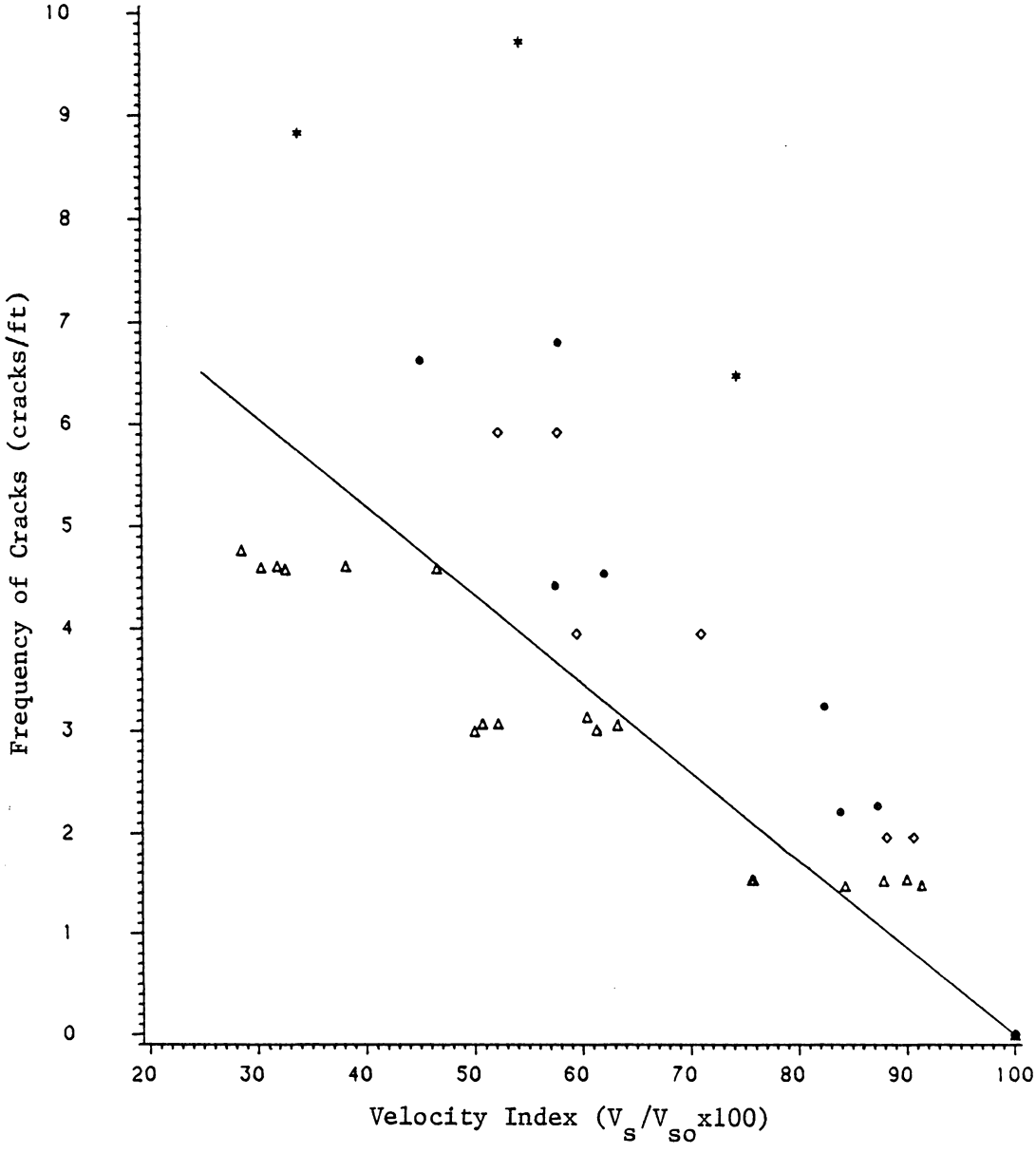


Figure 6.20 Effect of Cracks on the Velocity Index

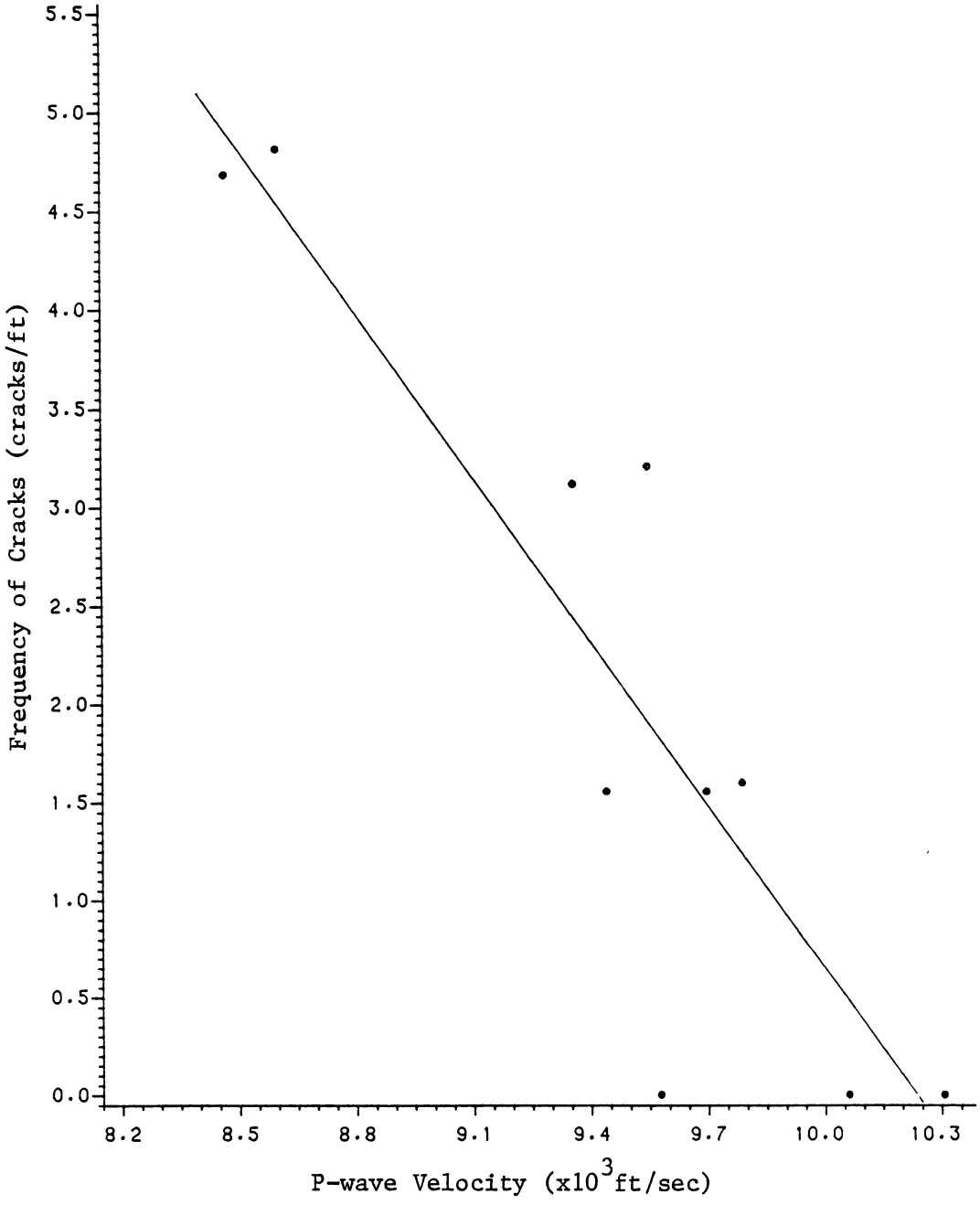


Figure 6.21 Effect of Cracks on P-wave Velocity, Wet Samples

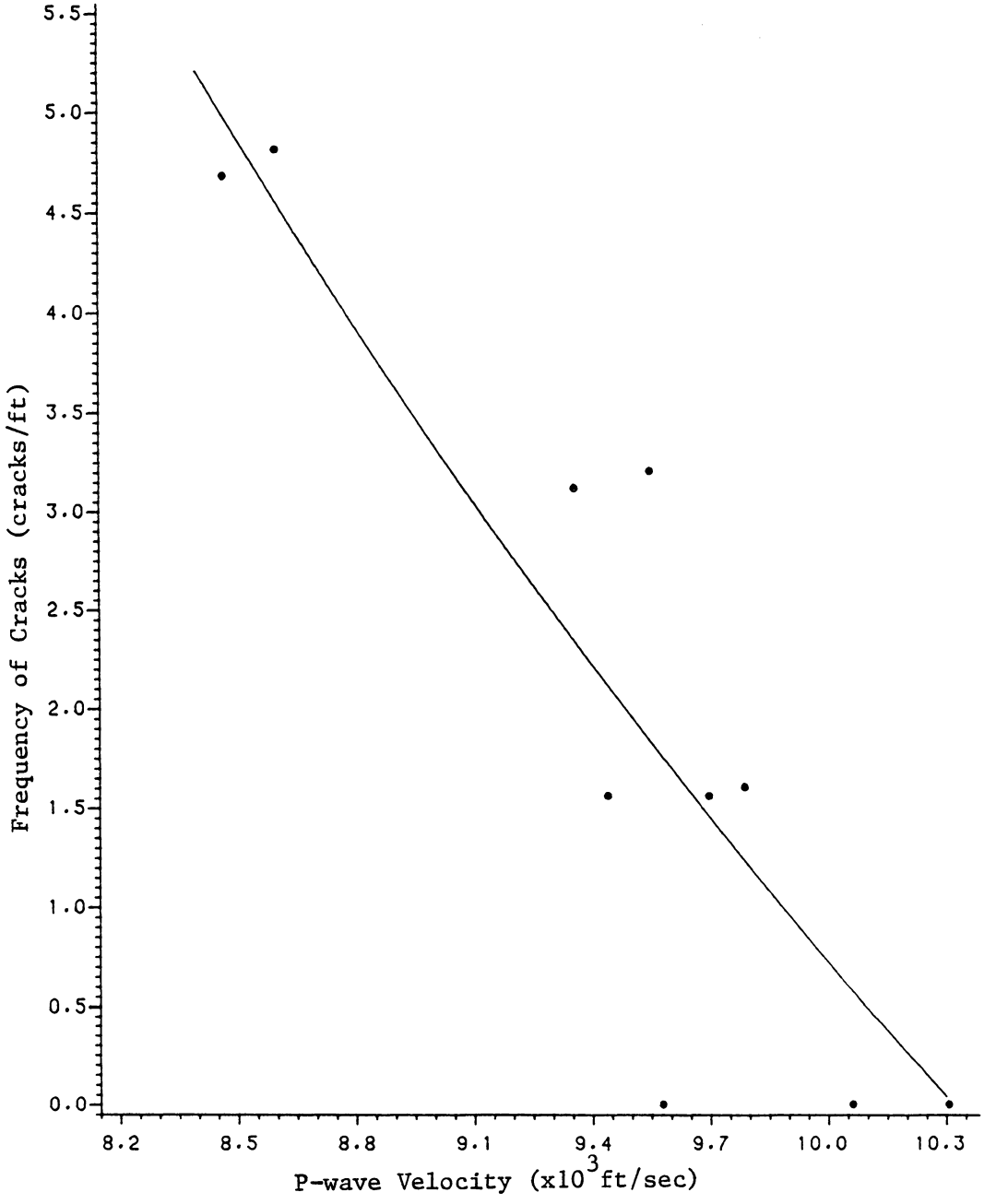


Figure 6.22 Effect of Cracks on P-wave Velocity, Wet Samples

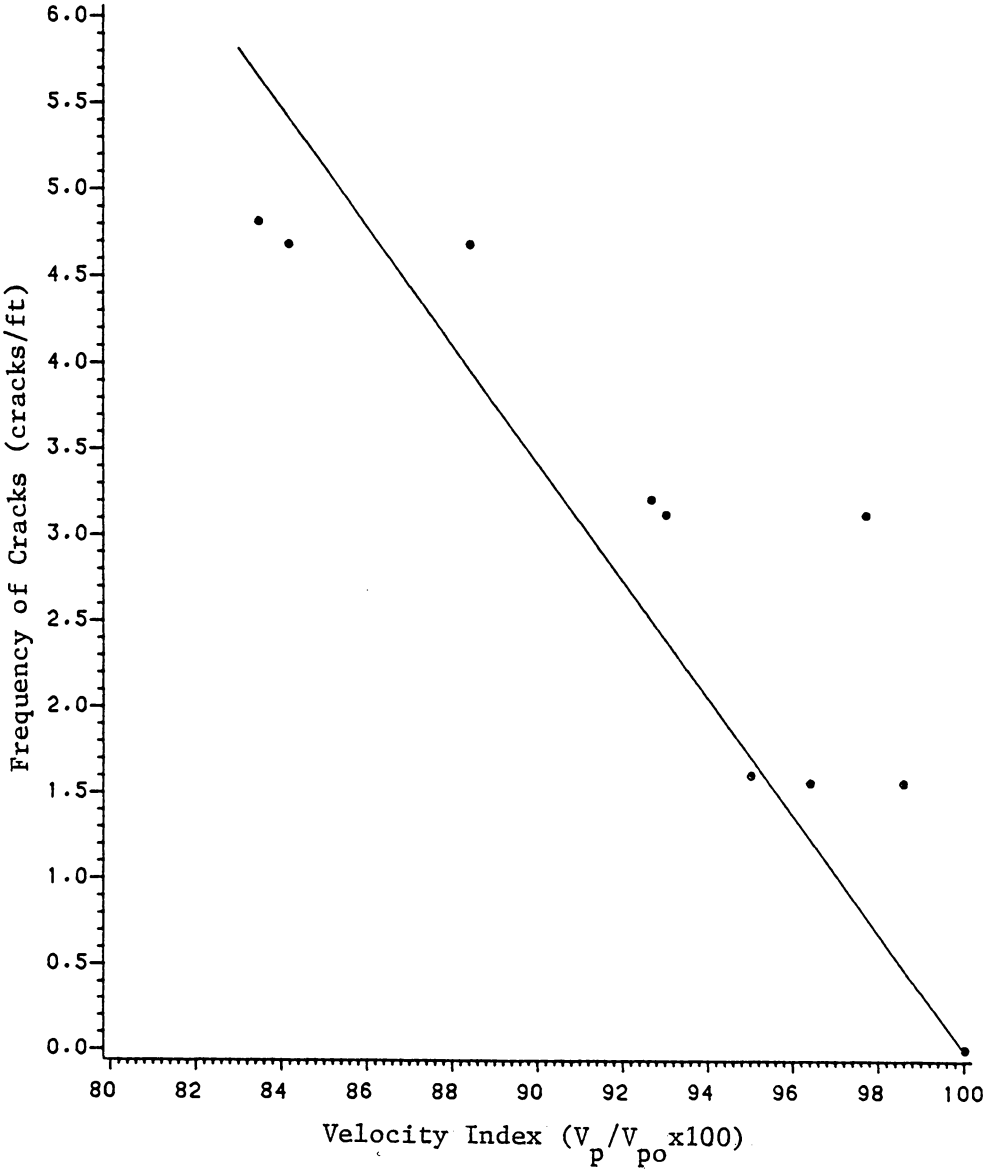


Figure 6.23 Effect of Cracks on the Velocity Index, Wet Samples

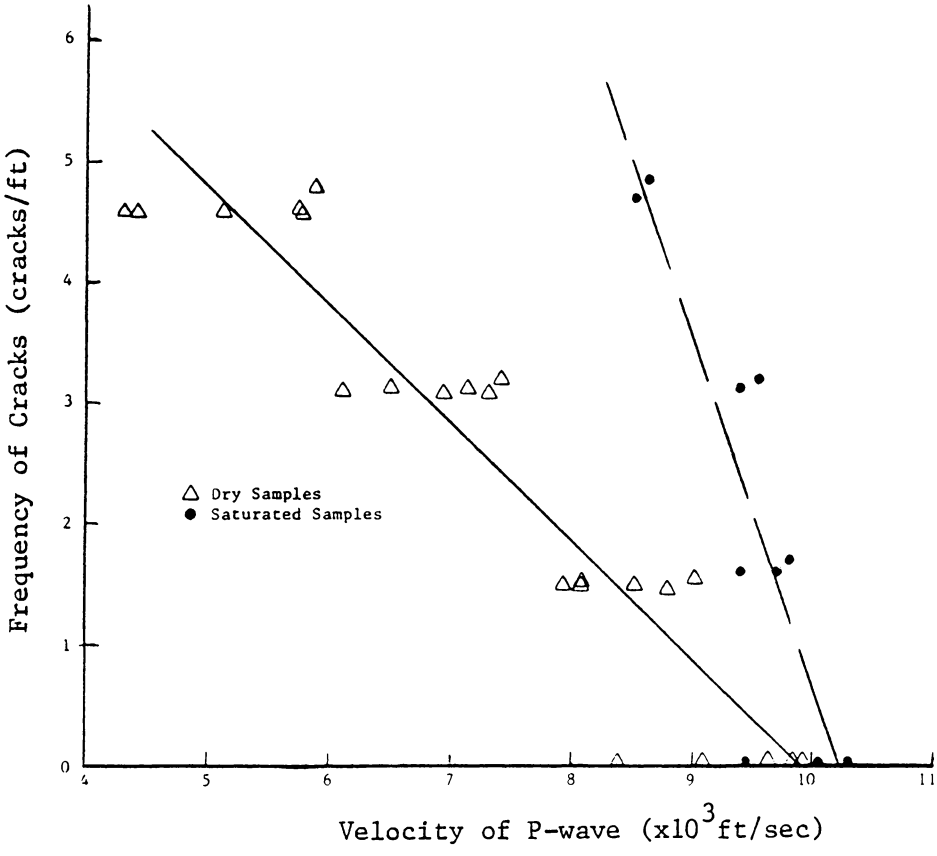


Figure 6.24 Comparison of Sonic Tests Between Dry and Wet Samples

6.3.3. Discussion of Results

A correlation between the frequency of joints and the velocity of P-waves and S-waves has been established, since the values of $\rho^2$ and the significance level are very satisfactory, for all relationships in Section 6.3.2. The simple model derived by the theoretical analysis in the form:

$$n/L = A \cdot \frac{1}{V} - B$$

should best describe such a correlation. However, since the linear model gives an estimation of the joint spacing with the same accuracy, it is preferred for field applications.

The relationships using $V_s$ to estimate the frequency of joints have a value of $\rho^2$ greater than similar relationships using $V_p$. However, for field tests, $V_p$ can be used to estimate the spacing of joints, if $V_s$ cannot be measured accurately.

Although the measurement of received wave amplitude was not accurate, a general observation was that shear wave amplitudes were significantly reduced when the joint surfaces were smooth.

# CHAPTER VII

## APPLICATION OF SONIC METHODS FOR ROCK CLASSIFICATION

### 7.1. The Classification of Intact Rock

Two properties are mainly used to classify rock material, the compressive strength ($C_o$) and the modulus of elasticity ($E_s$).

Figures 6.3 and 6.6 show that $E_d$ and $V_p$ can be used to estimate $E_s$, within satisfactory limits of accuracy. The compressive strength, however, cannot be estimated from dynamic tests because of the low correlation ($\rho^2$ around 0.3) with dynamic properties. If a field testing method is necessary, the Point Load Index can be easily used.

A modification of the Deere and Miller classification system is presented in Table 7.1 and Figure 7.1. The advantage of this system is that both tests (dynamic and Point Load Index) can be conducted in the field.

### 7.2. The Classification of Rock Mass

Dynamic tests can be used for estimating the spacing of joints, the condition of joint surfaces, the filling material and the water content. However, not all of these parameters can be determined from sonic tests. From Equation 2.13:

$$\frac{n}{L} = \frac{1}{t_c} \cdot \frac{1}{V_n} - \frac{1}{t_c V} = A \cdot \frac{1}{V_n} - B \qquad (2.13)$$

Table 7.1

Classification of Intact Rock

I. On Basis of Stength

| Class | Description | Point Load Index (psi) |
|---|---|---|
| A | Very High Strength | Over 2,400 |
| B | High Strength | 1,200-2,400 |
| C | Medium Strength | 600-1,200 |
| D | Low Strength | 300- 600 |
| E | Very Low Strength | Less than 300 |

II. On Basis of Modulus Ratio

| Class | Description | Modulus Ratio[1] |
|---|---|---|
| H | High Modulus Ratio | Over 20 |
| M | Average Modulus Ratio | 10-20 |
| L | Low Modulus Ratio | Less than 10 |

1) Modulus Ratio= $E_d/I_s$

where $E_d$= Dynamic Modulus of Elasticity

$I_s$= Point Load Index

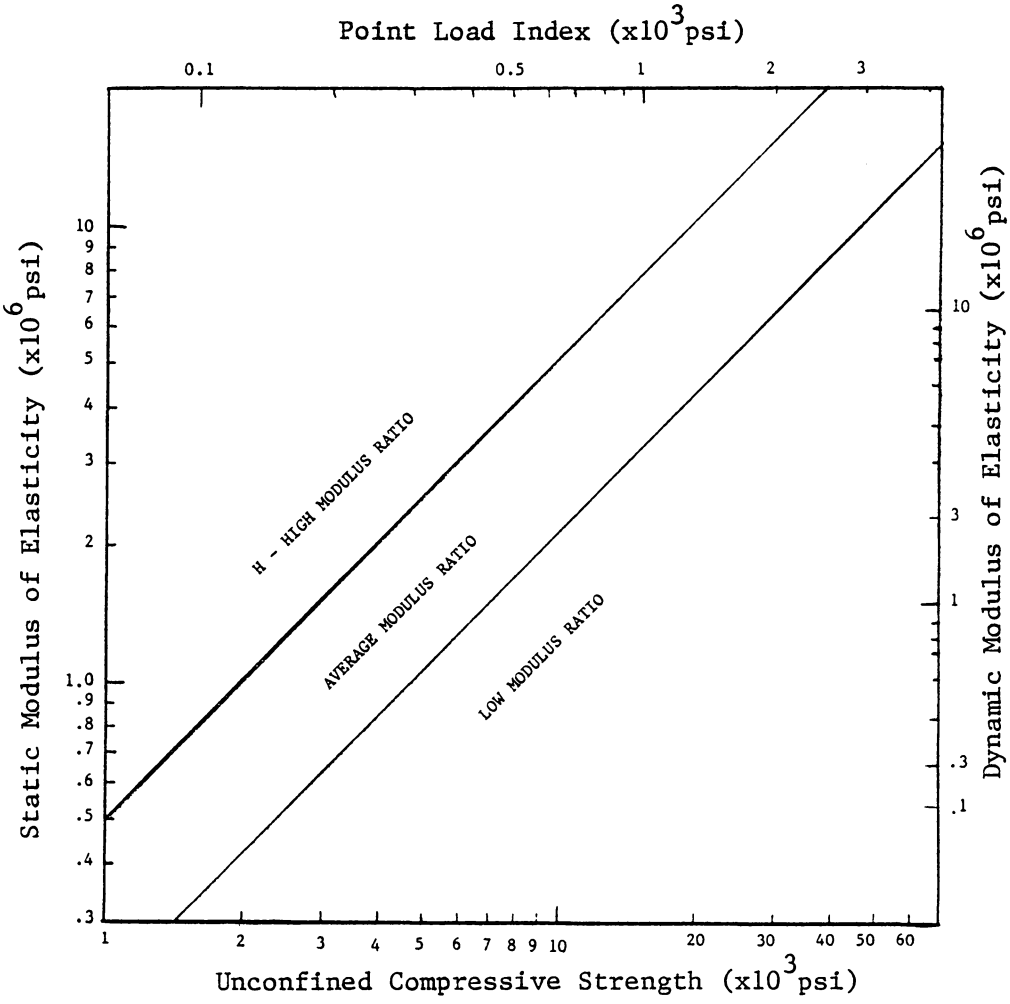


Figure 7.1 Classification of Intact Rock

where: n/L: the frequency of joints

$V_n$: the velocity of the P-wave or the S-wave

A, B: parameters defined by experiments, depending on rock type and joint characteristics.

However, it was shown in Chapter VI that a linear model can approximate this relationship, at least for a certain range of joint spacing; as shown below:

$$n/L = C - D \cdot V_n .$$

When the constants A, B, C or D are determined from field data or laboratory tests, simulating the conditions of the rock mass, the wave velocity can replace the spacing of joints in a classification system.

Another alternative would be to substitute the spacing of joints in a classification system by using the relationship:

$$n/L = E - F \left(\frac{V_n}{V_o}\right)$$

where: $\left(\frac{V_n}{V_o}\right)$: the velocity index ($I_v$)

$V_o$ : the wave velocity for intact rock

E, F : Constants.

The advantage of this relationship is that it is independent of the rock type, when the wave velocities do not differ by more than 5,000 ft/sec in intact samples.

A classification system has been developed, by modifying Franklin's Rock Quality Classification, (Franklin et al. 1971) and is presented

in Figure 7.2. It has to be emphasized that the correlation between $V_p$ or $V_s$ and the spacing of joints has to be determined for different joint conditions. Table 7.2 shows the effect of joint conditions on the shear wave propagation.

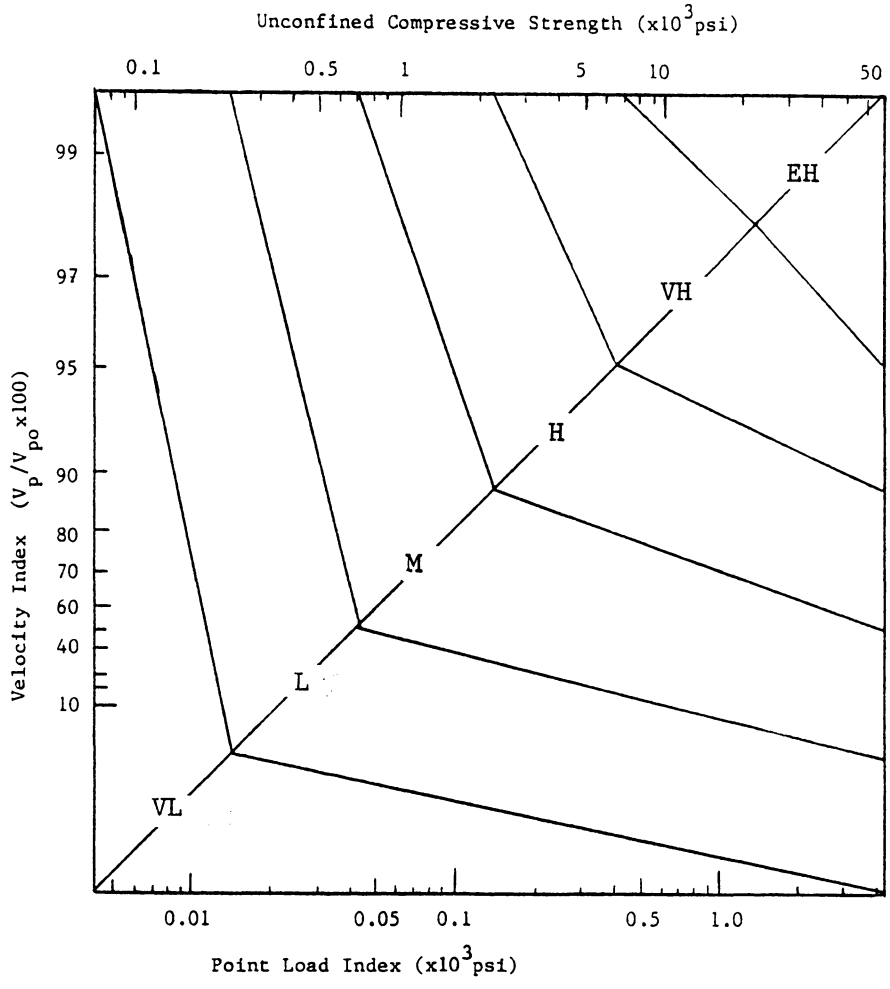


Figure 7.2 Classification of Rock Mass

Table 7.2

The Effect of Joint Conditions on the Shear Wave Propagation

| Condition of Joint | Effect on S-waves |
|---|---|
| Surfaces widely separated | S-waves discontinued |
| Wet fractures | Low frequencies - Low amplitudes |
| Fractures filled with wet clay | Very low frequencies (more sensitive than P-waves) - Medium amplitudes |
| Dry clay in joints | Medium frequencies - Medium amplitudes |
| Jointed but compact or under stress | Medium frequencies - High amplitudes |

# CHAPTER VIII

## CONCLUSIONS AND RECOMMENDATIONS

From the analysis of the experimental procedures and results, the following conclusions can be made:

(i) A linear relationship exists between the static and the dynamic modulus of elasticity. Calculation of the latter necessitates a knowledge of the shear wave velocity. If this is not possible, the velocity of the compressional wave can provide an excellent approximation of the static modulus of elasticity.

(ii) A relationship of the form:

$$n/L = A \cdot \frac{1}{V_n} - B$$

can be used successfully to predict the frequency of joints. In this relationship, the parameters A and B have to be calculated for each particular case, since they depend on the characteristics of the joints.

Within a certain range, of joint spacing, a linear relationship may be preferred because of its simplicity. As before, the parameters depen on the joint characteristics and have to be determined experimentally.

(iii) Joint characteristics (i.e., separation of joints, filling material, water content) can be determined qualitatively by measuring the amplitude and the frequency of the shear wave.

(iv) A correlation between the unconfined compressive strength and the wave velocities, or functions based on wave velocities, could not be established. If a field test is required for determining the unconfined compressive strength, the Point Load Index is suggested.

(v) The "Petite Sismique" method utilizes the frequency of the shear wave to determine the in-situ static modulus of deformation. Although the technique has demonstrated significant potential its application raises several questions. In particular, the nature of the received waves, when applying the method in the field (i.e., may include shear as well as surface waves), the influence of the distance between source and receiver on the recorded frequency and, finally, the influence of the resonant frequency of the receiver are yet to be fully understood.

(vi) The Velocity Index ($V_F/V_L$) is an excellent indication of rock quality and it may be a better ndex than that provided by the RQD. It is simple to measure, it can yield information pertaining to both frequency and condition of joints and, unlike RQD, it is not affected by external factors such as drilling machine, skill of operator, rate of drilling and relative angle of drilling.

(vii) This research demonstrated that sonic wave parameters have considerable potential for engineering rock mass or rock material classifications. Such parameters are easier to determine

experimentally, both in the field and laboratory, and can provide reliable qualitative and quantitative means of rock assessment.

Finally, from this research investigation the following recommendations can be made:

(i) Sonic testing of rocks should be standardized, particularly with regard to amplitude, frequency, mode of generation and other characteristics of the generated pulse.

(ii) Further research is necessary in order to develop meaningful and quantitative relationships between the amplitude and frequency of the compressional and shear waves and the joint characteristics.

(iii) The "Petite Sismique" method has yielded very encouraging results and its merits further investigation. The concept of the method should be further reviewed and its field application should be improved and standardized if it is to be accepted as an established technique.

(iv) The possibility of substituting dynamic for static properties in the existing engineering rock classification systems should be the subject of future research. In particular the introduction of the Velocity Index in place of the RQD and other joint parameters could greatly enhance the applicability and practical significance of two comprehensive and quantitative rock classification systems, i.e., Bieniawski's Geomechanical Classification and Barton's Rock Quality Index.

## REFERENCES


Avilo, L. "Some Applications of Seismic Field Tests in Rock Media," Proceedings, 1st Congress of the International Society for Rock Mechanics, Lisbon, Vol. I, 1966.

Bandis, S., Lunsden, A. C. and Barton N. "Experimental Studies of Scale Effects on the Shear Behaviour of Rock Joints," International Journal of Rock Mechanics Mining Science and Geomechanics Abstracts, Vol. 18, pp. 1-21, 1981.

Barton, N., Lien, R. and Lunde, J. "Estimation of Support Requirements for Underground Excavations," Rock Mechanics, Vol. 6/4, 1973.

Bergland, G. D. "A Guided Tour of the Fast Fourier Transform," IEEE Spectrum, July, 1969.

Bieniawski, Z. T. "Engineering Classification of Jointed Rock Masses," The Civil Engineer in South Africa, December, 1973.

Bieniawski, Z. T. "Case Studies: Prediction of Rock Mass Behaviour by the Geomechanics Classification," Proceedings, 2nd Australian and New Zealand Conference on Geomechanics, Brisbane, 1975.

Bieniawski, Z. T. "Elandsberg Pumped Storage Scheme - Rock Engineering Investigations," Proceedings of the Symposium on Exploration for Rock Engineering, Johannesburg, November, 1976.

Bieniawski, Z. T. "Determining Rock Mass Deformability: Experience from Case Histories," International Journal of Rock Mechanics Mining Science and Geomechanics Abstracts, Vol. 15, pp. 237-247, 1978.

Bieniawski, Z. T. "The Geomechanics Classification in Rock Engineering Applications," Proceedings, 4th International Congress for Rock Mechanics, International Society for Rock Mechanics, Montreux, 1979.

Bieniawski, Z. T. "Estimating Safe Roof Spans in Coal Mines Using Rock Mass Classification," Proceedings, 11th Annual Institute on Coal Mining Health, Safety and Research, Blacksburg, August, 1981.

Bur, T. R., Thill, R. E. and Hjelmstad, K. E. "An Ultrasonic Method for Determining the Elastic Symmetry of Materials," Report of Investigation 7333, U.S. Bureau of Mines, 1969.

Cannaday, F. S. and Leo, G. M. "Piezoelectric Pulsing Equipment for Sonic Velocity Measurements in Rock Samples from Laboratory Size to Mine Pillars," Report of Investigation 6810, U.S. Bureau of Mines, 1966.

Cannaday, F. X. "Piezoelectric Pulsing Equipment for Shear Wave Velocity Measurements in Rock Samples," Report of Investigation 7065, U.S. Bureau of Mines, 1968.

Coon, R. F. and Merritt, A. H. "Predicting In-Situ Modulus of Deformation Using Rock Quality Indexes," ASTM STP 477, American Society for Testing and Materials, pp. 154-173, 1970.

Darracott, B. W. and Orr, C. M. "Geophysics and Rock Engineering," Proceedings of the Symposium on Exploration for Rock Engineering, Johannesburg, November, 1976.

Desai, C. S. and Christian, J. T. Numerical Methods in Geotechnical Engineering, McGraw Hill, 1977.

Farmer, I. W. Engineering Properties of Rocks, E. & F. N. Spon Ltd., London, 1968.

Franklin, J. A., Broch, E. and Walton, G. "Logging the Mechanical Character of Rock," Transactions, Institution of Mining and Metallurgy, January, 1971.

Furcron, A. S. "James River Iron and Marble Belt, Virginia," Virginia Geological Survey, Bulletin 39, 1935.

Goodman, R. E. Methods of Geological Engineering in Discontinuous Rocks, West Publishing Company, 1976.

Gray, D. R., Lowry, W. D., Read, J. F. and Schulz, A. P. "Nature of Thrusting Along the Allegheny Front Near Pearisburg and of Overthrusting in the Blacksburg-Radford Area of Virginia," Guidebook for the 11th Annual Virginia Geological Field Conference, Blacksburg, Virginia, October, 1979.

Heuze, F. E. "Scale Effects in the Determination of Rock Mass Strength and Deformability," Rock Mechanics, 12, 1980.

Heuze, F. E. "Geomechanics of the Climax "Mine-By", Nevada Test Site," Proceedings, 22nd U.S. Symp. R. Mech., MIT, 1981, pp. 428-438.

Hoar, R. J. and Stokoe, K. H. "Generation and Measurement of Shear Waves In-Situ," Dynamic Geotechnical Testing, ASTM STP 654, American Society for Testing and Materials, pp. 3-29, 1978.

Just, G. D. and Walter, G. W. "Engineering Potential of Seismic Methods of Assessing Rock Breakage Characteristics," Rock Breaking Symposium, The Australian IMM Melbourne Branch, November, 1978.

Lama, R. D. and Vutukuri, V. S., Handbook on Mechanical Properties of Rocks, Vol. II, Trans Tech Publications, 1966.

Londe, P. "Field Measurement in Tunnels," International Symposium on Field Measurements in Rock Mechanics, Zurich, April, 1977.

McKenzie, C. K., Stacey, G. P. and Gladwin, M. T. "Ultrasonic Characteristics of a Rock Mass," International Journal of Rock Mechanics Mineral Science and Geomechanics Abstracts, Vol. 19, pp. 25-30, 1982.

Mooney, H. M. "Seismic Shear Waves in Engineering," Journal of the Geotechnical Engineering Division, ASCE, Vol. 100, August, 1974.

Palmer, S. P., Smith, J. A. and Waters, K. H. "Fracture Detection in Crystalline Rock Using Ultrasonic Reflection Techniques," International Journal for Rock Mechanics Mining Science & Geomechanics Abstracts, Vol. 18, pp. 403-413, 1981.

Roberts, A., Geotechnology. An Introductory Text for Students and Engineers, Pergamon Press, 1977.

Roegiers, J.-C., Thill, R. E. "Rock Characterization at a Geothermal Site," Proceedings, 17th Annual Rock Mechanics Symposium, Snowbird, Utah, 1976.

Roussel, J.-M. "Etude théoretique et expérimental du module dynamique de massif rocheux," Revue de 1' Industrie Minérale, Paris, August, 1968.

Rummel, F. and Vantleerden, W. L. "Suggested Methods for Determining Sound Velocity," International Journal of Rock Mechanics Mining Science and Geomechanics Abstracts, Vol. 15, pp. 53-63, 1978.

Schneider, B. "Contribution a 1'étude de massifs de fondation de barrages," (thése), Trans. de labor. de geol. de la fac. des sci. de Grenoble, Monsoir No. 7, Grenoble, 1967.

Schneider, B. "Moyens nouveau de reconnaissance de massifs rocheux," Annales de 1' Institut Technique du Batiment et des Travaux Publics, France, 1967.

Stacy, T. R. "Seismic Assessment of Rock Masses," Proceedings, Symposium on Exploration for Rock Engineering, Johannesburg, 1976.

Statton, C. T., Auld, B. and Fritz, A. "In-Situ Seismic Shear-Wave Velocity Measurements and Proposed Procedures," Dynamic Geotechnical Testing, ASTM STP 654, American Society for Testing and Materials, 1978.

Stephenson, R. W. "Ultrasonic Testing for Determining Dynamic Soil Moduli," Dynamic Geotechnical Testing, ASTM STP 654, American Society for Testing and Materials, 1978.

Sweet, P. C., Directory of the Mineral Industry in Virginia - 1980, Virginia Division of Mineral Resources, Charlottesville, Virginia, 1981.

Thill, R. E., McWilliams, J. R. and Bur, T. R. "An Acoustical Bench for an Ultrasonic Pulse System," Report of Investigation 7164, U.S. Bureau of Mines, 1968.

Thill, R. E. and Bur, T. R. "An Automated Ultrasonic Pulse Measurement System," Geophysics, Vol. XXXIV, No. 1, February, 1969.

Thill, R. E. "Acoustic Methods for Monitoring Failure in Rock," Proceedings, 14th Symposium on Rock Mechanics, University Park, Pennsylvania, June, 1972.

Thill, R. E. "Acoustic Cross-Borehole Apparatus for Determining In-Situ Elastic Properties and Structural Integrity of Rock Masses," Proceedings, 19th U.S. Symposium on Rock Mechanics, May, 1978.

Thill, R. E. and Jessup, J. A. "Engineering Properties of Coal Measure Rocks," Proceedings, AIME Annual Meeting, Dallas, Texas, February, 1982.

Van Schalwyk, A. "Rock Engineering Testing in Exploratory Boreholes," Proceedings, Symposium on Exploration for Rock Engineering, Johannesburg, November, 1976.

# APPENDIX A

## LOAD VERSUS DEFORMATION RESULTS

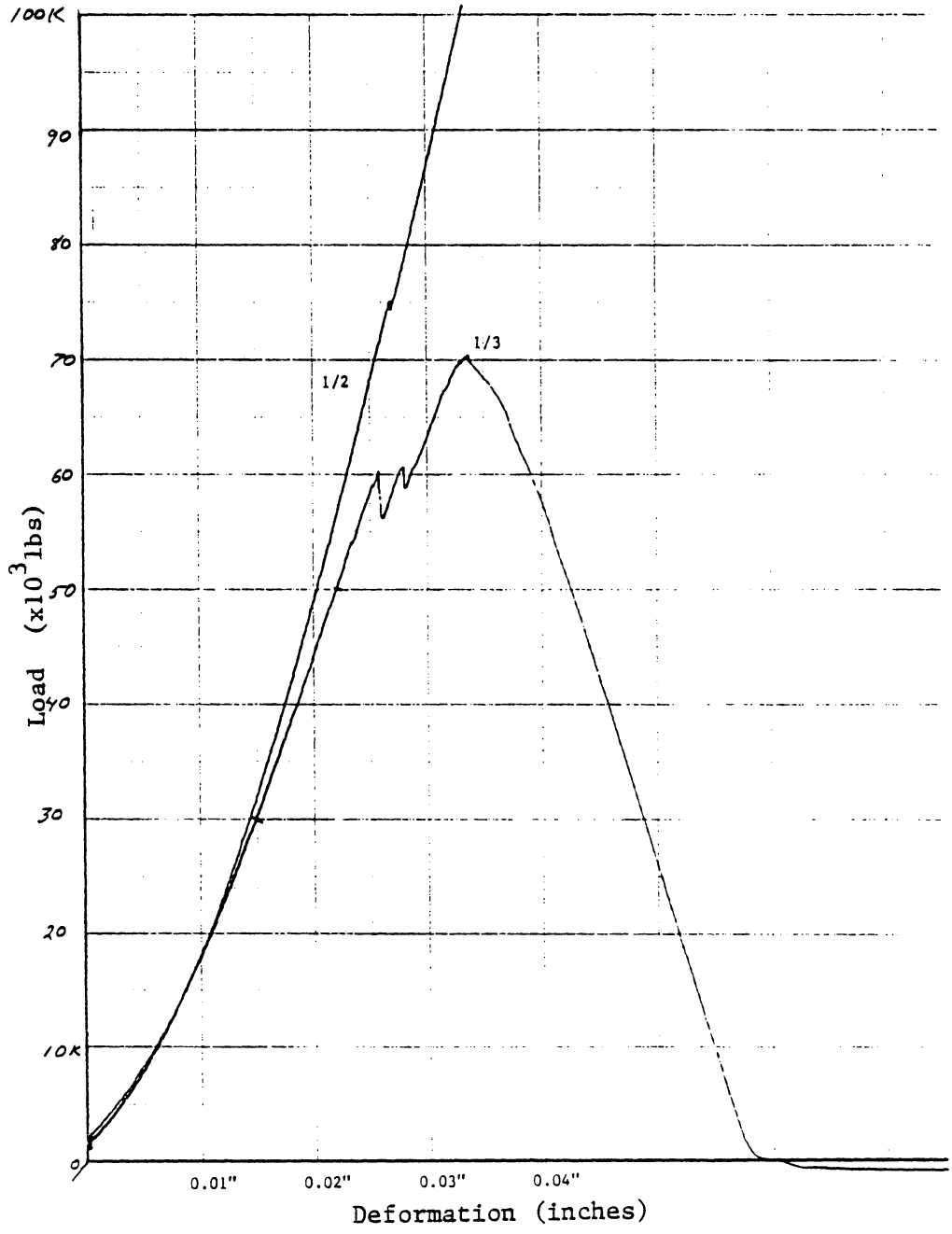


Figure A.1 Load-Deformation Diagram
Samples 1/2,1/3

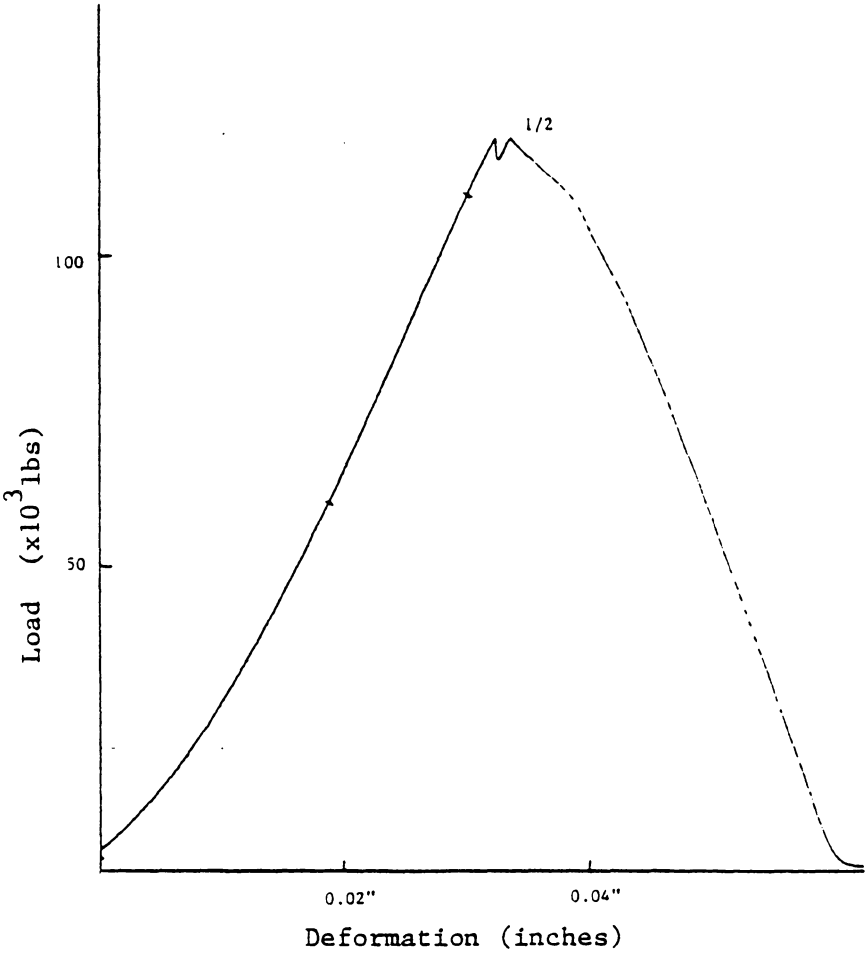


Figure A.2 Load-Deformation Diagram-
Sample 1/2

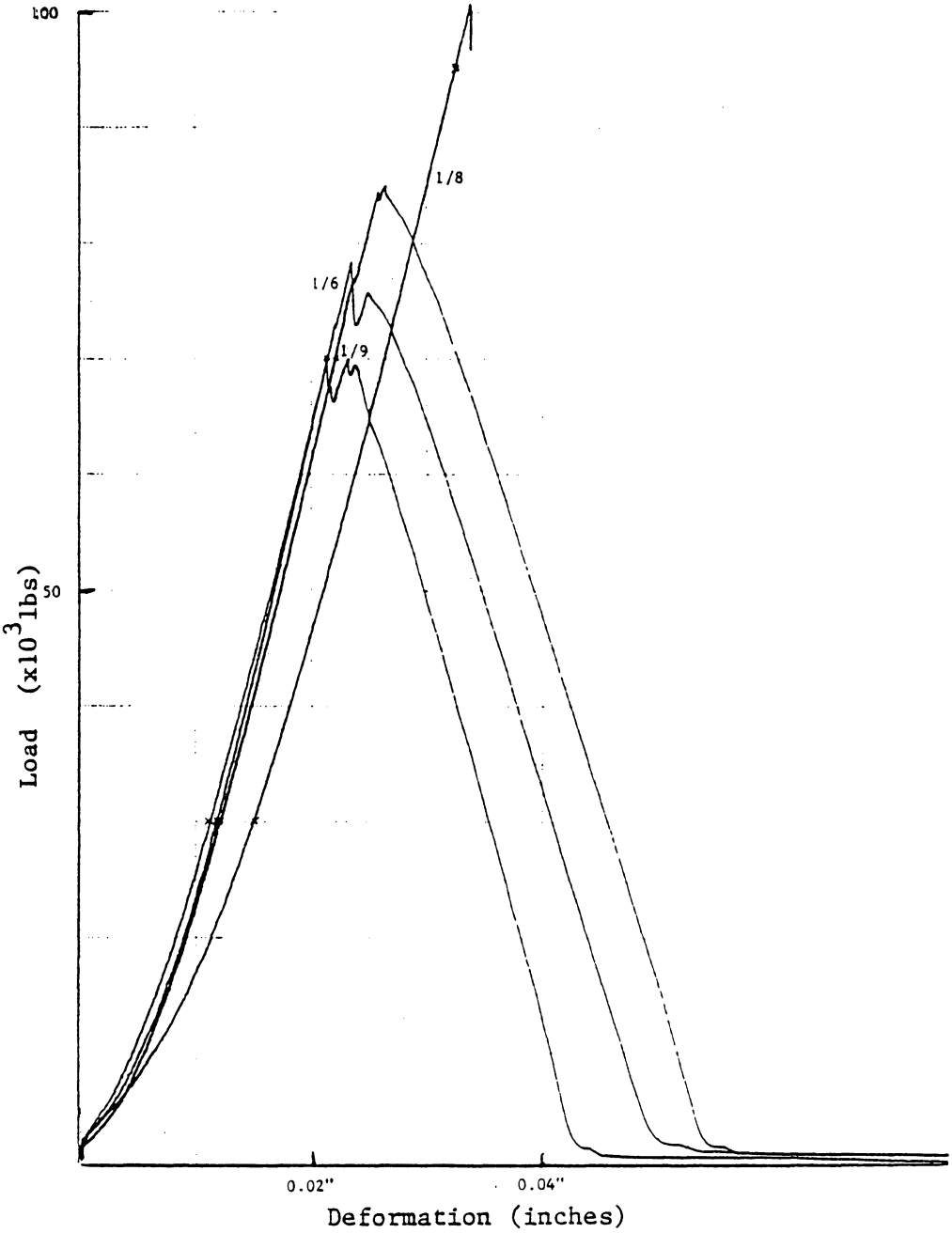


Figure A.3 Load-Deformation Diagram-
Samples 1/6,1/8,1/9

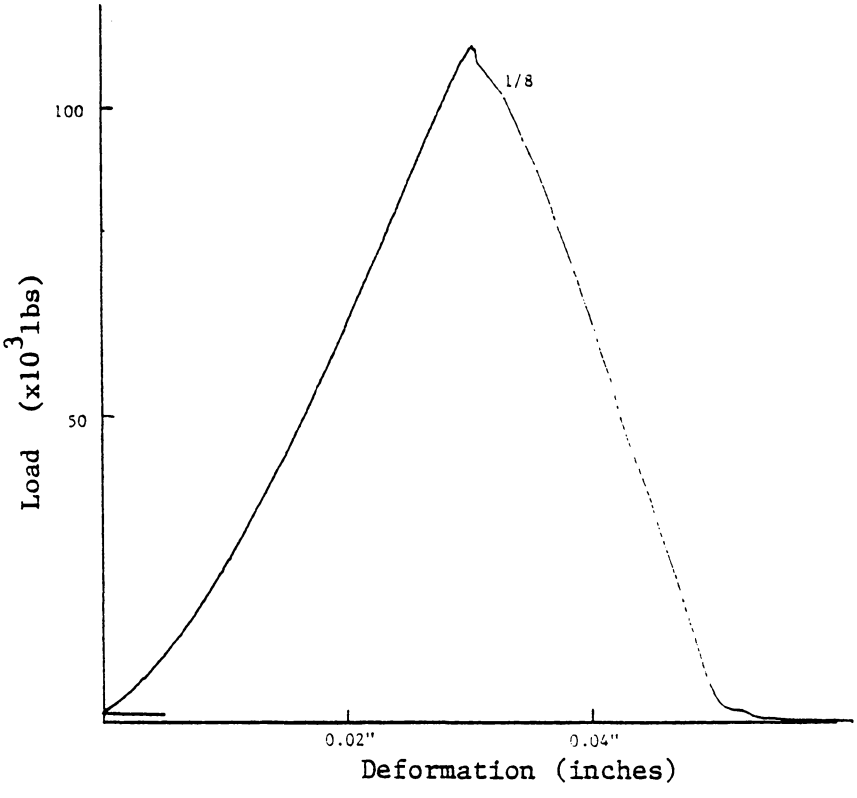


Figure A.4 Load-Deformation Diagram-
Sample 1/8

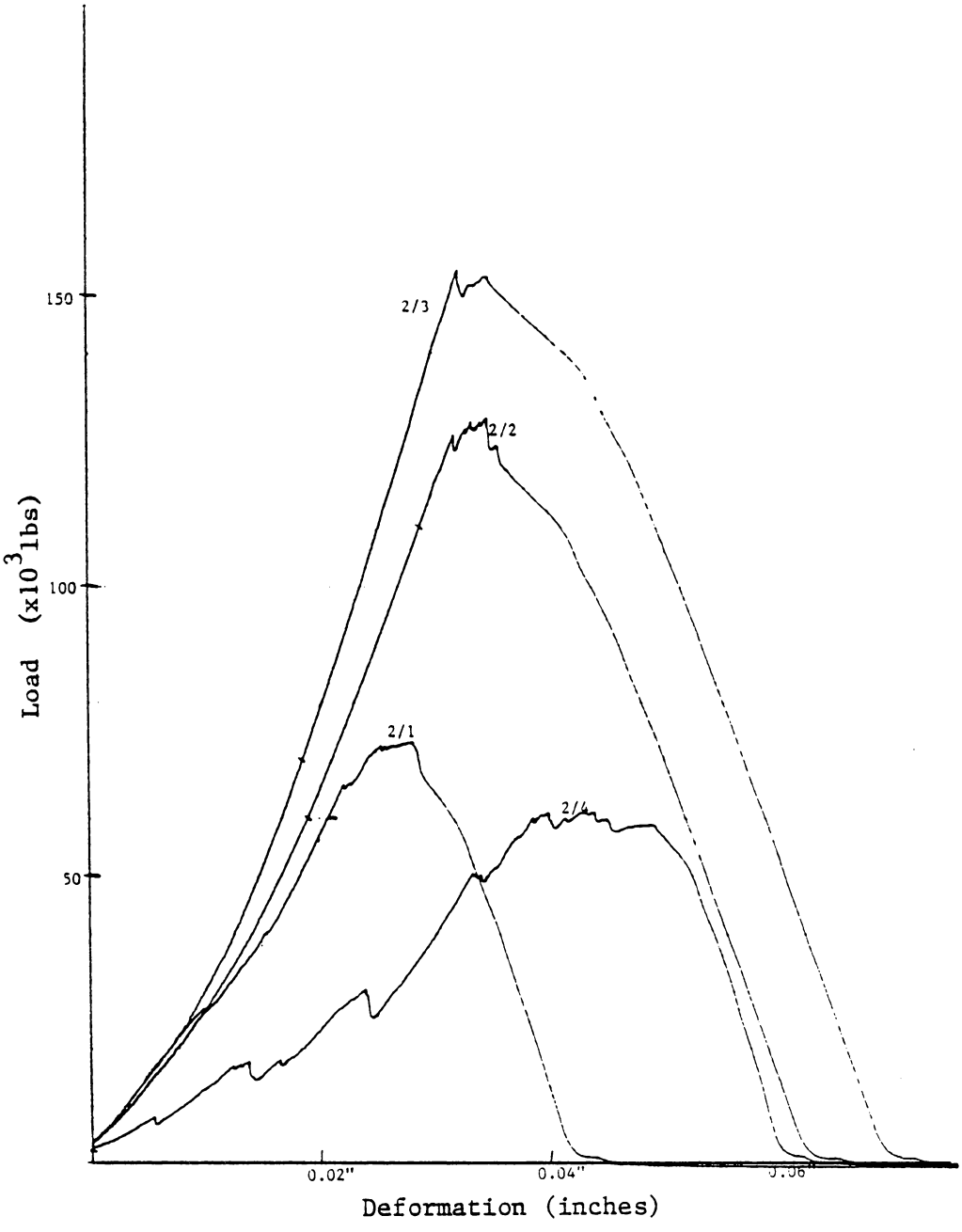


Figure A.5 Load-Deformation Diagram-
Samples 2/1,2/2,2/3,2/4

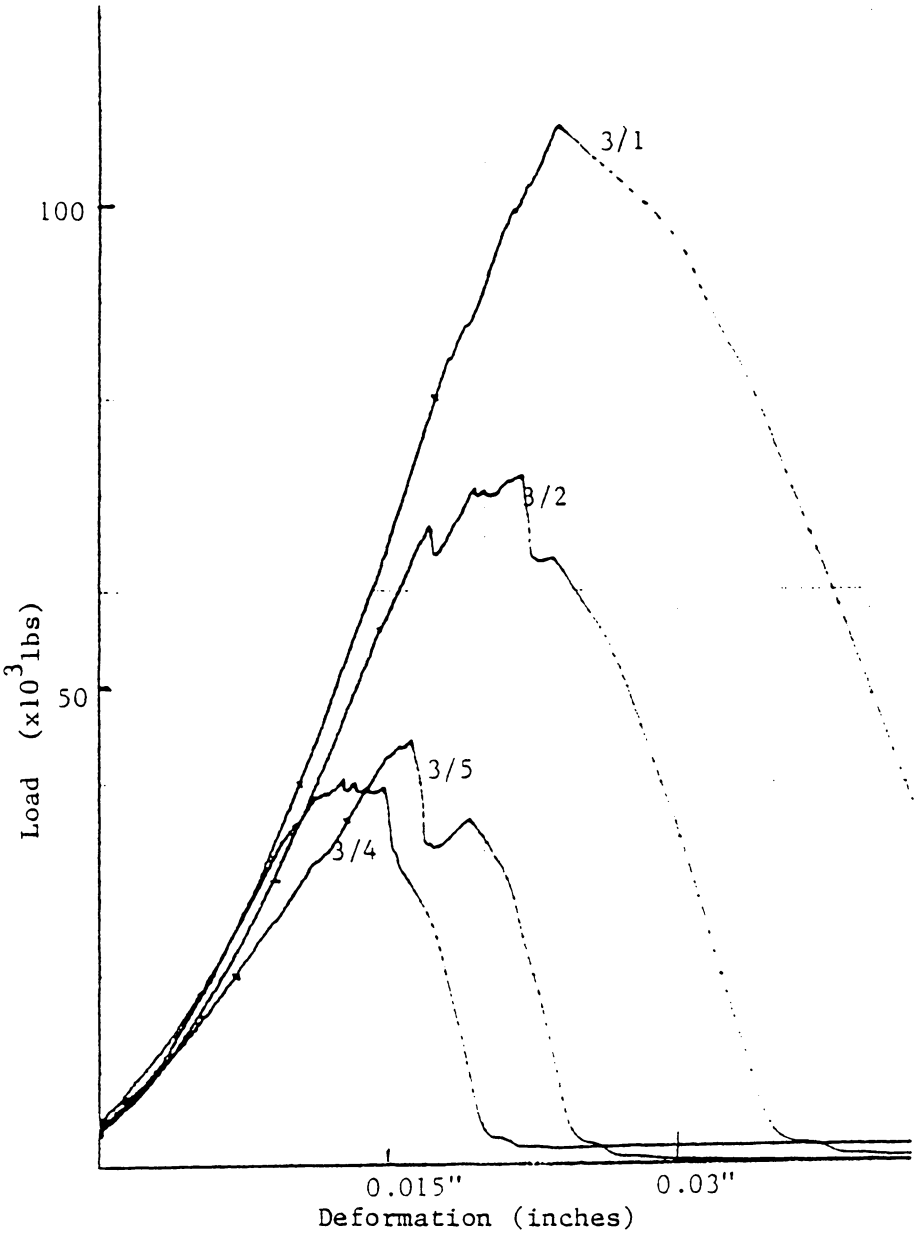


Figure A.6 Load-Deformation Diagram-
Samples 3/1,3/2,3/4,3/5

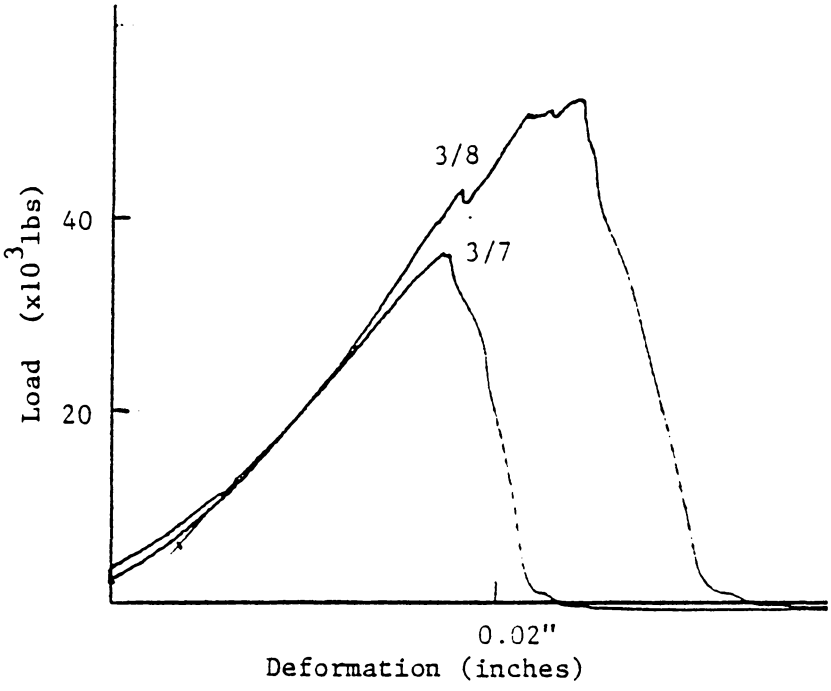


Figure A.7 Load-Deformation Diagram-
Samples 3/7,3/8

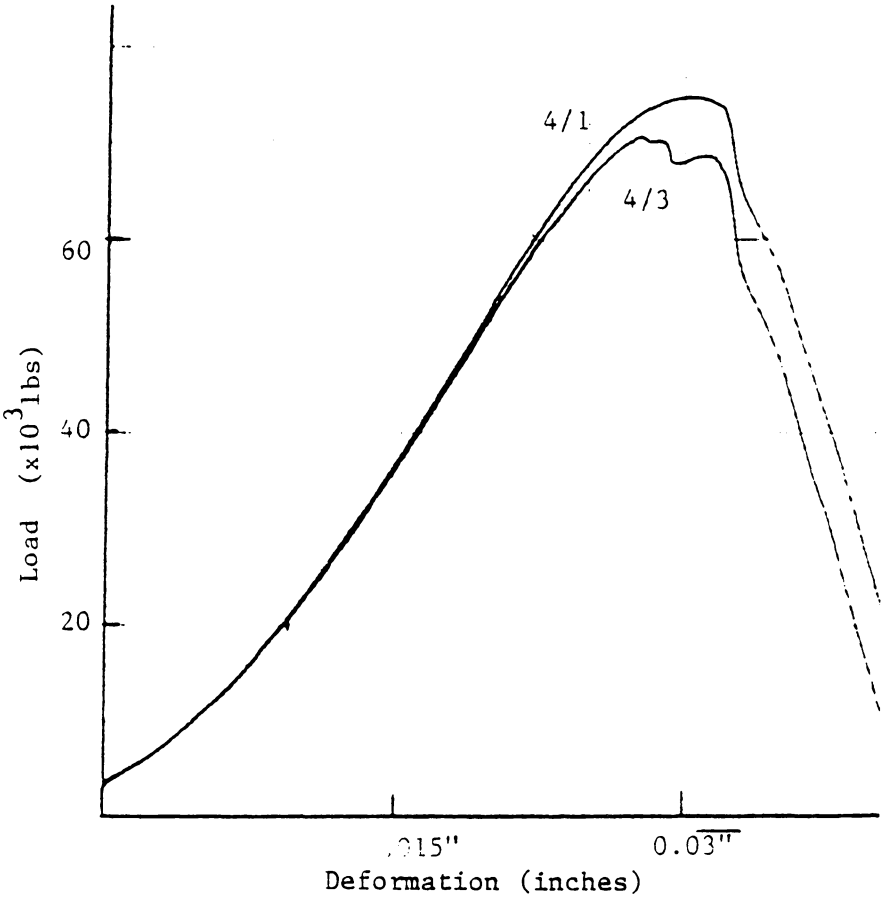


Figure A.8 Load-Deformation Diagram-
Samples 4/1,4/3

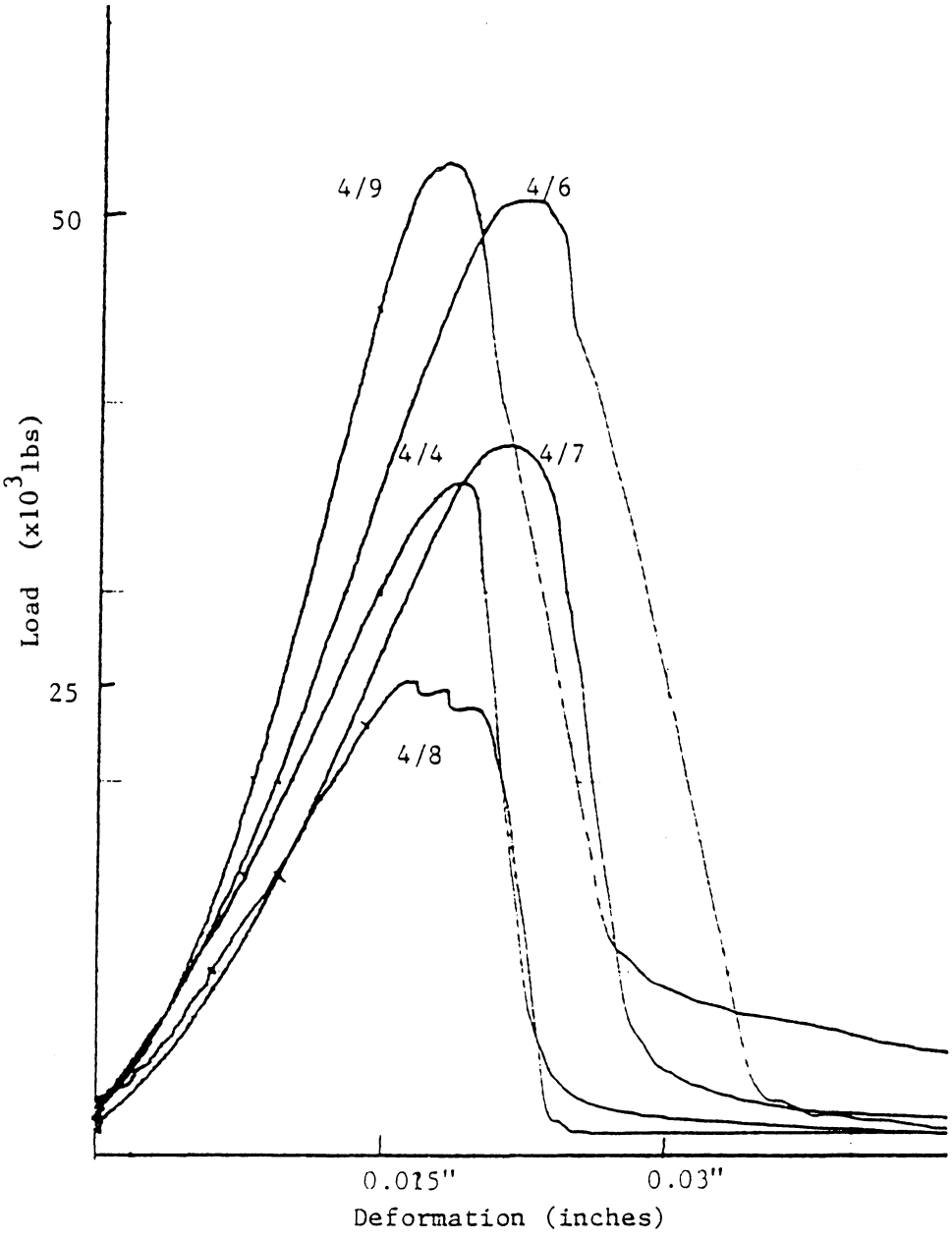


Figure A.9 Load-Deformation Diagram-
Samples 4/4,4/6,4/7,4/8,4/9

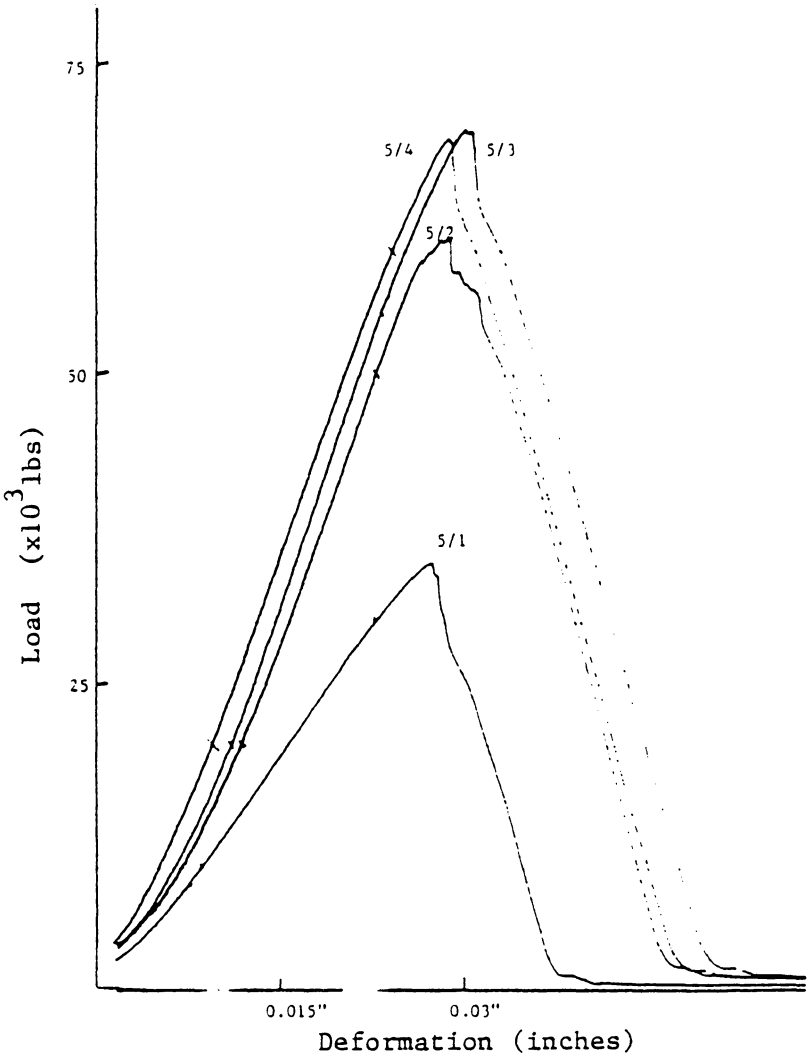


Figure A.10 Load-Deformation Diagram-
Samples 5/1,5/2,5/3,5/4

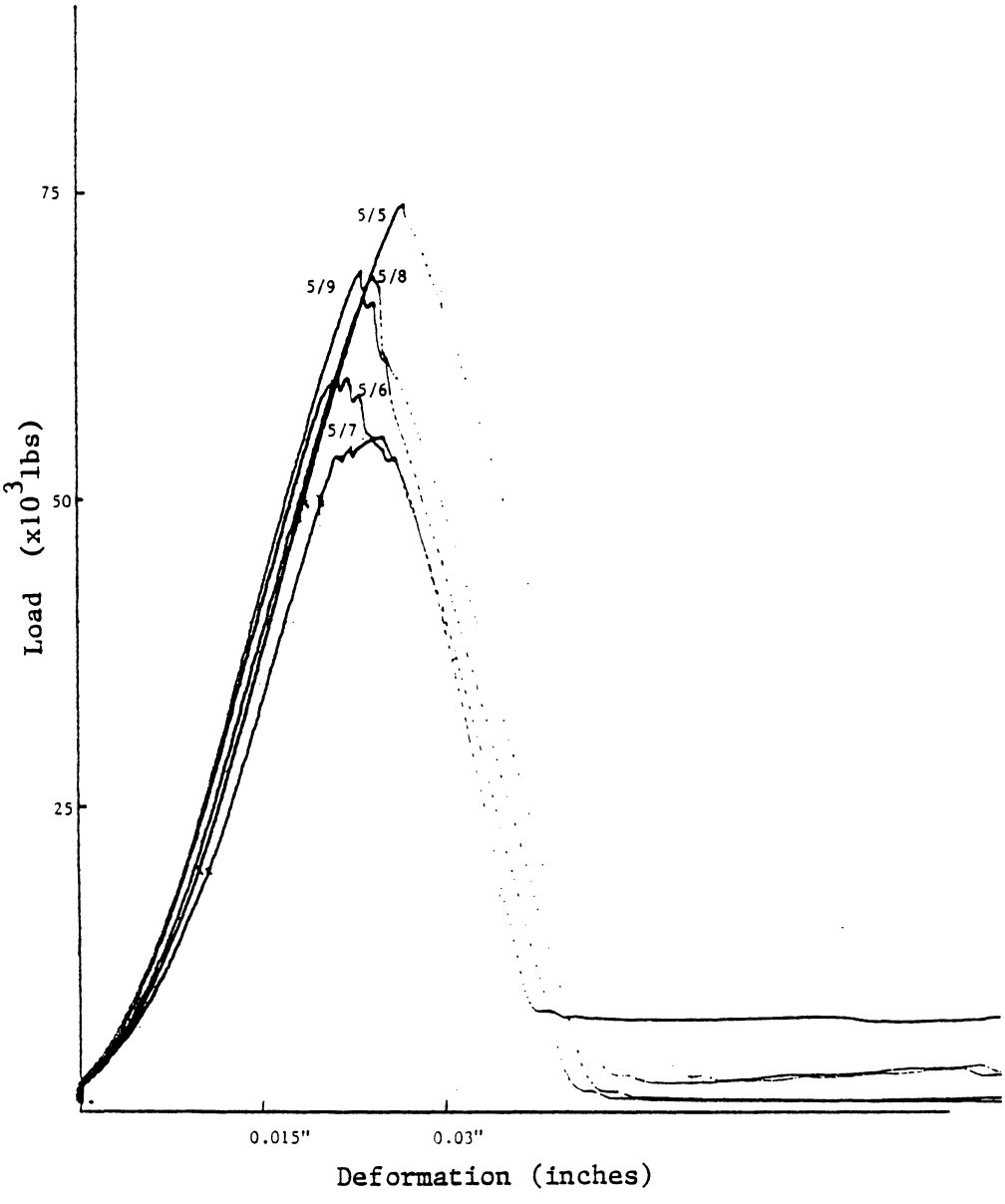


Figure A.11 Load-Deformation Diagrams-
Samples 5/5,5/6,5/7,5/8,5/9

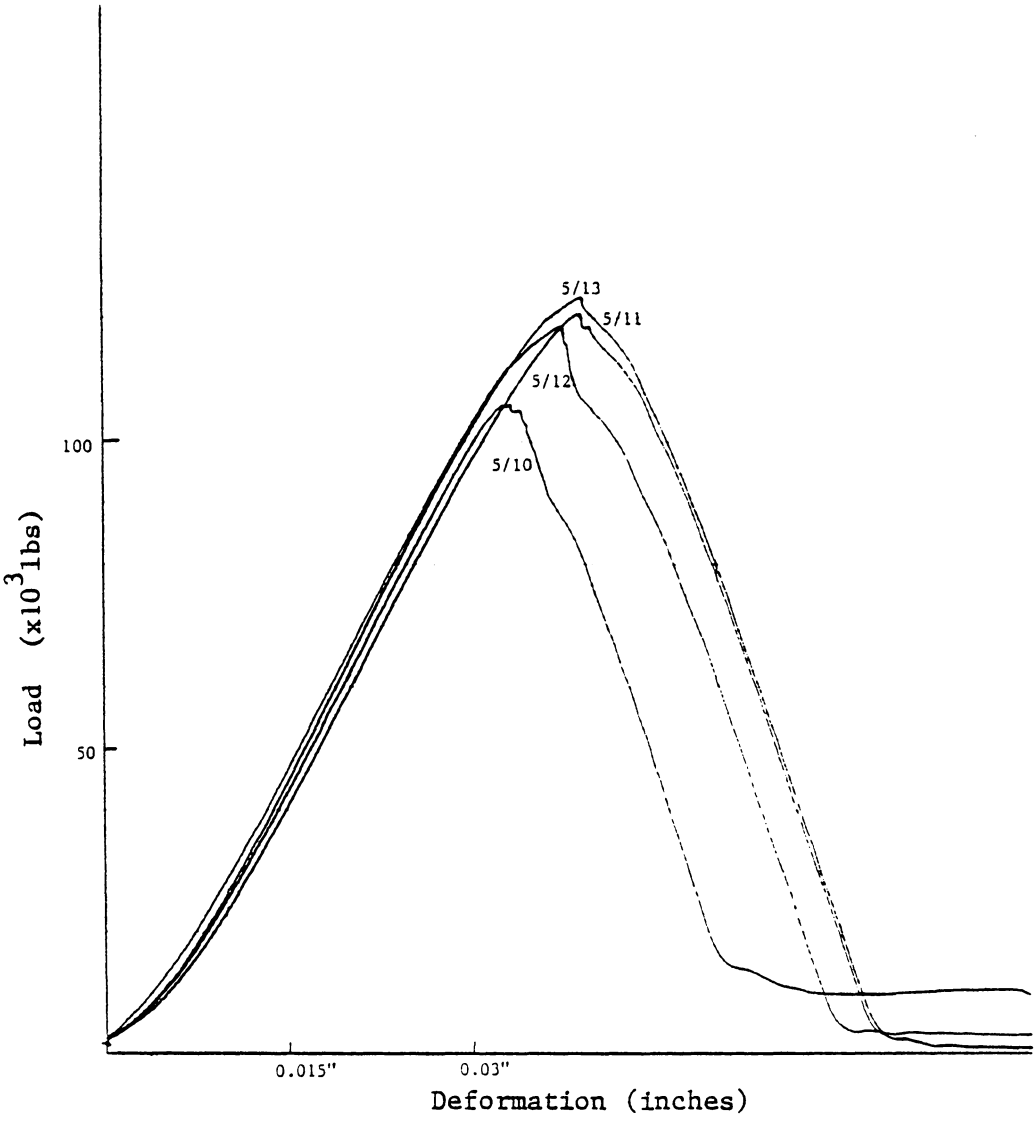


Figure A.12 Load-Deformation Diagram-
Samples 5/10,5/11,5/12,5/13

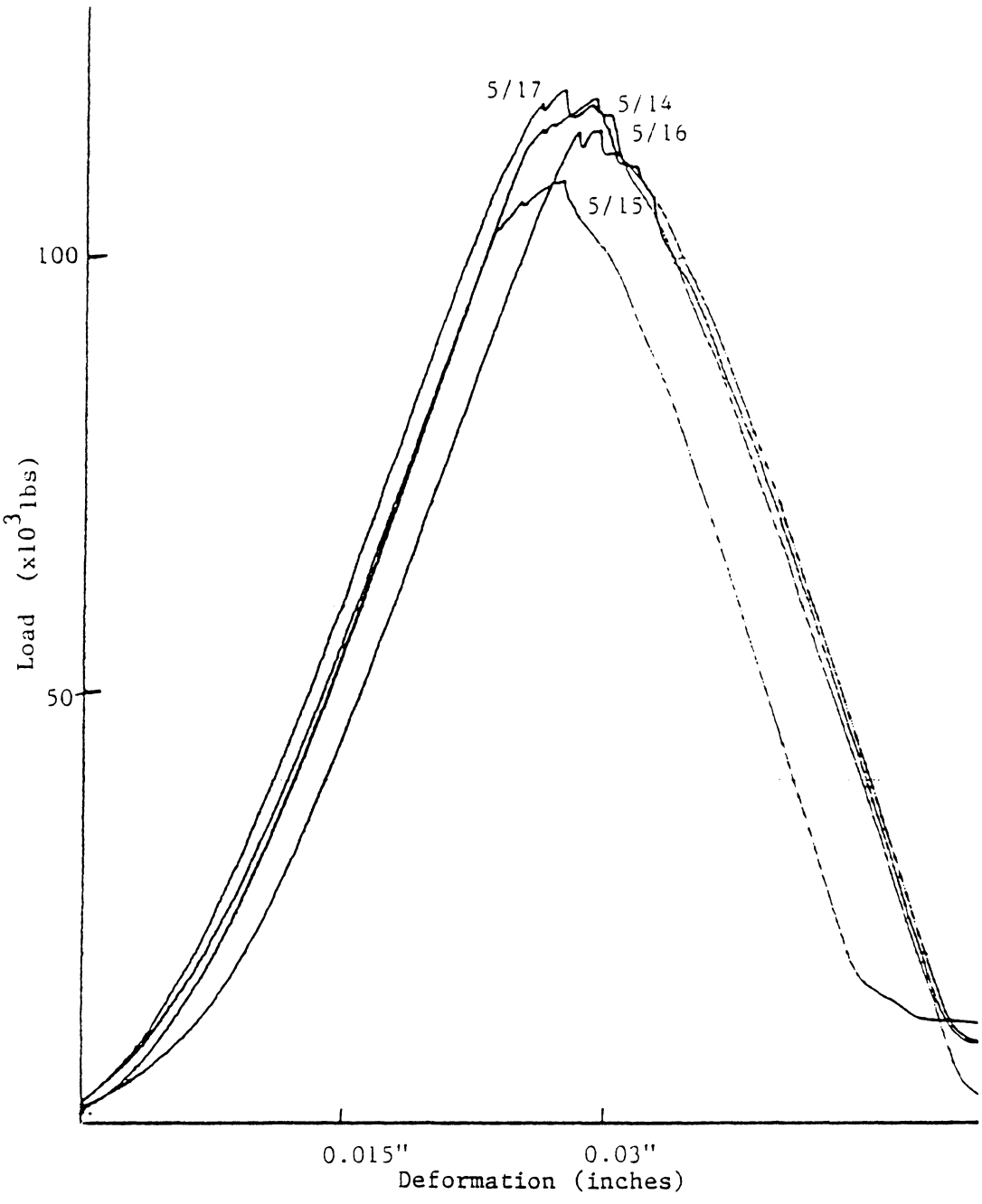


Figure A.13 Load-Deformation Diagram-
Samples 5/14,5/15,5/16,5/17

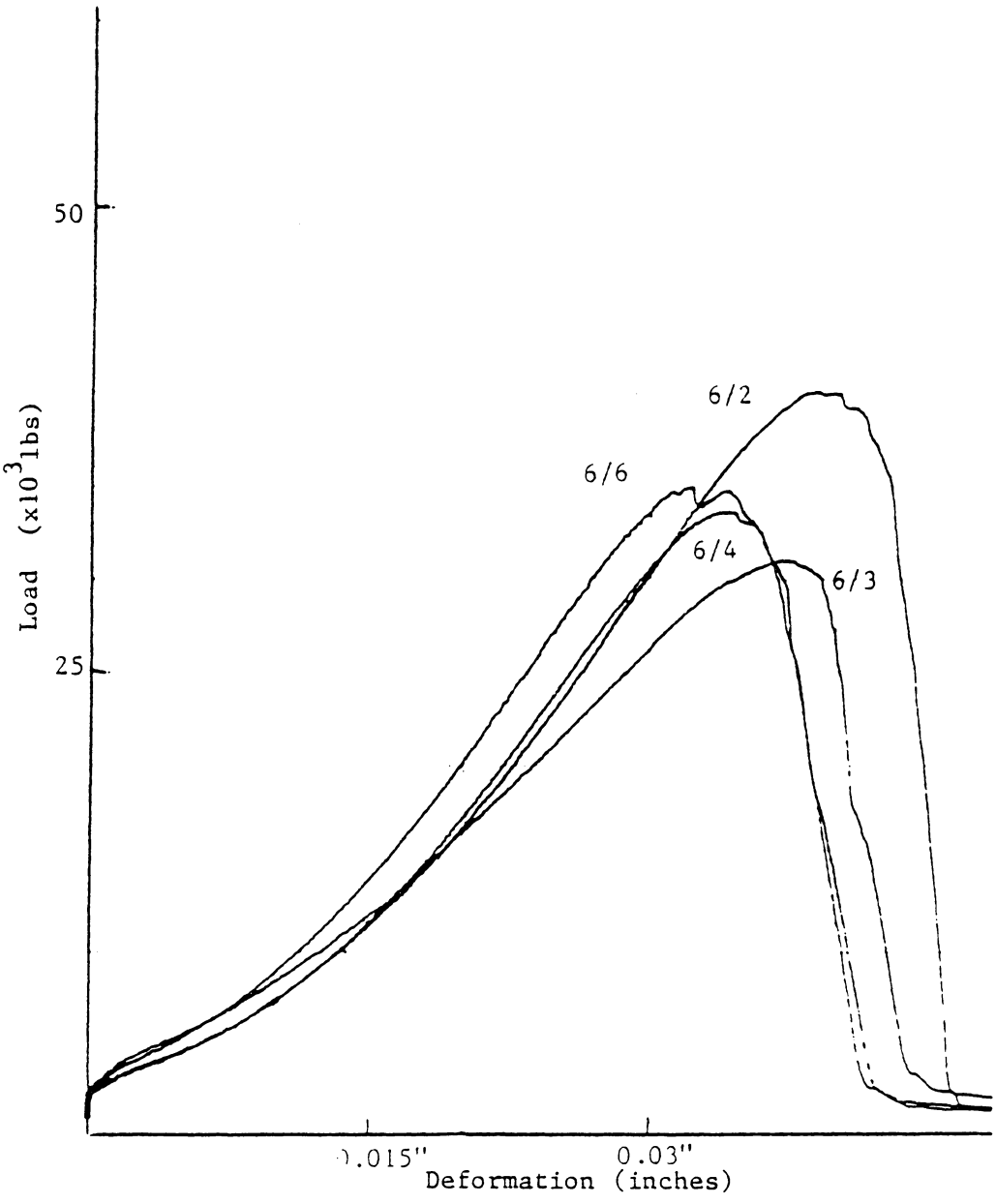


Figure A.14 Load-Deformation Diagram-
Samples 6/2,6/3,6/4,6/6

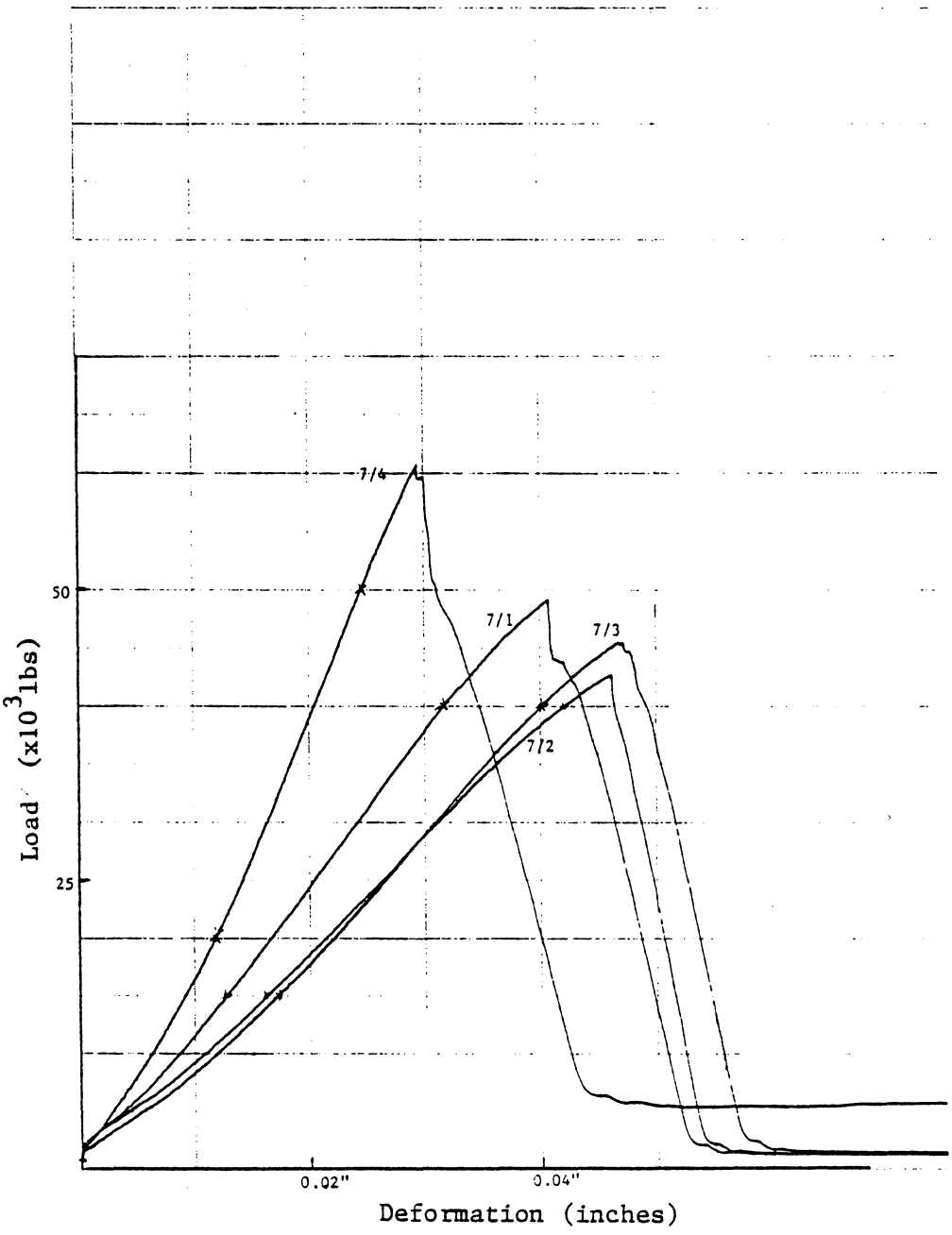


Figure A.15 Load-Deformation Diagram-
Samples 7/1,7/2,7/3,7/4

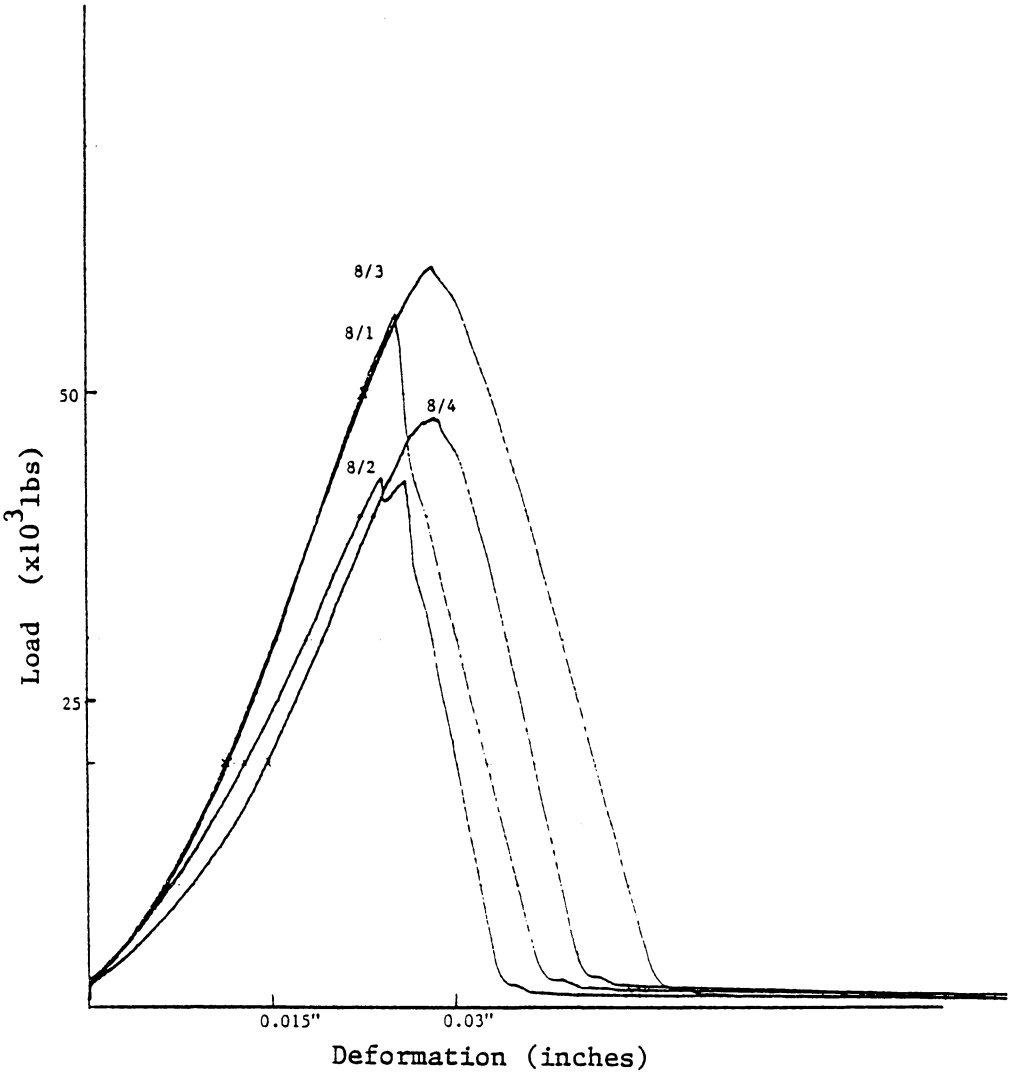


Figure A.16 Load-Deformation Diagram-
Samples 8/1,8/2,8/3,8/4

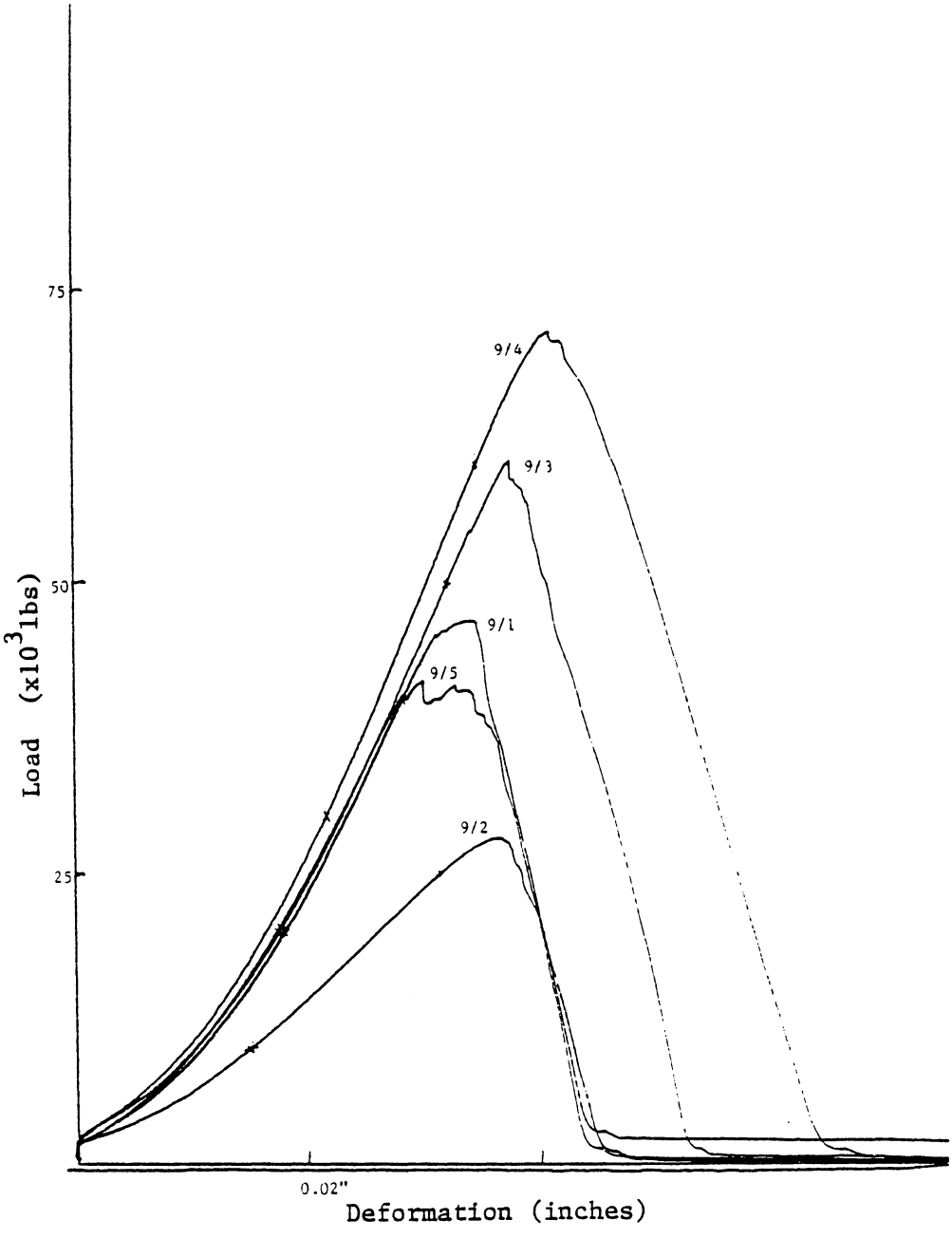


Figure A.17 Load-Deformation Diagram-
Samples 9/1,9/2,9/3,9/4,9/5

# APPENDIX B

# EFFECT OF FRACTURES ON WAVE VELOCITIES

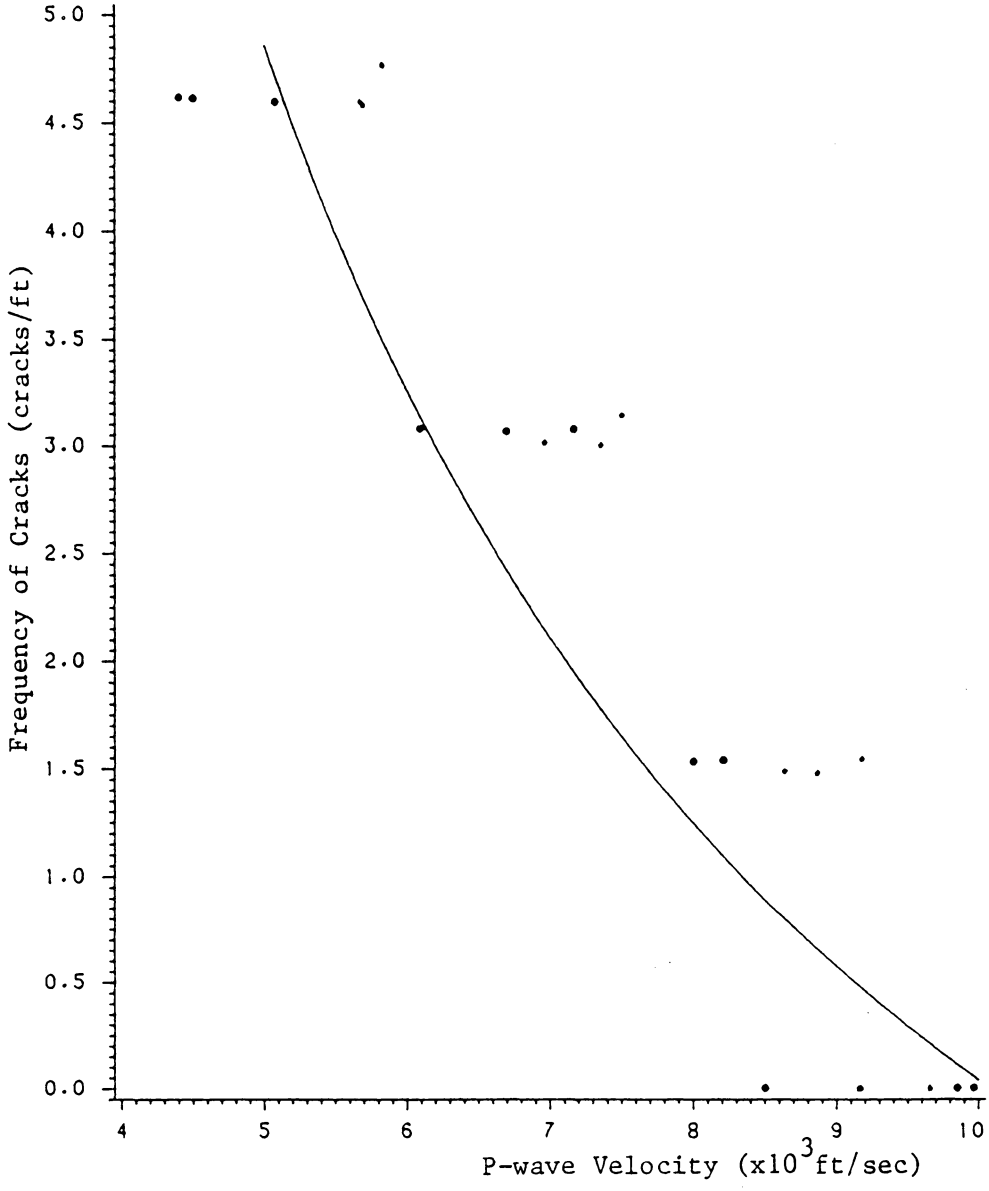


Figure B.1 Effect of Cracks on P-wave Velocity, Rock Type #6

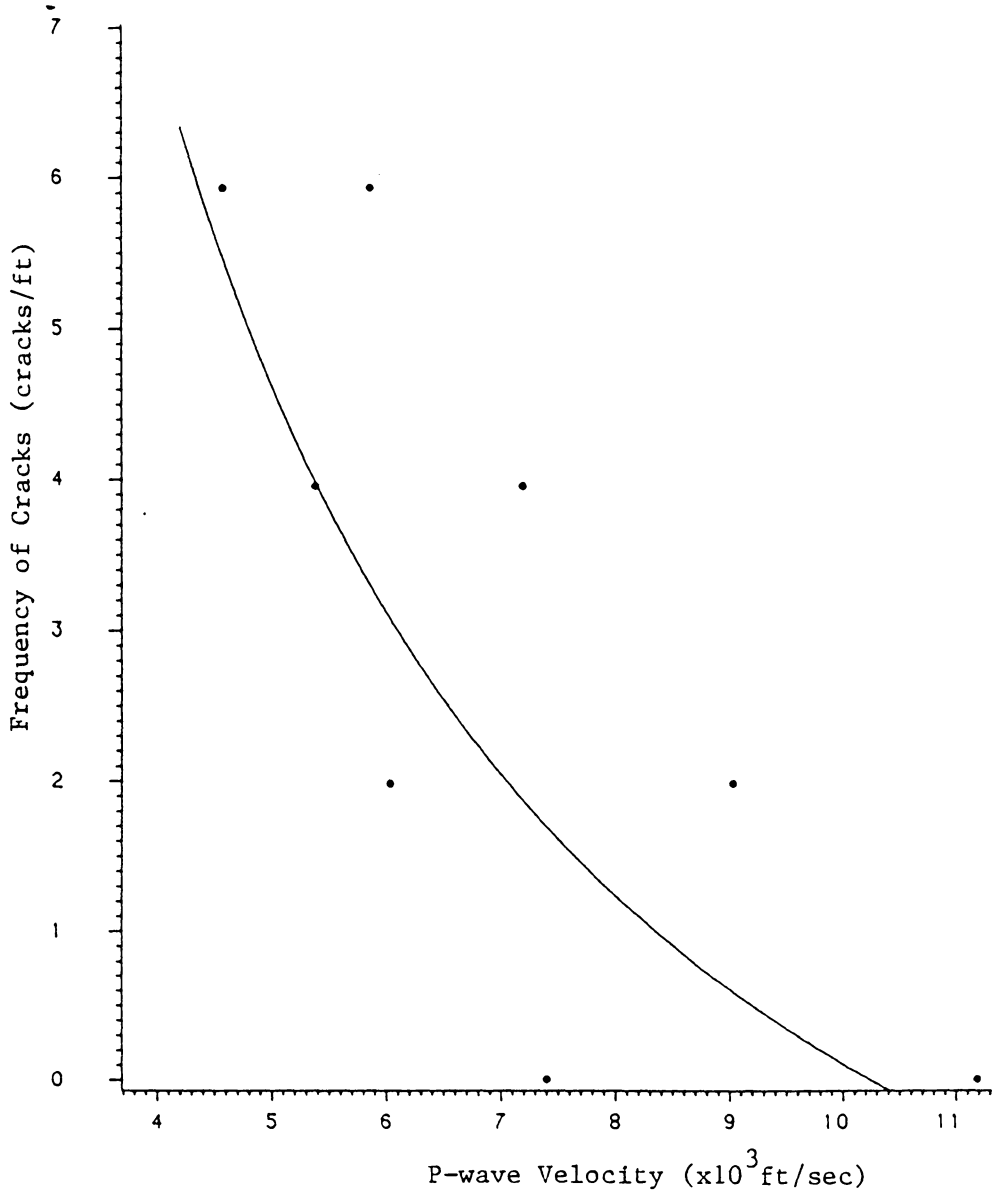


Figure B.2 Effect of Cracks on P-wave Velocity, Rock Type #9

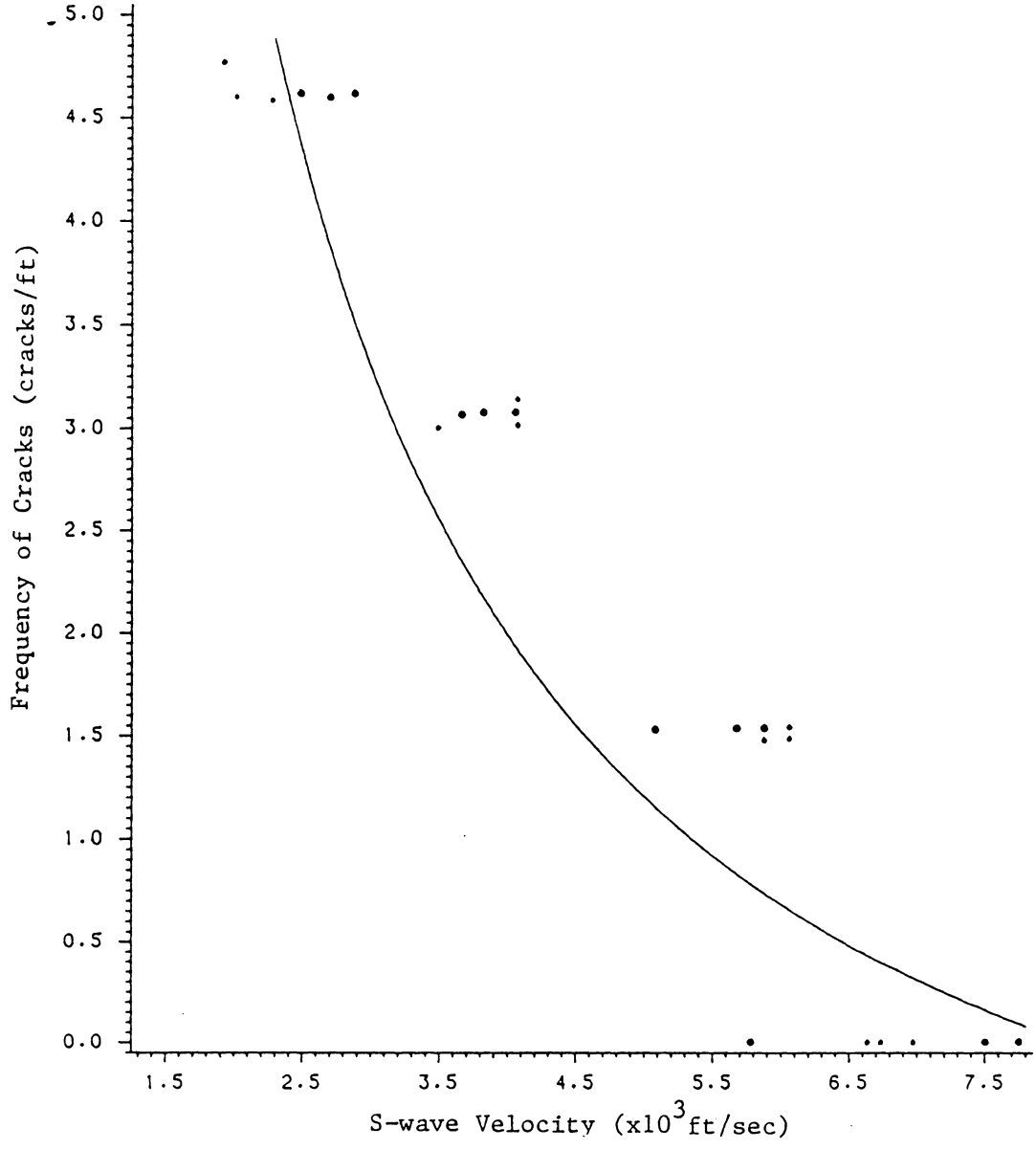


Figure B.3 Effect of Cracks on S-wave Velocity, Rock Type #6

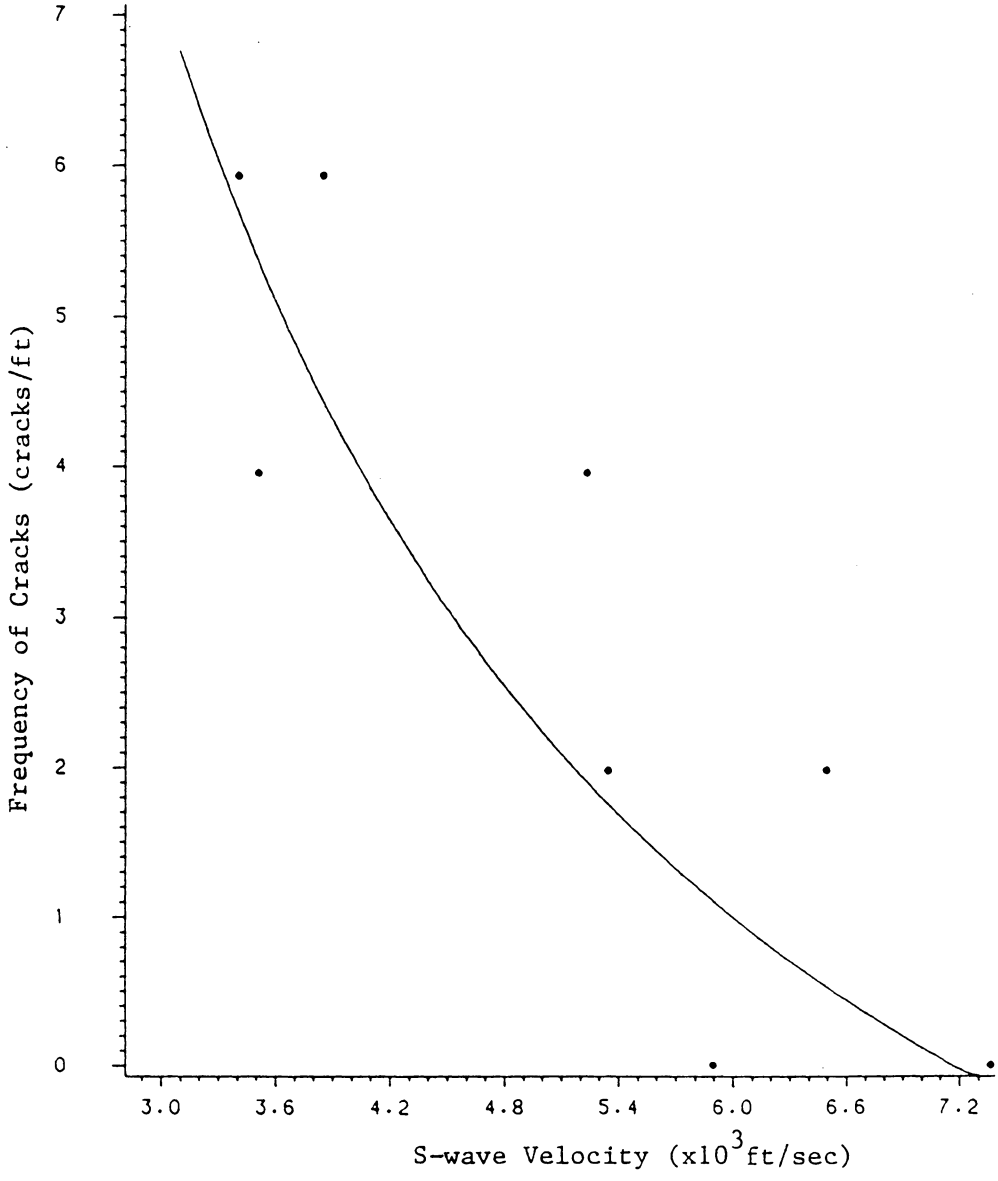


Figure B.4 Effect of Cracks on S-wave Velocity, Rock Type #9

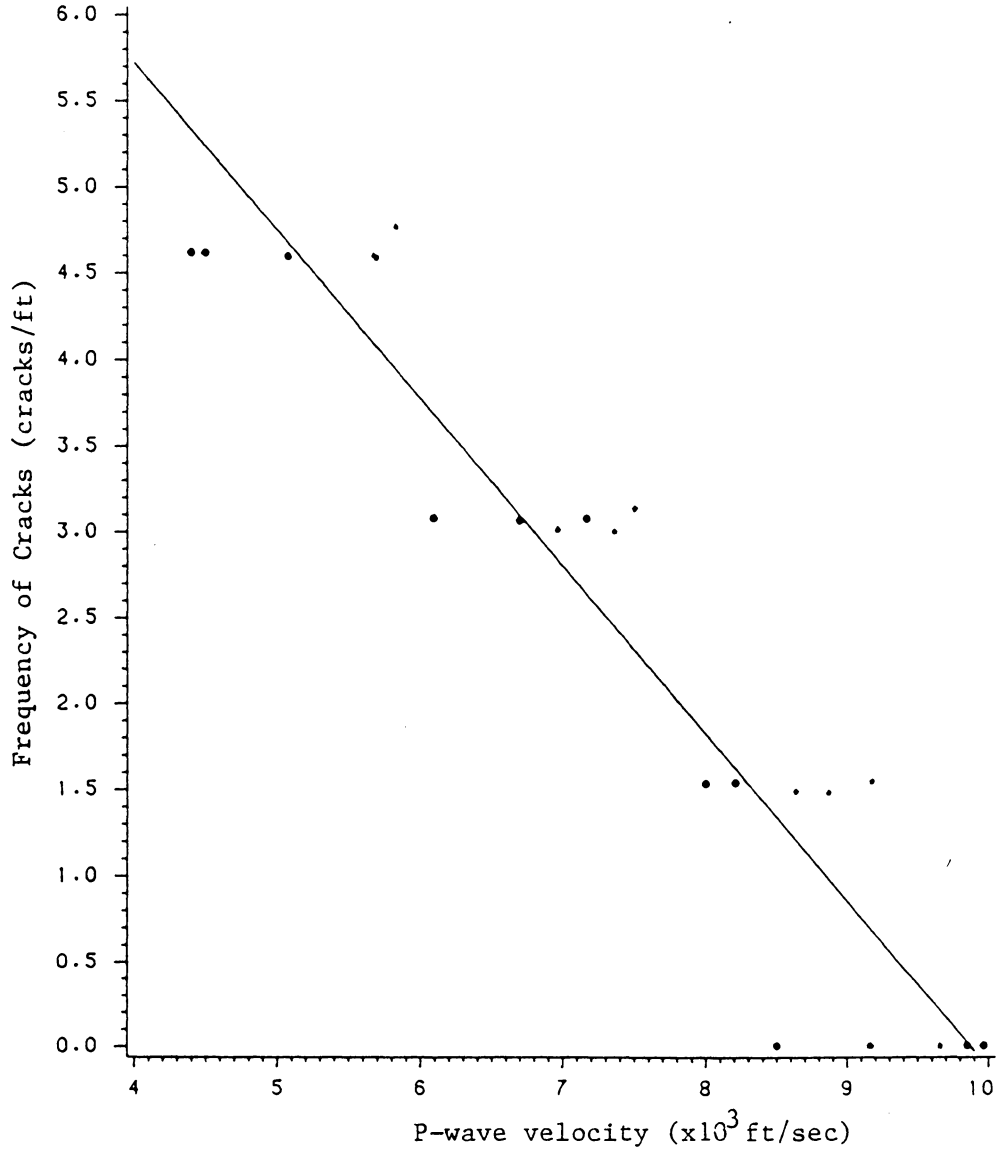


Figure B.5 Effect of Cracks on P-wave Velocity, Rock Type #6

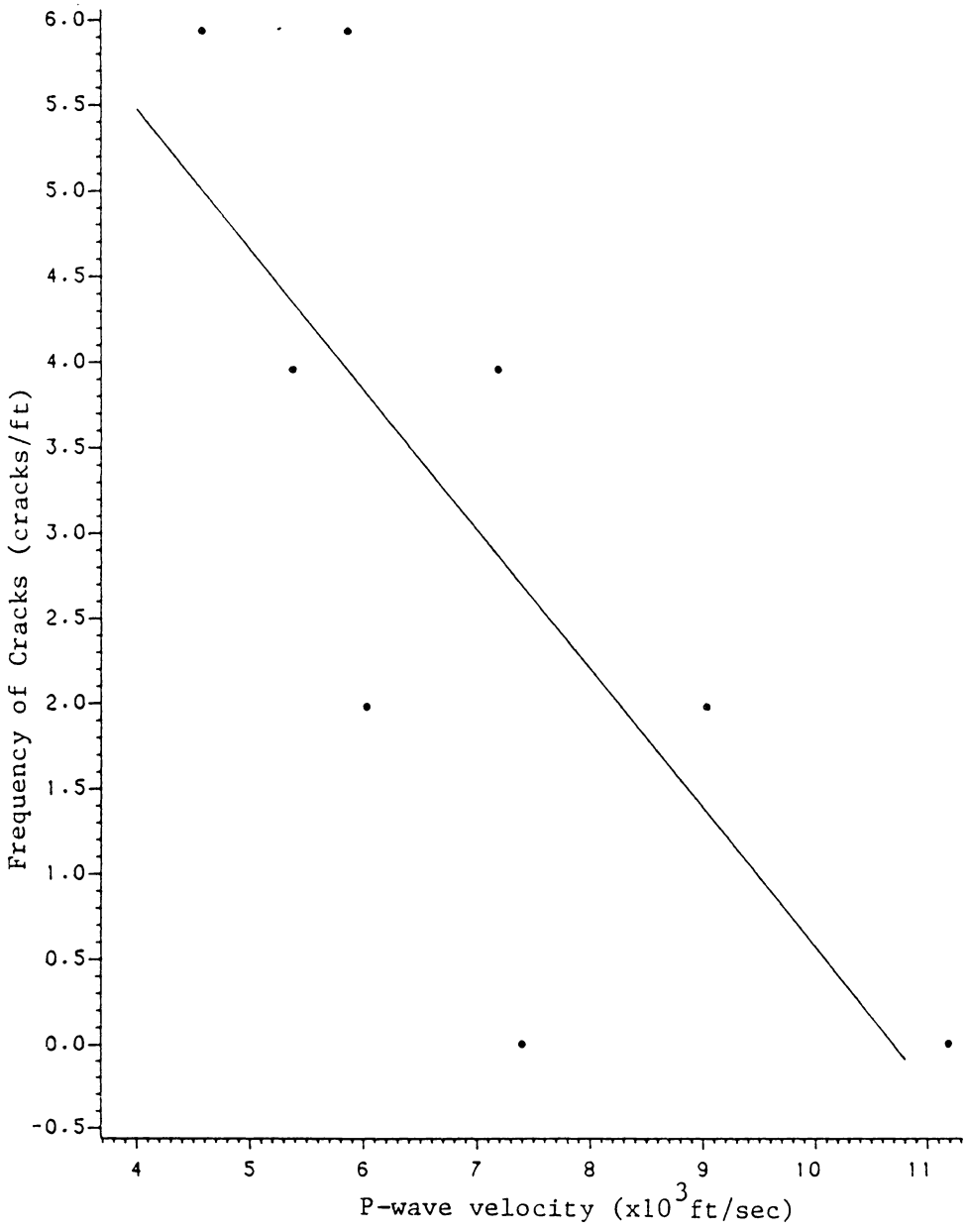


Figure B.6 Effect of Cracks on P-wave Velocity, Rock Type #9

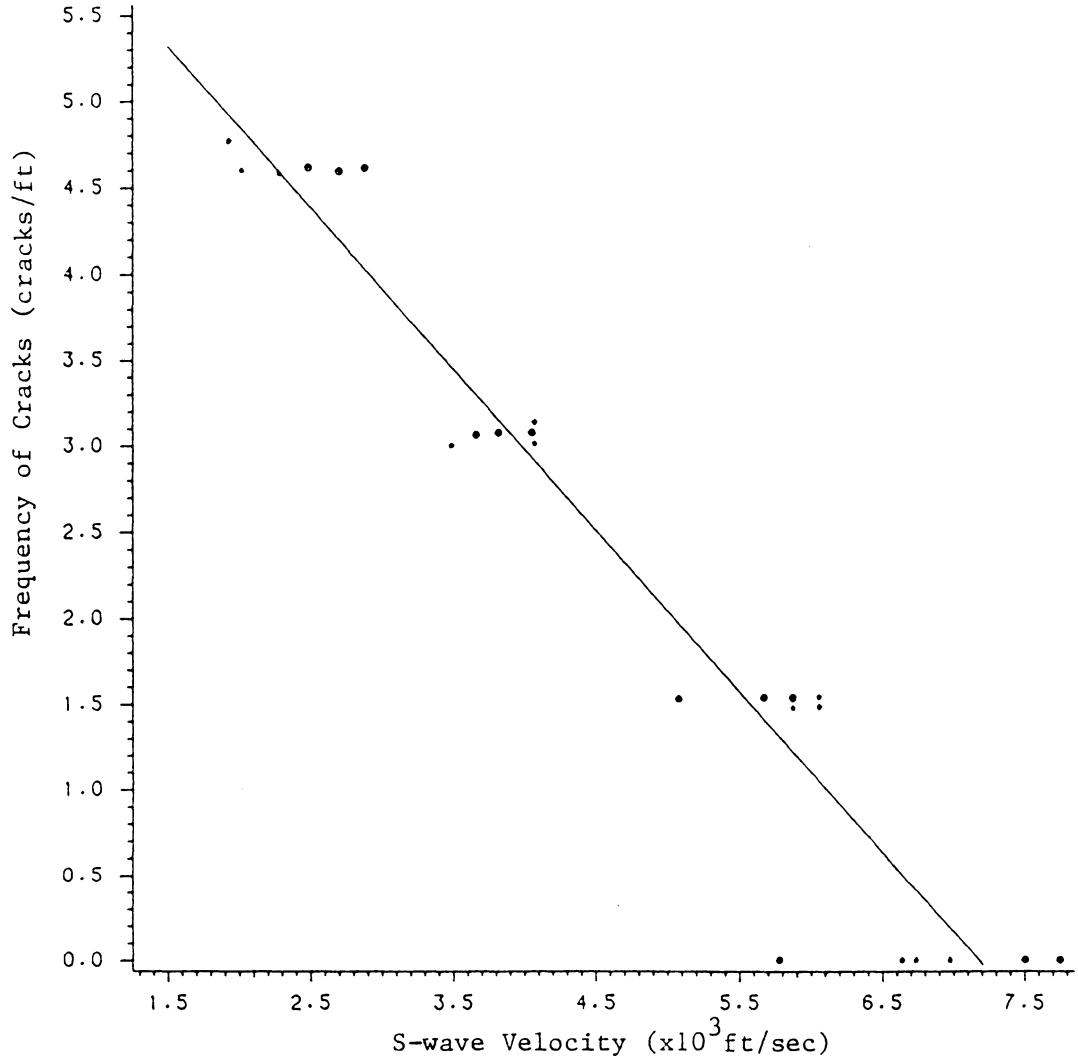


Figure B.7 Effect of Cracks on S-wave Velocity, Rock Type #6

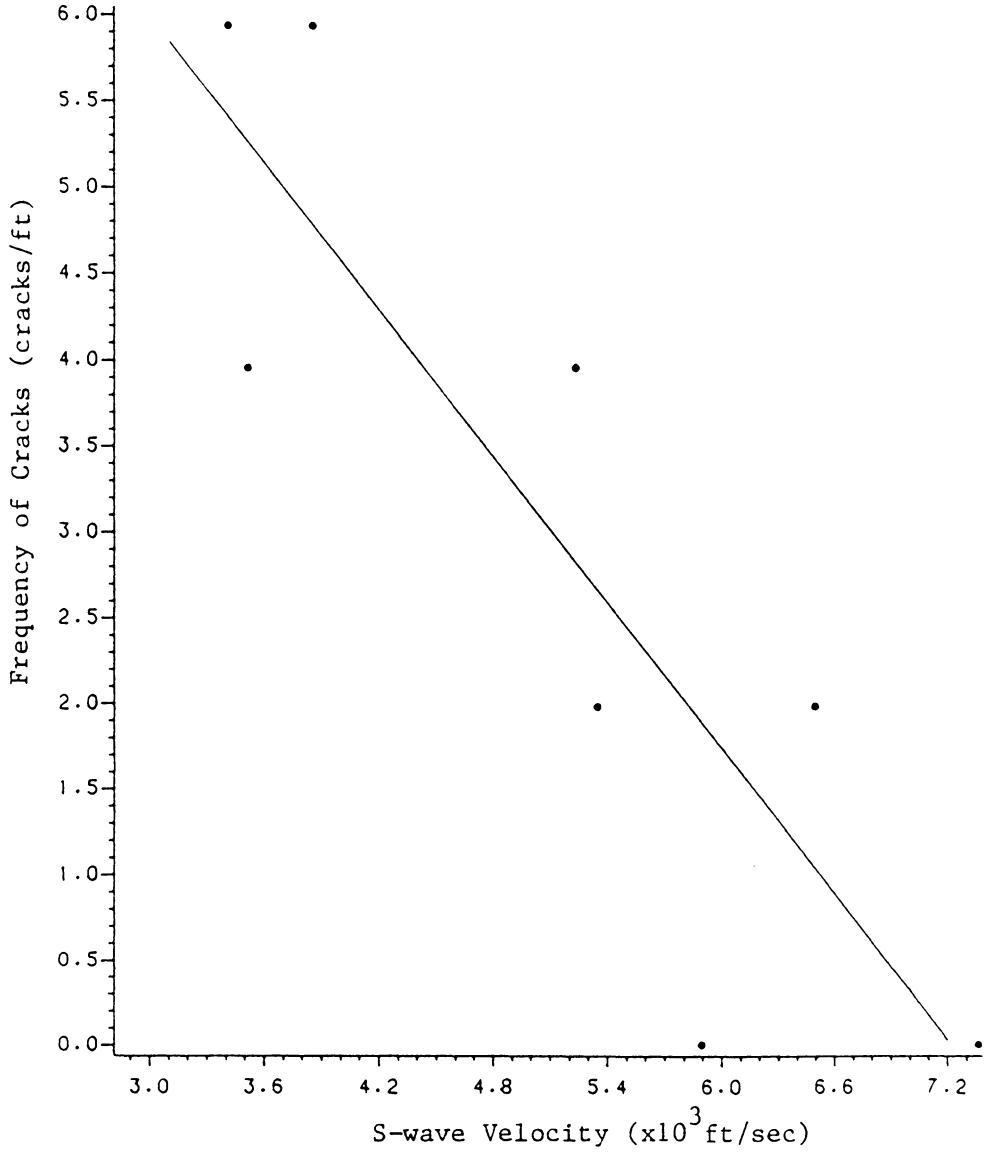


Figure B.8 Effect of Cracks on S-wave Velocity, Rock Type #9

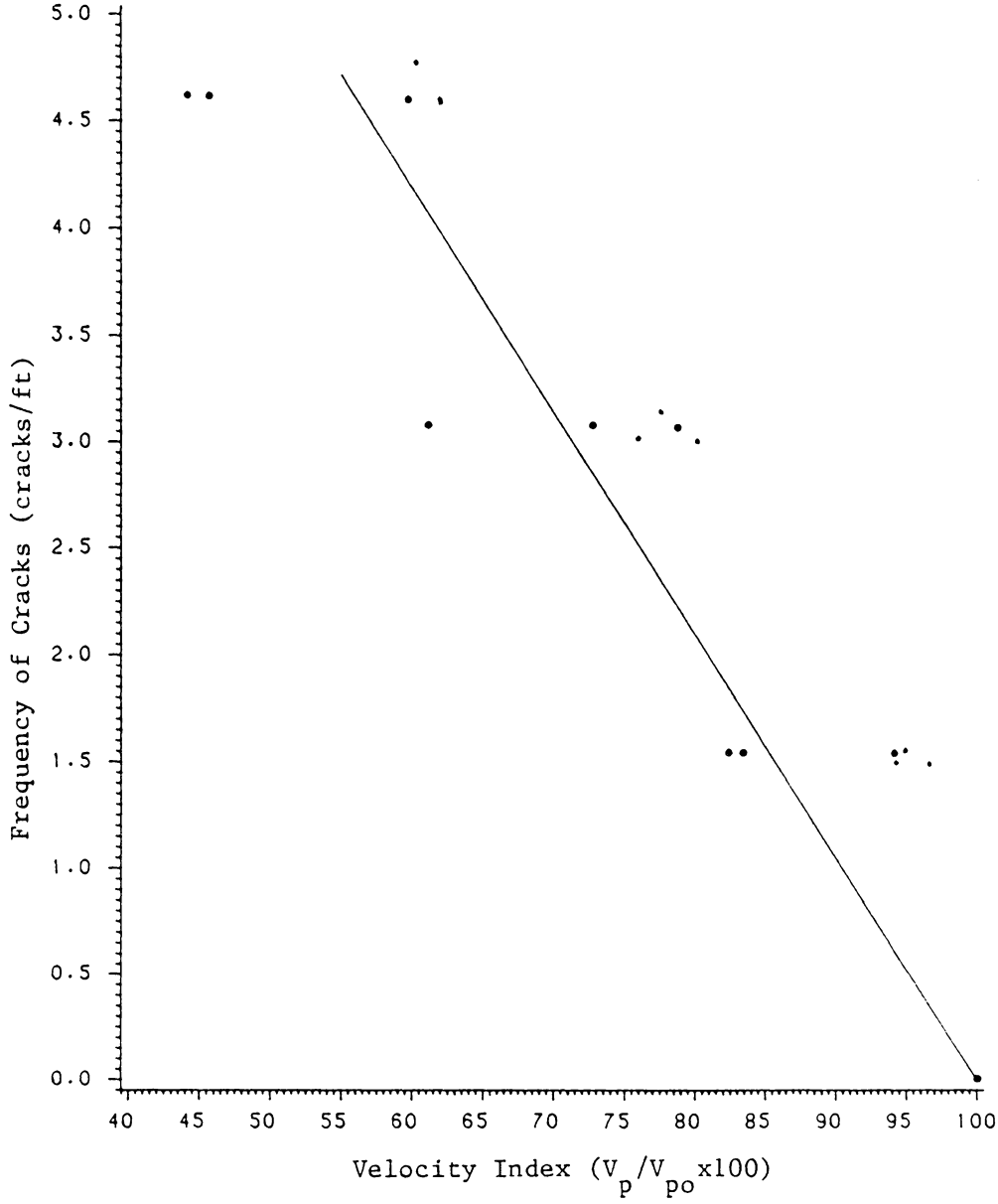


Figure B.9 Effect of Cracks on the Velocity Index, Rock Type #6

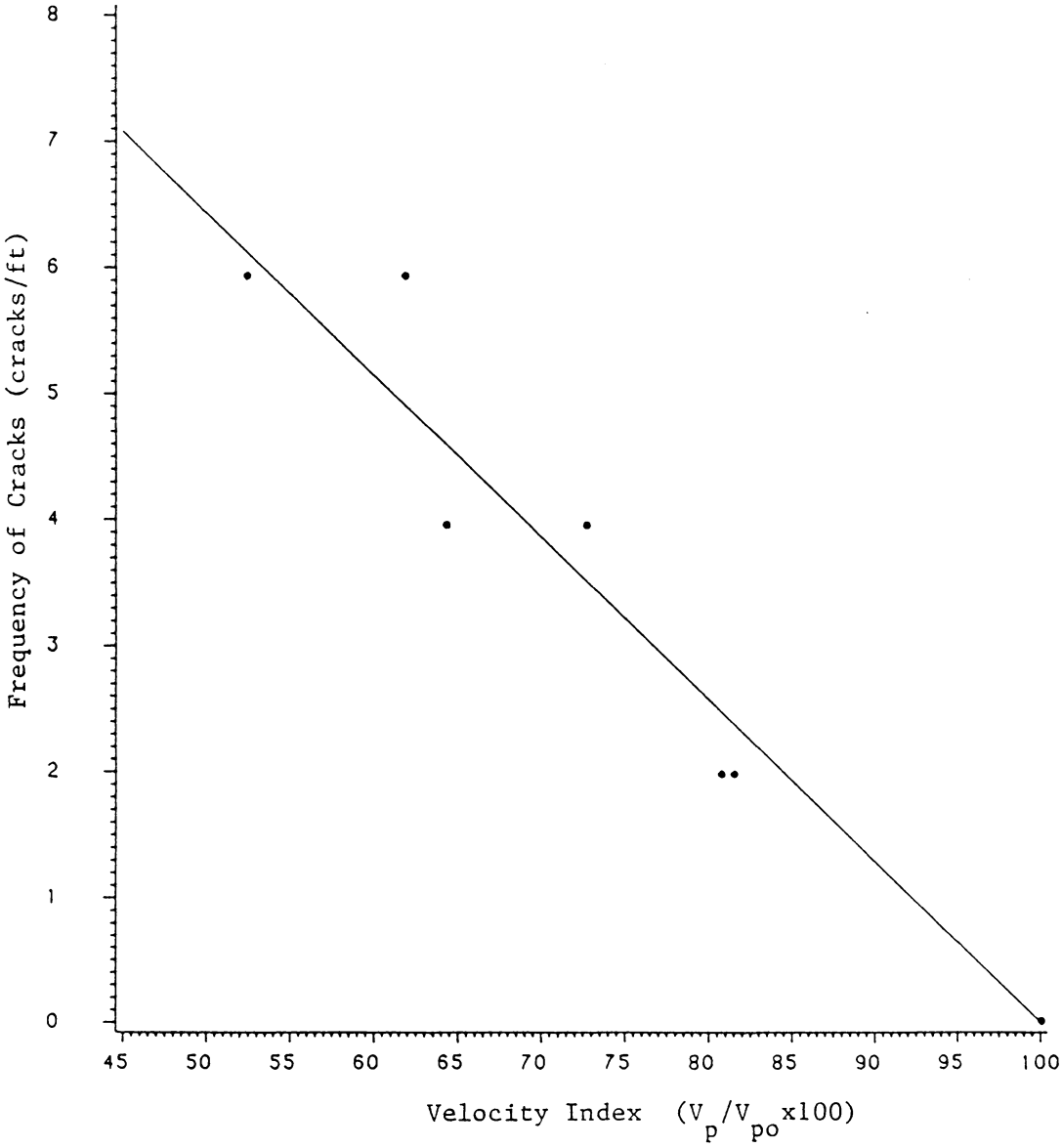


Figure B.10 Effect of Cracks on the Velocity Index, Rock Type #9

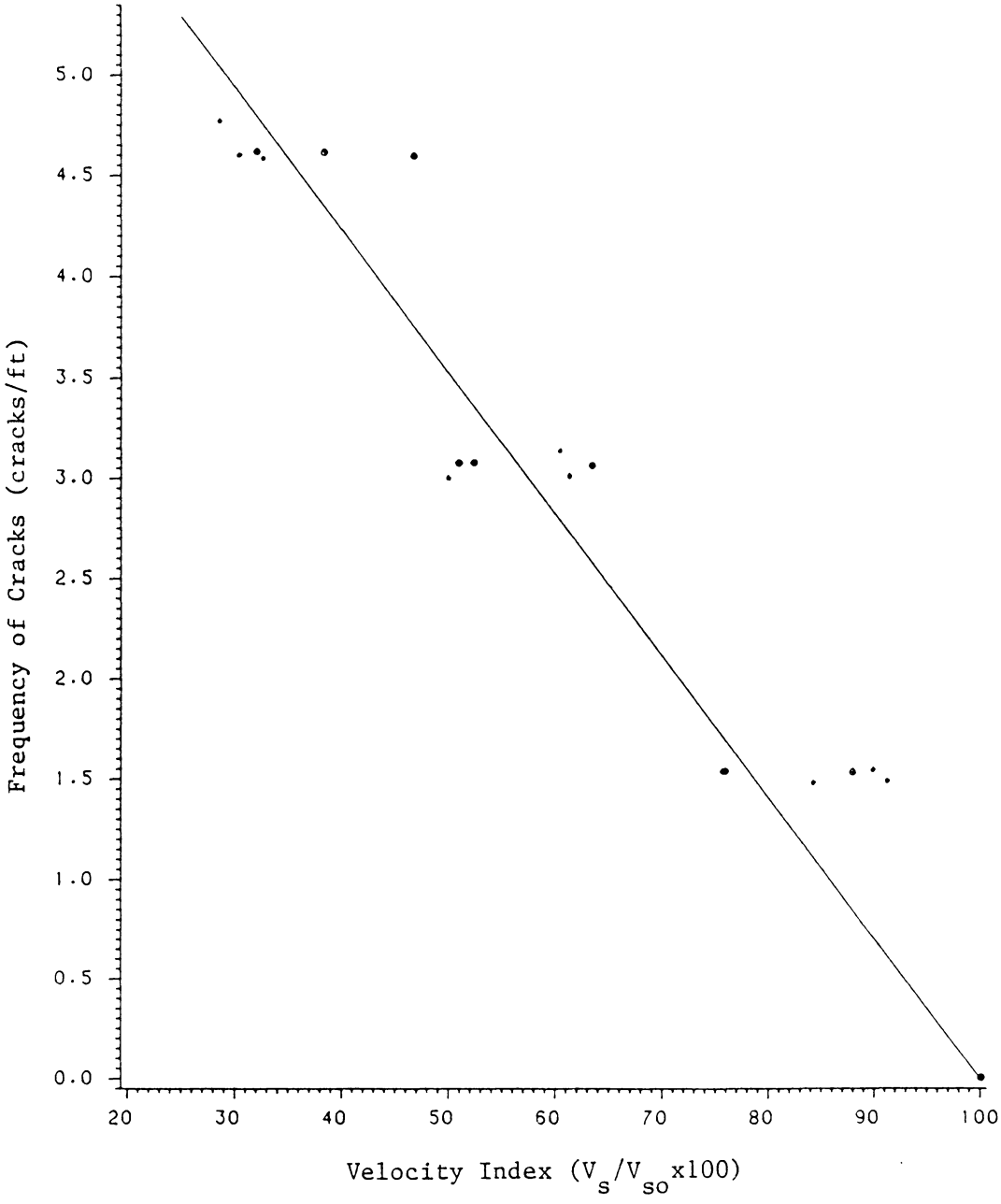


Figure B.11 Effect of Cracks on the Velocity Index, Rock Type #6

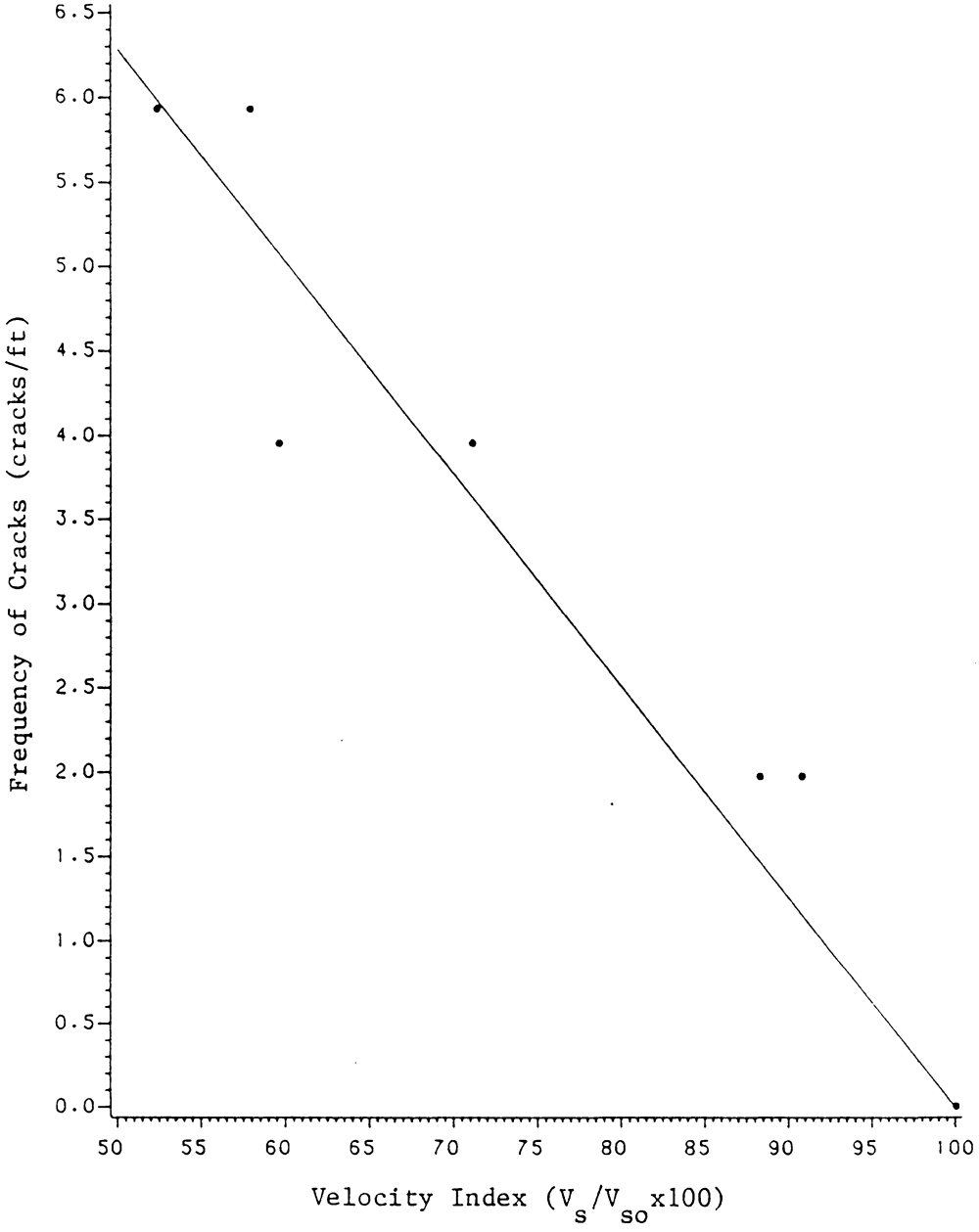


Figure B.12 Effect of Cracks on the Velocity Index, Rock Type #9

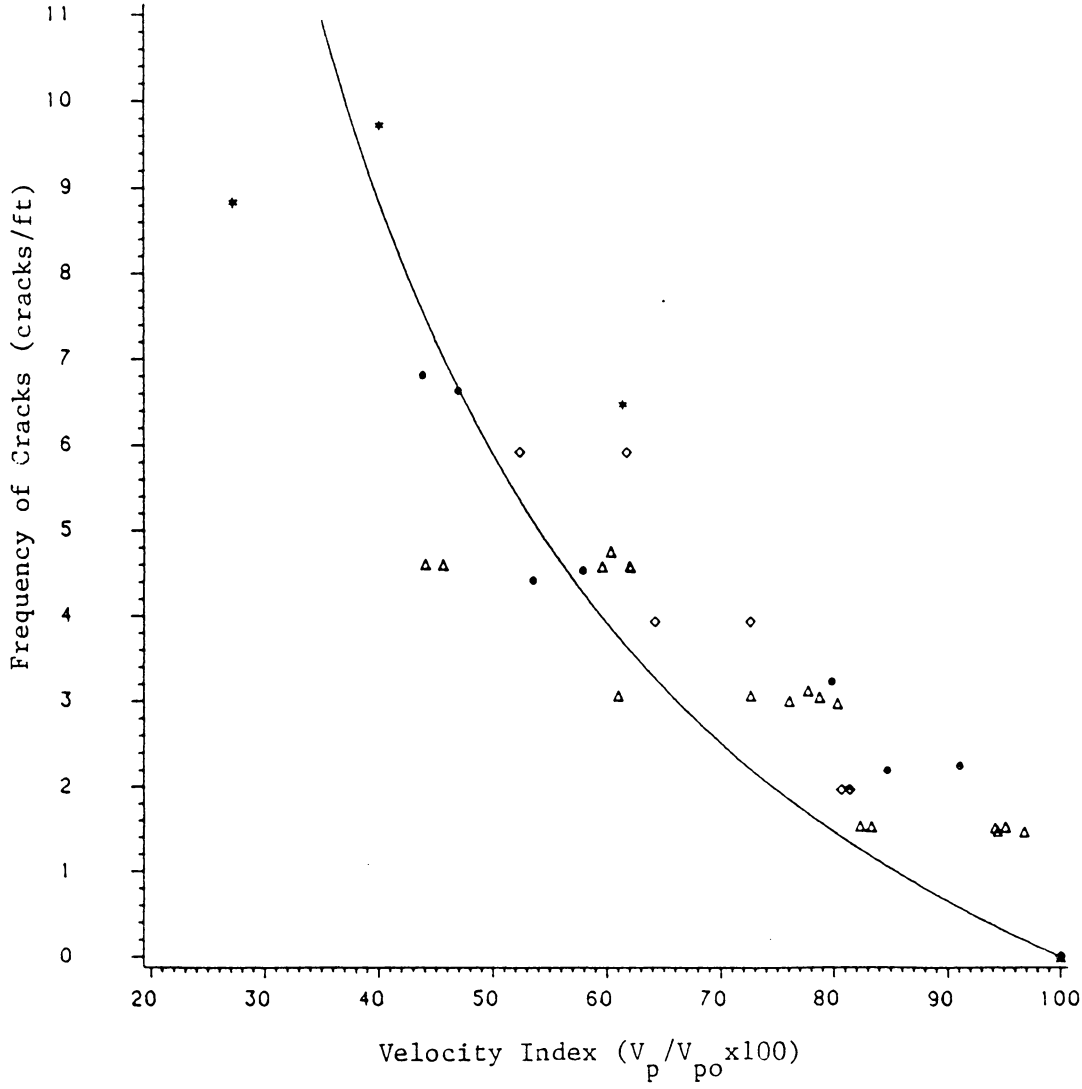


Figure B.13 Effect of Cracks on the Velocity Index

The vita has been removed from the scanned document

# THE POTENTIAL OF SONIC WAVE PROPAGATION IN ENGINEERING ROCK CLASSIFICATION

by

Paul P. G. Schilizzi

(ABSTRACT)

Sonic wave methods can be used to provide information on the engineering properties of rocks. The advantages of such techniques include minimal sample preparation, fast site preparation for field tests, reproducible and nondestructive tests, and capability for large scale testing.

During this research an extensive review of the most widely accepted engineering rock classification systems was undertaken and their principles, advantages and disadvantages are presented in detail.

The mathematical equations describing wave propagation through elastic and viscoelastic media are analyzed in order to determine the dynamic parameters most likely related to static properties.

A detailed description of the instrumentation and experimental procedures used for sonic testing is presented. Based on the experimental data, a correlation between the most characteristic static and dynamic properties was established. These relationships can be used to modify existing engineering rock classification systems, by appropriately substituting static properties by the much easier to measure, in the field and in the laboratory, sonic wave parameters. Furthermore, a classification scheme was developed, incorporating information pertaining to the static modulus of elasticity and frequency of joints from sonic wave information.